Electric Vehicle Managed Charging: Forward-Looking Estimates of Bulk Power System Value

Elaine Hale, Luke Lavin, Arthur Yip, Brady Cowiestoll, Jiazi Zhang, Paige Jadun, and Matteo Muratori

NREL is a national laboratory of the U.S. Department of Energy
Office of Energy Efficiency & Renewable Energy
Operated by the Alliance for Sustainable Energy, LLC

This report is available at no cost from the National Renewable Energy Laboratory (NREL) at www.nrel.gov/publications.

Contract No. DE-AC36-08GO28308

Technical Report
NREL/TP-6A40-83404
September 2022

Electric Vehicle Managed Charging: Forward-Looking Estimates of Bulk Power System Value

Elaine Hale, Luke Lavin, Arthur Yip, Brady Cowiestoll, Jiazi Zhang, Paige Jadun, and Matteo Muratori

Suggested Citation
Hale, Elaine, Luke Lavin, Arthur Yip, Brady Cowiestoll, Jiazi Zhang, Paige Jadun, and Matteo Muratori. 2022. *Electric Vehicle Managed Charging: Forward-Looking Estimates of Bulk Power System Value*. Golden, CO: National Renewable Energy Laboratory. NREL/TP-6A40-83404. https://www.nrel.gov/docs/fy22osti/83404.pdf.

NREL is a national laboratory of the U.S. Department of Energy
Office of Energy Efficiency & Renewable Energy
Operated by the Alliance for Sustainable Energy, LLC

This report is available at no cost from the National Renewable Energy Laboratory (NREL) at www.nrel.gov/publications.

Contract No. DE-AC36-08GO28308

Technical Report
NREL/TP-6A40-83404
September 2022

National Renewable Energy Laboratory
15013 Denver West Parkway
Golden, CO 80401
303-275-3000 • www.nrel.gov

NOTICE

This work was authored by the National Renewable Energy Laboratory, operated by Alliance for Sustainable Energy, LLC, for the U.S. Department of Energy (DOE) under Contract No. DE-AC36-08GO28308. Funding provided by U.S. Department of Energy Office of Energy Efficiency and Renewable Energy Strategic Analysis Team and Vehicle Technologies Office. The views expressed herein do not necessarily represent the views of the DOE or the U.S. Government.

Cover Photos by Dennis Schroeder: (clockwise, left to right) NREL 51934, NREL 45897, NREL 42160, NREL 45891, NREL 48097, NREL 46526.

Acknowledgments

The authors would like to thank Ookie Ma, Jacob Ward, Raphael Isaac, and Kara Podkaminer of the U.S. Department of Energy (DOE) for supporting this work and providing reviews throughout the project. We also thank our technical review committee—Anthony Giacomoni (PJM), Chris Irwin (DOE), Danial Nazemi (PJM), Josh Quinnell (CEE), Greg Vaudreuil (Mosaic Power), Henry Yoshimura (ISO-NE)—for providing feedback on an early version of the results; and Nongchao Guo (NREL) for implementing linearization techniques for the optimal time-of-use formulation. We thank Mike Meshek for editing support and Ookie Ma, Adria Brooks, Paul Spitsen (DOE), Anthony Giacomoni (PJM), Josh Quinnell (CEE), Henry Yoshimura (ISO-NE), Jennie Jorgenson, Adarsh Nagarajan and Jaquelin Cochran (NREL) for their manuscript reviews. We thank Sarah Garman (DOE) and Gian Porro (NREL) for their programmatic support. As authors, we are grateful for all of these efforts by others that have made this work possible and improved the final results and report; and in turn, we take full responsibility for any remaining errors, omissions, and other faults.

Acronyms

BEV	battery electric vehicle
CEE	Center for Energy and Environment
DA	day-ahead
DCFC	direct current fast charging
DCOPF	DC optimal power flow
DLC	direct load control
DOE	U.S. Department of Energy
DZ	dispatch zone
EV	electric vehicle
EVMC	electric vehicle managed charging
ISO	independent system operator
ISO-NE	ISO New England
LDV	light-duty vehicle
LE	low-error
LMP	locational marginal price
MAE	mean average error
MINLP	mixed-integer nonlinear program
MIQP	mixed-integer quadratic program
MR	maximum revenue
NEL	net energy for load
NREL	National Renewable Energy Laboratory
OA	outer approximation
PCM	production cost model
PHEV	plug-in hybrid electric vehicle
RP	ramp penalty
RT	real-time
RTP	real time price
SEAMS	Interconnections Seam Study
SOA	scaled outer approximation

SOC state of charge

TEMPO Transportation Energy & Mobility Pathways Options (model)

TOU time of use

UC unit commitment

USE unserved energy

USR unserved reserves

V1G one-way vehicle charge scheduling

V2G vehicle-to-grid

VG variable generation

VO&M variable operating and maintenance

ZEV zero-emission vehicle

Executive Summary

When and where electric vehicle (EV) charging occurs has significant implications for power systems supporting widespread EV adoption, especially with high shares of wind and solar generation. Numerous studies have estimated the value of scheduling or otherwise managing electric vehicle charging in such power systems. This study improves on those works by leveraging detailed simulation models for EV adoption, EV use, EV charging, and bulk power system operations, and by linking them with methods for describing charging flexibility at both the individual vehicle and aggregate levels.

This technical potential study focuses on how the value of EV managed charging (EVMC) changes depending on charging flexibility type (within-charging session or within-week scheduling), dispatch mechanism (direct load control or one of several price-based mechanisms), and managed charging participation rate, assuming ubiquitous availability of vehicle charging infrastructure and on-time completion of all trips. The study is based on a passenger light-duty vehicle (LDV) adoption scenario with 100% electric vehicle sales by 2035 and an envisioned 2038 New England power system for which within-ISO generation is 84% clean.[1]

We show that naively aggregating EV charging flexibility from individual vehicles into megawatt-scale resources grossly overestimates the flexibility of the fleet, because such aggregate models can unrealistically pair, e.g., one already-fully-charged vehicle's ability to increase load with another already-charging vehicle's ability to accept more charge, effectively requesting a charging rate that is infeasible for the latter vehicle. We then propose a heuristic, experimental method for identifying scaling factors that, when multiplied with bounds on aggregate EV charging behavior, yield megawatt-scale resources with desirable properties. In our study, decreasing the aggregate ability of vehicles to increase charging, decrease charging, and delay the accumulation of energy in vehicle batteries by 50% creates megawatt-scale pseudo-storage resources for which dispatch requests can be fulfilled by individual vehicles with low error at hourly resolution. We also find that aggregators might want to make full use of all vehicles' ability to delay energy accumulation (100% scaling factor for within-charging session flexibility) or both ability to decrease charging and ability to delay energy accumulation (100% scaling factor for within-week flexibility) to maximize EVMC market revenues. Although this "maximize expected revenue" scaling can be expected to result in higher dispatch errors, if all discrepancies are settled against hourly energy prices, the times when aggregate EVMC "over-performs" generally more than make up for the times when aggregate EVMC "underperforms" its requested dispatch. Nonetheless, despite the possible implementation of scalings that maximize revenue in real-world operations, this study uses the low error scaling factors (50% for all parameters, for within-session and within-week flexibility) in most cases when examining direct load control dispatch mechanisms, because the performance of this heuristic is well-characterized at the aggregate level. That is, using low error scaling factors avoids the computationally expensive step of disaggregating aggregate dispatch requests to individual vehicles to determine the actual impact on real-time power system operations.

[1] EVs comprise 45% of LDV stock, or 5.3 million vehicles in New England, in the 2038 study year. 80% of EVs are battery electric vehicles. Clean generation is defined to include wind, solar, biomass, hydropower, and nuclear generation.

At low participation rates, individual vehicles responding to hourly real-time prices or a simple two-block time-of-use rate produce per-vehicle savings of the same order of magnitude as direct load control with low error scaling. In fact, we find that at 5% participation (2% of the LDV fleet), hourly real-time prices can outperform low-error direct load control by 15%–130%, where the latter number corresponds to within-week flexibility. At higher participation rates (e.g., at or above 30%, which in this study corresponds to 14% of the LDV fleet being fully responsive to charging prices) we find that dispatch mechanisms where individual EV charging responds to a predefined price signal (price-taking) requires some degree of coordination to provide system-level benefit. However, how price-based EVMC could be made to work at high participation rates was not within the scope of this study. The low-error direct load control mechanism enables feasible, coordinated dispatch of EVs alongside other resources on the bulk power system, and unlike price-taking mechanisms, reduces system costs across all participation levels (from 5% to 100%).

Per-vehicle value is highest at low participation rates for all dispatch mechanisms. Factoring in production cost savings, avoided firm capacity savings, and combustion-related power sector emissions savings,[2] we estimate the value of EVMC at low participation rates (5%) to be $33/vehicle-year to $69/vehicle-yr for within-session charging flexibility and $40/vehicle-yr to $120/vehicle-yr for within-week charging flexibility in an envisioned 2038 New England power system and monetary value reported in 2016 U.S. dollars. At 100% participation, per-vehicle value declines to $25/vehicle-yr to $31/vehicle-yr for within-session charging flexibility and to $29/vehicle-yr to $36/vehicle-yr for within-week charging flexibility; however, 100% participation yields the highest total system savings: 4.4% of production costs, 5.2% of power sector emissions, and 780 MW of firm capacity for within-session flexibility, and 5.6% of production costs, 6.9% of power sector emissions and 830 MW of firm capacity for within-week flexibility in a net-importing power system with 28.9 GW peak load and 20.8 GW net-peak load.

[2] CO_2 emissions savings were valued at $45/metric ton in 2016$ in the operational dispatch and the EVMC valuation analysis.

Table of Contents

List of Figures

List of Tables

1 Introduction

Widespread adoption of electric vehicles (EVs) will significantly impact future power systems (Muratori et al. 2021). In particular, in future power systems with more wind and solar generation, when and where charging occurs will be a key driver of electric grid expansion needs and system costs (Mai et al. 2018; Cochran et al. 2021a; Murphy et al. 2021; Zhou and Mai 2021; Muratori and Mai 2020). At the bulk power level, new EV loads require more electricity supply and could require additional generation or transmission and distribution capacity. Will the load shapes align well or poorly with low marginal cost generation (including wind and solar)? Will they exacerbate system peak loads and thus necessitate additional generation capacity, or will new charging infrastructure result in higher localized peaks that require more transmission capacity? Although it is perhaps not indicative of future unmanaged EV charging load shapes, current EV charging profiles tend to peak in the evenings after people come home from work and plug their vehicles into residential outlets or dedicated chargers (Kaluza, Almeida, and Mullen 2016; Wood et al. 2017). Such profiles exacerbate and extend current residential load peaks and, if borne out in the future at higher EV shares, could cause system stress and make decarbonization more challenging, especially in solar-heavy grid systems (Muratori 2018). EV managed charging (EVMC) can alleviate such issues by changing the charging load shape to better match electricity supply while holding mobility service constant with high probability (Zhang et al. 2020; Szinai et al. 2020). EVMC can thus lower costs, reduce required system expansion, and increase system reliability. However, the grid services EVMC can provide and its value to the power system have not yet been fully assessed (Anwar et al. 2022).

This study builds on recent capability development at the National Renewable Energy Laboratory (NREL) to estimate the potential resource size and value of EVMC for personal LDVs in a possible future bulk power system (Figure 1). EV adoption and vehicle charging are estimated for a high EV adoption scenario using the Transportation Energy & Mobility Pathway Options (TEMPO)^{TM} model[3] run at the county level considering county-specific demographic distributions, vehicle distributions, and weather. Grid operations are simulated using a nodal production cost model (PCM) that describes a future ISO New England (ISO-NE) system that was isolated from the Interconnections Seam Study (SEAMS) [4] continental-scale model. EV charging flexibility is estimated using the demand-side grid flexibility model (dsgrid-flex). We chose to model ISO-NE in 2038 because ISO-NE is a well-defined regional power system and the 2038 model year available from SEAMS provides a good starting point for exploring how a future system with significant shares of wind and solar generation might operate with and without managed charging at different levels of managed charging participation.

Broadly speaking, EVMC consists of scheduling or otherwise modulating EV charging and possibly discharging in response to grid signals. Currently, although two-way vehicle-to-grid (V2G) services that allow discharging electricity from EVs back into the grid have been piloted (CEC 2019; Black et al. 2018; Das and Sanchari 2020) and shown to provide more value than one-way vehicle charge scheduling (V1G) in recent analyses (Anwar et al. 2022), most utility EV programs are one-directional (V1G, which does not discharge vehicle batteries to provide power to

[3] "TEMPO: Transportation Energy & Mobility Pathway Options," NREL, https://www.nrel.gov/transportation/tempo-model.html

[4] "Interconnections Seam Study," NREL, https://www.nrel.gov/analysis/seams.html

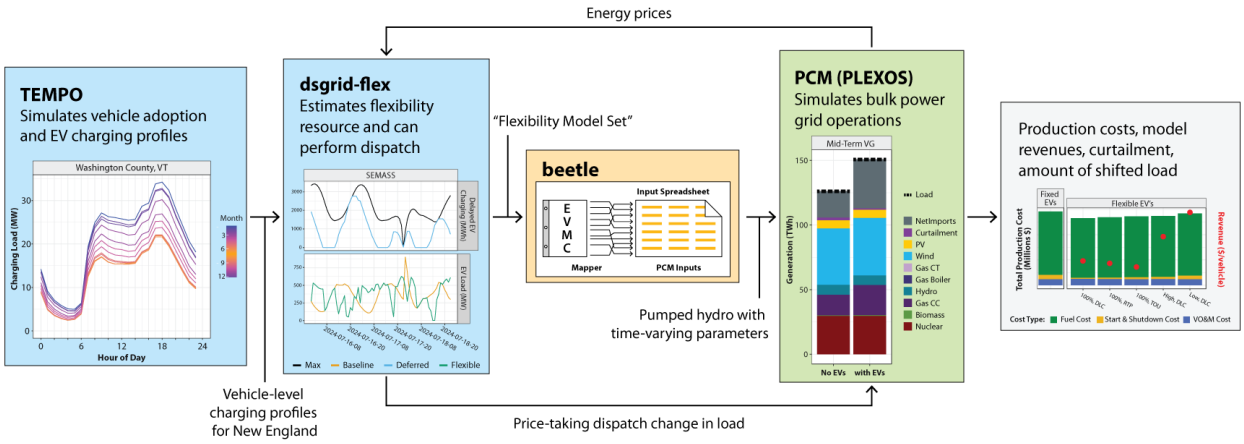

Figure 1. Value of EVMC in bulk power systems modeling workflow

the grid) (SEPA 2021). V1G has lower communication and control requirements, as well as less risk of vehicle range limitations and less uncertain battery degradation impacts (Noel et al. 2019; Guo et al. 2019). We therefore study only V1G for this report. On the grid services side, this report focuses on the three services in the bulk power system that are responsible for 95% or more of costs: energy, capacity, and transmission (Denholm, Sun, and Mai 2019). Specifically, EVMC can reduce energy costs, reduce generation capacity requirements, and alleviate transmission congestion via intentional scheduling of EV charging. At the vehicle level, managed charging could be actively controlled by an aggregator; be affected through customer-facing vehicle, charger, or smart phone software; or be achieved behaviorally (similar to how gasoline vehicle drivers currently factor price into their choice of gas station). At the bulk power level, managed charging could bid into and be dispatched in day-ahead (DA) or real-time (RT) markets; be anticipated by short-term load forecasts; or simply show up in the real-time, actual load. This study is agnostic about most of these details, but in the interest of understanding the bulk power system value of EVMC, we do compare the performance of three stylized EV charging dispatch mechanisms: (1) direct load control (DLC) in which the grid operator dispatches storage-like megawatt-scale aggregations of EV charging load alongside supply-side resources to minimize system costs, (2) real-time pricing (RTP) in which individual vehicle charging is scheduled to minimize charging costs as defined by DA wholesale electricity prices, and (3) time-of-use (TOU) tariffs, which are similar to RTP profiles but use coarser price signals, with different energy prices depending on season and time block (up to 32 prices per year rather than the 8,760 in RTP). In all cases, we model EVMC as fully respecting mobility constraints, that is, EVMC does not hinder the ability of vehicles to complete all trips.

Numerous studies have estimated the value of EVMC in bulk power systems (Anwar et al. 2022). We improve on earlier estimation methods by:

- Starting from sample vehicle energy profiles differentiated by vehicle type, household type, and location (location impacts weather and EV energy use)
- Estimating charging bounds for both within-charging session and within-week scheduling flexibility, thus exceeding the common assumption of a 24-hour flexibility window

- Computing both individual-level and aggregate-level dynamic flexibility models
- Comparing aggregate flexibility dispatch to vehicle-level flexibility dispatch and using those comparisons to scale aggregate flexibility parameters (i.e., ability to increase charging, decrease charging, or delay the accumulation of energy in vehicle batteries) to create low-error and maximum-revenue megawatt-scale resources
- Starting from a bulk power system production cost model that meets basic standards for reliability under baseline charging assumptions and realistically incorporates widespread EV adoption into a system with high wind and solar shares[5]
- Examining how managed charging value and complexity change depending on flexibility type (within-session, or within-week) and dispatch mechanism (DLC, RTP, or TOU).

Similar to some other studies, we:

- Capture charging flexibility by determining as-early-as-possible (immediate) and as-late-as-possible (delayed) charging bounds that preserve mobility service
- Make a "ubiquitous charging" assumption that a charger is always available when an EV is parked
- Analyze a fixed power system and do not directly estimate how EVMC could change utility-scale generation, transmission and storage investment or retirement decisions
- Directly compute electricity production (operational) cost impacts and estimate capacity value using heuristic methods
- Estimate the value of EVMC as a function of participation rate without attempting to estimate fixed and variable costs, realistic participation rates, or demand bids
- Analyze only bulk power system benefits and costs, implicitly assuming the distribution system can handle additional EV load.

The result is a technical potential study focused on how the value of EVMC changes depending on participation level, dispatch mechanism, and whether the charging flexibility is represented per-charging session or over the course of an entire week. Although the geography and temporal focus of the study (ISO-NE in 2038 with a single grid build-out and single EV deployment scenario) is limited, and the value results are subject to the usual caveats that modeled grid service prices are often less volatile than real-world grid service prices (Gagnon et al. 2021; Seel and Mills 2021), both the methodology and the results should interest readers who would like to better understand how large shares of EVs could be efficiently integrated into bulk power systems with high shares of variable generation.

In the remainder of this report, we describe our EV adoption projection and unmanaged charging profile (chapter 2), reference production cost model (chapter 3), dynamic models of EVMC resource (chapter 4), and bulk power system value of EVMC results (chapter 5) before discussing the implications of our results (chapter 6) and providing concluding remarks (chapter 7).

[5]Reliability was confirmed by computing loss of load expectation (LOLE) and normalized expected unserved energy (NEUE) with the Probabilistic Resource Adequacy Suite[6].

2 Electric Vehicle Adoption and Unmanaged Charging

The Transportation Energy & Mobility Pathways Options (TEMPO^{TM}) model generates long-term scenarios of energy use for the United States transportation sector. TEMPO includes all passenger and freight transportation modes (i.e., walking, biking, public transport, LDVs, freight trucks, rail, maritime, and aviation) (Figure 2); however, the scope of this study is limited to personal LDVs, including cars, sport utility vehicles, vans, and pickup trucks. LDV adoption and use is modeled at the household level, and households are differentiated by income, urbanity (e.g., rural, suburban, urban, etc.), and number of drivers (Muratori et al. 2020; Muratori et al. 2021). TEMPO preserves travel needs and behaviors while simulating the adoption and use of new options. Transitions from the current petroleum-dominant paradigm to alternative fuels and vehicles can be modeled through projections of technology and fuel evolution over time (i.e., cost and performance improvements) and various policies (e.g., zero-emission vehicle [ZEV] sales mandates). In addition, TEMPO includes county-level geographic resolution for input data on household types and vehicles preferences. EV efficiency estimates also vary with outdoor temperature as measured at 975 weather stations across the contiguous United States. These geographically resolved data allow TEMPO to reflect heterogeneity in the estimated vehicle stock and use and to project heterogeneous EV adoption and charging profiles for future scenarios (Yip et al., n.d.).

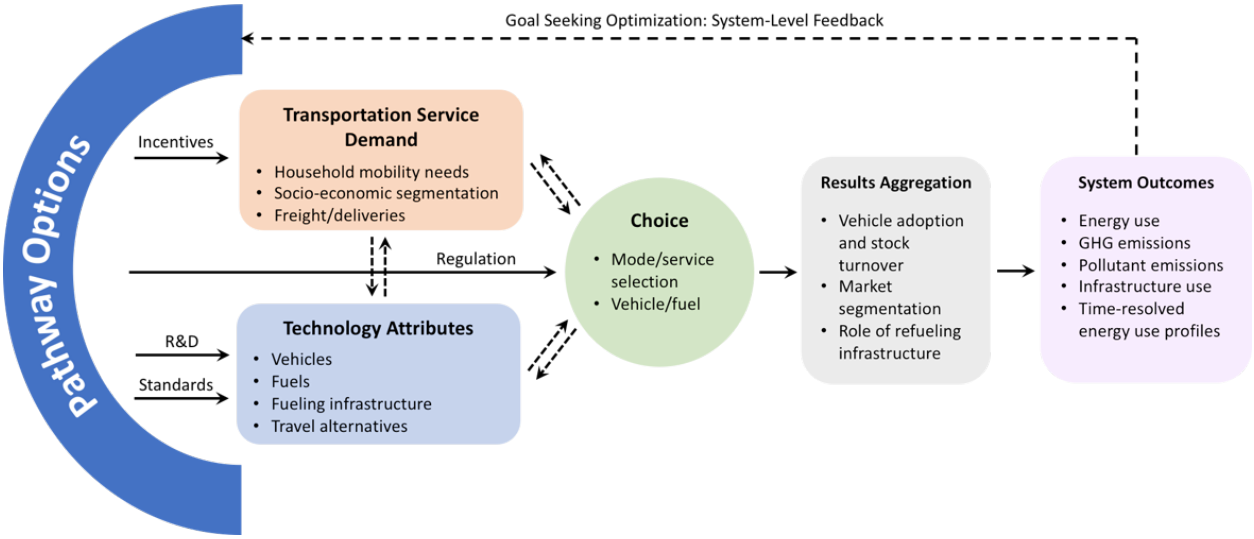

Figure 2. The TEMPO model is a comprehensive transportation demand macro model. TEMPO can explore long-term scenarios of energy use across all passenger and freight transportation modes and assess synergies with energy supply.

In this study, we focus on a future ISO-NE system with significant shares of plug-in electric LDVs (EVs). We create a simulated population of New England EVs in 2038 by running a scenario that nationally achieves 50% EV sales by 2030 and 100% EV sales by 2035 to align with goals and targets such as 50% zero emissions sales nationally by 2030 (Biden 2021) and California and New York ZEV regulations that approach 100% ZEV sales by 2035 (Yip et al., n.d.). We disaggregate EV adoption by county by anchoring each county to empirical county-level vehicle registration data in historical years and then applying the national-level EV growth rate trends uniformly across all counties. This approach captures the current heterogeneity in EV

adoption observed across counties in the United States and extends this into the future, achieving high-level EV sales goals while assuming similar positioning of counties in terms of EV adoption either leading or lagging national averages. In 2021, many counties, particularly in states with ZEV programs mandating ZEV sales, had EV sales shares well over the national average of 5%.

U.S.-wide county-level projected EV sales shares are shown in Figure 3, with New England county sales shares highlighted in red. The heterogeneity built into county-level TEMPO projections is evident. New England county sales shares mostly fall near and below the U.S. average EV sales shares.

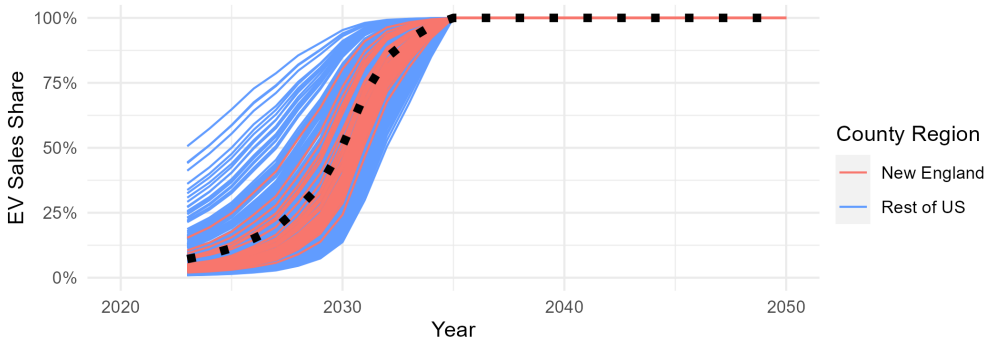

Figure 3. Personal light-duty EV sales shares over time by county in the All EV Sales by 2035 scenario. The national average is shown as a black dashed line. The New England counties are plotted in red.

Figure 4 shows New England LDV sales shares by vehicle type. This TEMPO scenario assumes a solid majority of EV sales will be battery electric vehicles (BEVs) in the longer term. Plug-in hybrid electric vehicles (PHEVs) are assumed to be 20-30% of the total EV sales share in the 2025-2035 transition time frame before tapering off to 0% by 2045, based on expert opinion and latest trends in BEV technology, infrastructure, and policies.

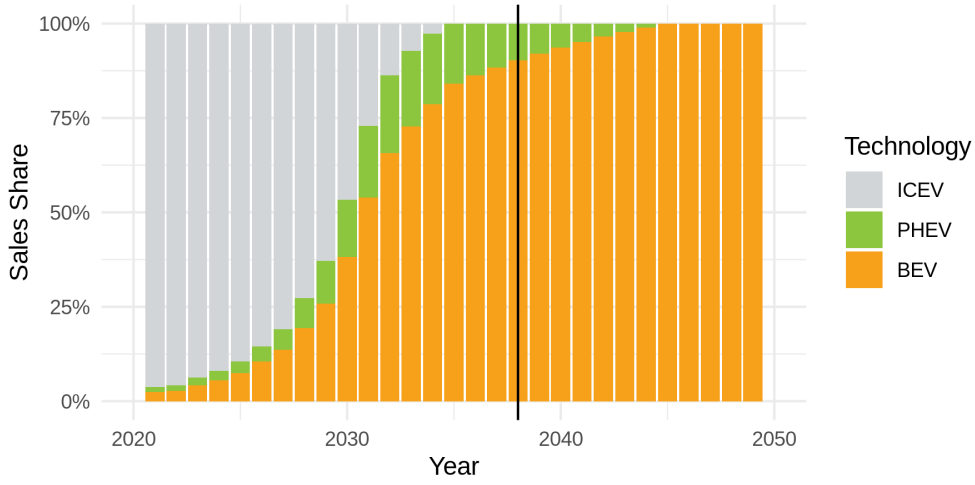

Figure 4. Personal LDV sales shares by vehicle technology type and year for New England in the All EV Sales by 2035 scenario. Powertrains depicted: internal combustion engine vehicles, plug-in hybrid electric vehicles (PHEVs), and battery electric vehicles (BEVs). The vertical line indicates 2038, the year of the data for this study.

The resulting New England LDV stock is shown in Figure 5. Because only about 6% of the LDV fleet turns over each year (Jacobsen and Benthem 2015), sales shares are a leading indicator of

stock shares, and national average 100% EV sales by 2035 translates into a New England LDV stock EV share of only 81% in 2050. In this study, we explore the value of EVMC for the 2038 All EV Sales by 2035 scenario EV stock. That scenario projects 5.3 million EVs in New England in 2038, 80% of which are BEVs, with the remainder being PHEVs. Overall, EVs are 45% of the New England LDV stock in 2038.

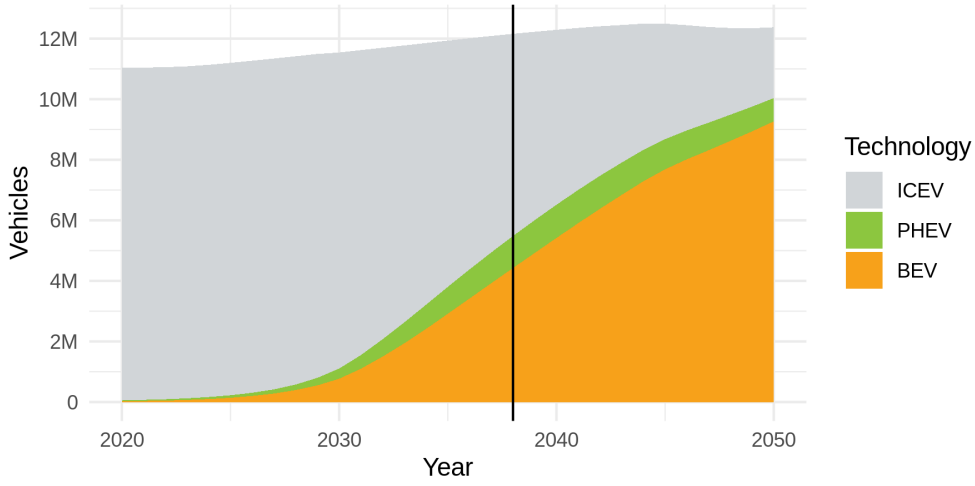

Figure 5. New England LDV stock in TEMPO, 2020-2050. The total 2038 LDV stock is 12.2 million vehicles, including 4.3 million BEVs and 1.0 million PHEVs. The vertical line indicates 2038, the year of the data for this study.

County-level heterogeneity for LDVs per capita, EV share and EVs per capita is depicted for the 2038 New England All EV Sales by 2035 scenario in Figure 6. The counties with higher numbers of EVs per capita are those with more LDVs per capita, higher EV shares, or both. The more-urban counties tend to have average or higher EVs per capita because, although urban counties have fewer LDVs per capita, they have higher shares of EVs. There are therefore few counties with relatively low numbers of EVs per capita (e.g., only 4 of 67 counties have less than 0.3 EVs per capita for this particular scenario).

Unmanaged EV charging is simulated by TEMPO assuming vehicles plug in and charge after every trip until either they are fully charged or another trip is started. We refer to this as the Immediate charging strategy. This charging strategy assumes charging infrastructure is ubiquitous, always available for EVs to plug-in whenever they are parked, and has the outcome of maximizing vehicle state of charge at all times. It thus represents a bounding case that minimizes range anxiety. For this study, we assume all charging between trips is either 120 volt Level-1 (L1) charging at 1.4 kW or 240 volt Level-2 (L2) charging at 7.2 kW. High power direct current fast charging (DCFC) is simulated only when required to complete a trip. Vehicles are assigned to either L1 (5% of vehicles) or L2 (95% of vehicles) between-trip charging. In the final unmanaged profiles, charging is 88% L2, 5% L1 and 7% DCFC. The average per-vehicle charging load profiles of the Immediate charging strategy and how they vary by county based on heterogeneity in household types, vehicle preferences, and weather are shown in Figure 7.

In Figure 7, a wider spread across different months for the same county indicates more severe winter weather that reduces vehicle energy efficiency in cold months. Counties with higher charging demand per vehicle than the regional average either have larger EVs (e.g., more pickup

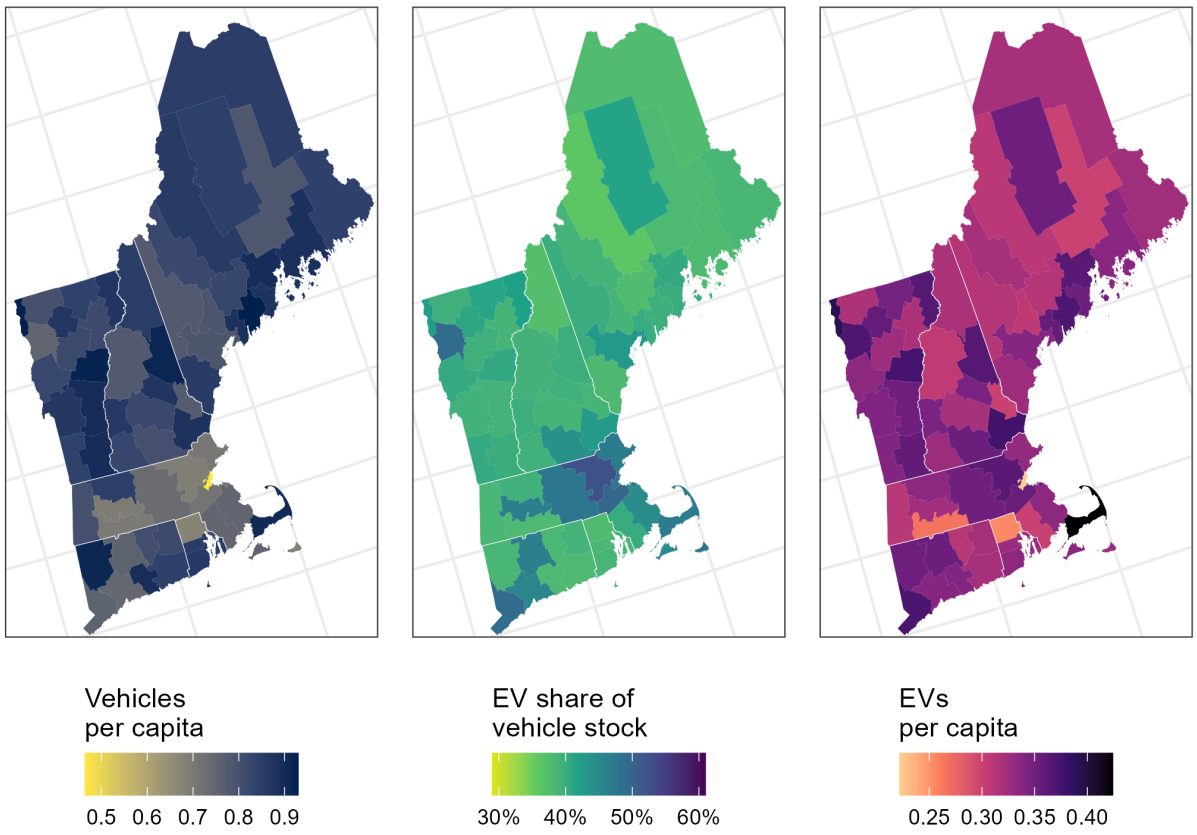

Figure 6. New England LDV stock in TEMPO, 2038 by county

trucks or sport utility vehicles), more driving activity, or more temperature extremes than the regional averages or a combination of these characteristics. From the figure and a basic knowledge of New England geography, we observe higher than average per-EV charging load in more rural counties and larger differences in energy use by month in more northern or mountainous counties that are regularly subject to severe winter weather.

Applying sample weights to TEMPO's 101,031 sample vehicle profiles for 2038 New England produces the aggregate profile shown in Figure 8. We assume all charging takes place on the distribution system and incurs uniform, average losses of 5.3% (Cohen et al. 2019). The overall charging load as it would be measured at the meter is 16.27 TWh/yr or 8.41 kWh/vehicle-day; including the 5.3% losses, the generation required to serve this load is 17.13 TWh/yr. In what follows, charging load refers to EV load as measured at the meter; generation includes grossing up for distribution losses. With EVMC, this amount of load, and thus mobility service, is unchanged, but we change the charging load profiles (charging shape) to better align electricity demand with electricity supply, thereby reducing system operating costs. TEMPO simulates a single week of charging for each sample vehicle for each month of the year to capture the impacts of temperature, which in Figure 8 manifests as identical weekly profiles for each month. The unmanaged charging profile peaks at 3.79 GW on winter (simulated February) Monday evenings during the local time hour ending at 6 p.m. (i.e., January 30, February 6, February 13, and February 20 for 2012), and has at least 0.284 GW of EV charging load in all hours during the year.

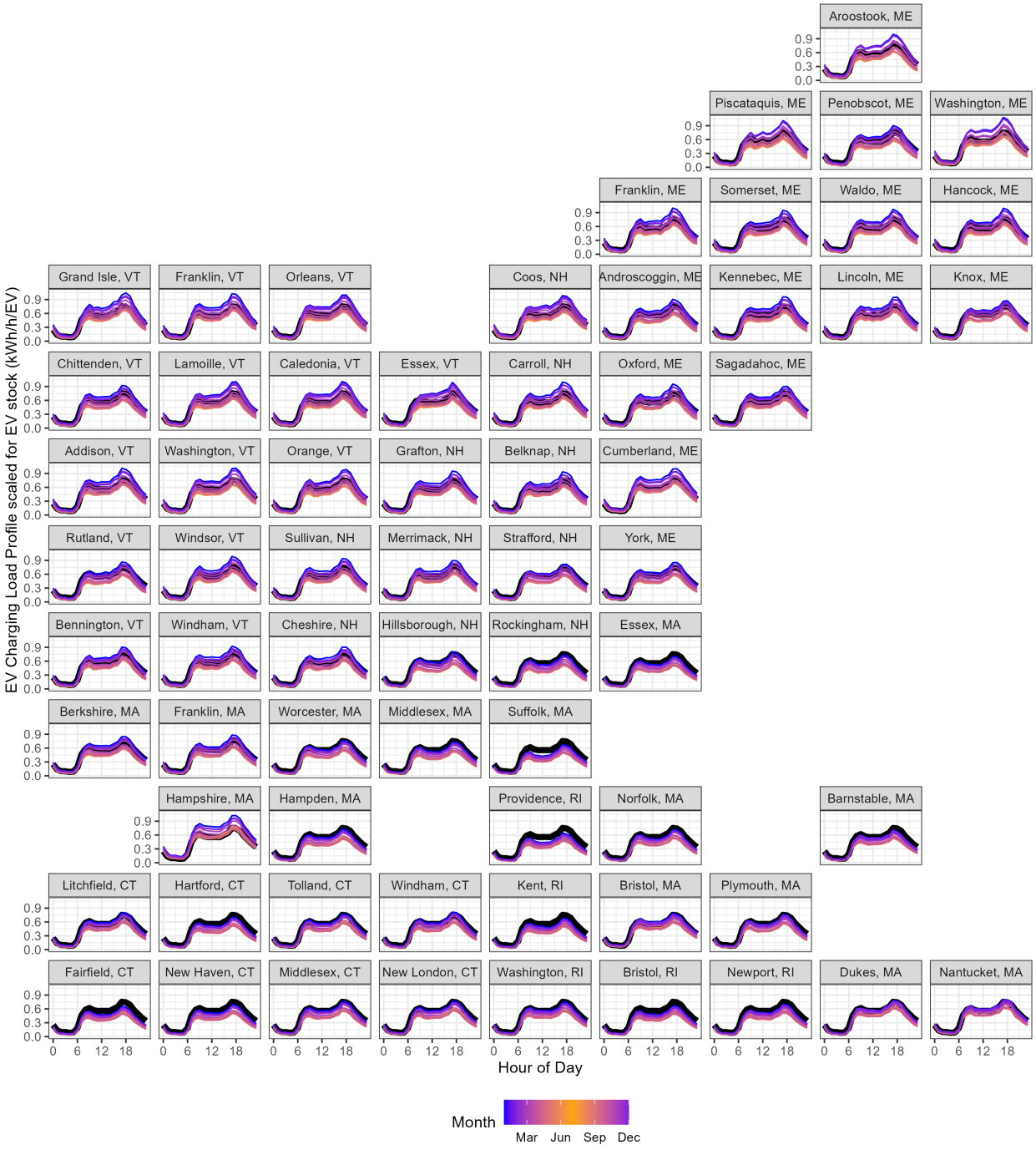

Figure 7. County-level Immediate EV charging strategy average load profiles in 2038. Average load profiles are normalized to be per vehicle (kWh/h/EV). The black line shown in all facets is the per-vehicle average weekday load for all of New England.

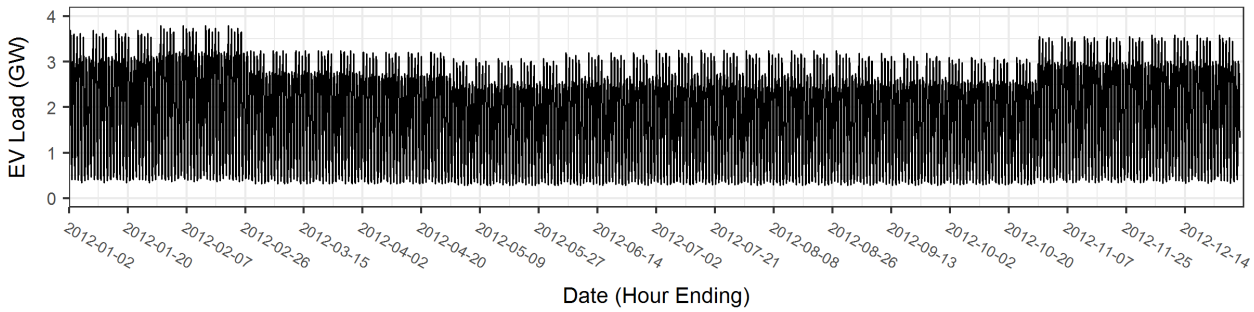

Figure 8. TEMPO unmanaged EV charging hourly profile (as measured at the meter) for New England in 2038 using weather year 2012. The profile was created by simulating Immediate charging under a ubiquitous charger assumption. Charging 5.3M EVs requires 16.27 TWh of annual energy, with a peak demand of 3.79 GW at 6 p.m. on the coldest weekday evenings, and a minimum demand of 0.284 GW across all hours.

Table 1 summarizes the 2038 New England EV stock, unmanaged charging profile, and set of sample vehicles used in this study.

Table 1. TEMPO 2038 ISO-NE EV Adoption, Unmanaged Charging, and Sample Vehicles Summary

Vehicle Stock	2038	Unmanaged Charging	2038	Sample Vehicles	2038
EV Stock [millions]	5.3	Electricity Load [TWh][a]	16.3	Number [thousands]	101
EV Share of LDVs	45%	Peak [GW][a]	3.79	Avg. Sample Weight	52.5
BEV Share of PEVs	80%	Peak Time	5 p.m.-6 p.m. January 30[b]	Avg. Load [kWh/veh-day]	8.41

[a] Load measured at the meter. Serving this load requires 17.1 TWh of generation, 3.99 GW at peak, to cover distribution losses of 5.3%.

[b] The peak charging load occurs on Monday evenings in February in TEMPO's representative-week simulations. January 30 has February data because most of the week January 30–February 5 occurs in February.

3 Bulk Power System Operations

We demonstrate the value of EVMC in a production cost model (PCM) indicative of a future ISO-NE power system. ISO-NE is an independent system operator (ISO) covering six northeastern U.S. states: Connecticut, Rhode Island, Massachusetts, Vermont, New Hampshire, and Maine (Figure 9).[7] We chose ISO-NE for this case study because it is moderately-sized and geographically well-defined, and because it has a limited number of connections to other power systems. The PCM was initially extracted from the Interconnections Seam Study[8] (SEAMS) 2038 model (Bloom et al. 2022). We also developed an ISO-NE PCM from the SEAMS 2024 model, which we use here to illustrate (approximately) how the 2038 system differs from ISO-NE as it exists today. For this study of ISO-NE, the SEAMS ISO-NE subnetwork was extracted and assigned fixed import and export schedules based on full SEAMS model runs. Hydroelectric generator dispatch was also fixed to the results of full SEAMS model runs, to facilitate comparisons of models with and without EVMC.

Figure 10 shows the annual generation for New England in the 2024 model, the 2038 model (without EV load), and the 2038 model with the TEMPO All EV Sales by 2035, 2038 Immediate charging profile added.[9] The latter PCM is the Reference scenario for this study. Currently, the ISO-NE system is predominately natural gas and nuclear generation with significant contributions from hydropower and non-hydropower renewables as well as imports.[10] However, much of the non-hydropower renewables is biomass; only 6.2% of generation and 5.3% of net energy for load (NEL) comes from within-ISO wind and solar, that is, variable generation (VG), in 2021 (ISO-NE 2022). In contrast, the 2024 SEAMS model has 14% VG and the 2038 SEAMS model has 35% VG counting only ISO-NE non-curtailed VG resources and measured against NEL. When 17.1 TWh of generation needed to serve EV charging load (direct consumption plus distribution losses) is added to the 2038 SEAMS model, the PCM serves additional load primarily through increased net imports (15.9 TWh) and increased natural gas combined cycle (gas combined cycle) generation (1.1 TWh).[11] Thus our 2038 +EV Reference scenario has within-ISO VG shares (excluding curtailment for both VG and total generation) of 47% of generation and 35% of NEL. Reference scenario within-ISO clean energy shares (inclusive of wind, solar, hydropower, biomass, and nuclear; excludes storage) are 84% of generation and 63% of NEL.

[7] https://www.iso-ne.com/

[8] https://www.nrel.gov/analysis/seams.html

[9] All PCM results in this report are generated from the ISO-NE PCMs isolated from SEAMS; that is, we do not report any results extracted directly from the original SEAMS models.

[10] 22.2 TWh/18.8 TWh in gross/net imports in ISO-NE in 2021; net imports were 15.8% of net-energy for load (NEL) (ISO-NE 2022).

[11] ISO-NE was isolated from the SEAMS model by using the full SEAMS model to compute import and export profiles under baseline conditions and then fixing those profiles in the isolated model. PLEXOS effectively modifies these net-import profiles by dumping energy at a cost of $20/MWh. In what follows we report net imports as the difference between load (inclusive of storage charging) and internal non-curtailed generation, effectively counting dumped energy against net imports. The 2038 model contains 56.6 TWh of fixed imports and 15.6 TWh of fixed exports, both implemented at select nodes, for up to 41.0 TWh of net imports.

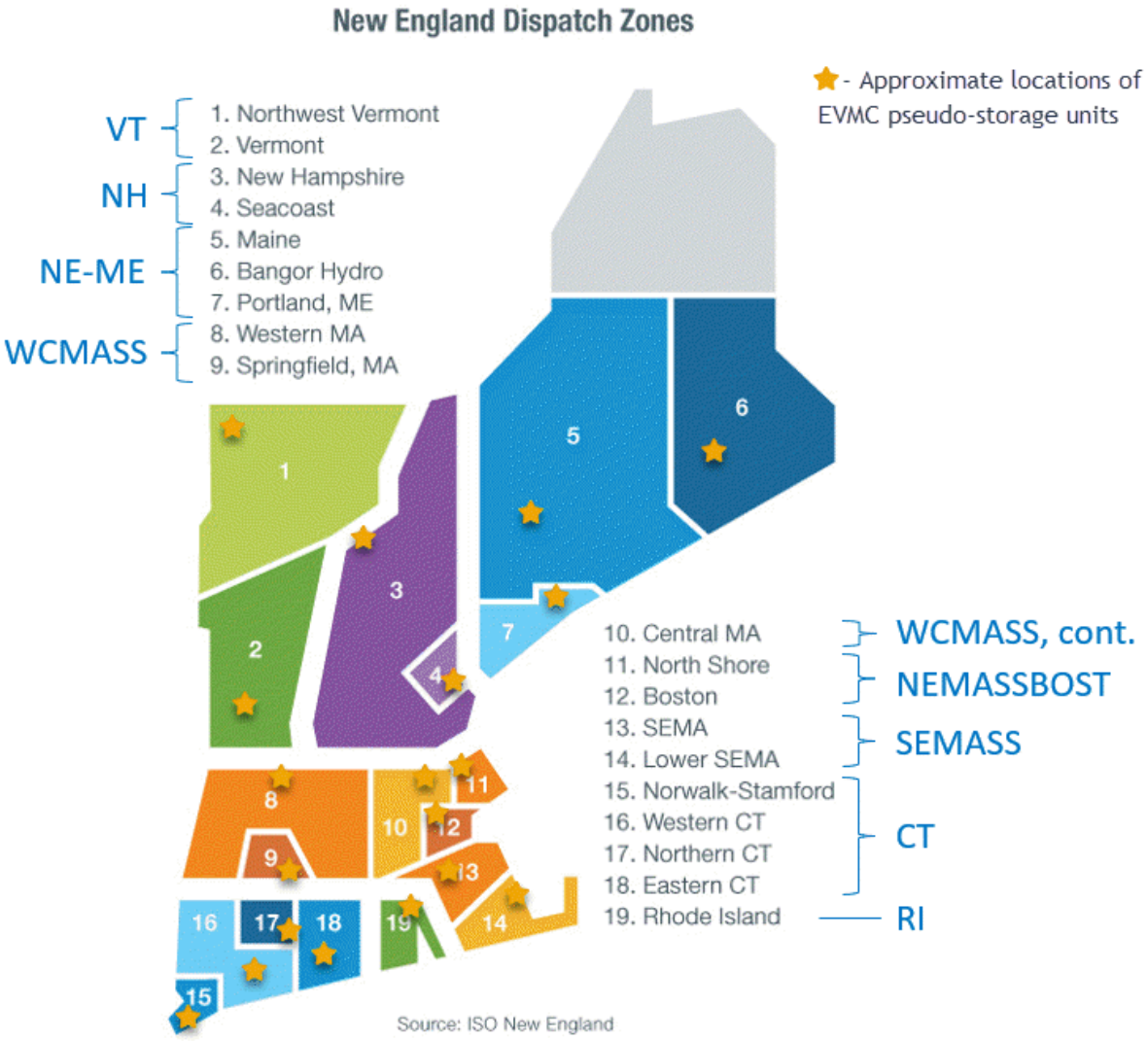

Figure 9. ISO-NE dispatch zones and load regions. ISO-NE's eight load regions are the indicated aggregations of 1–4 dispatch zones. Unmanaged EV load is represented at the load region level and then distributed to all load nodes via participation factors. EVMC flexibility models are represented in the DA PCM at the largest load node per dispatch zone (19 pseudo-storage units; approximate locations shown). In the RT PCMs EVMC outcomes are, as with unmanaged EV load, represented at the load region level and distributed to all load nodes via participation factors.

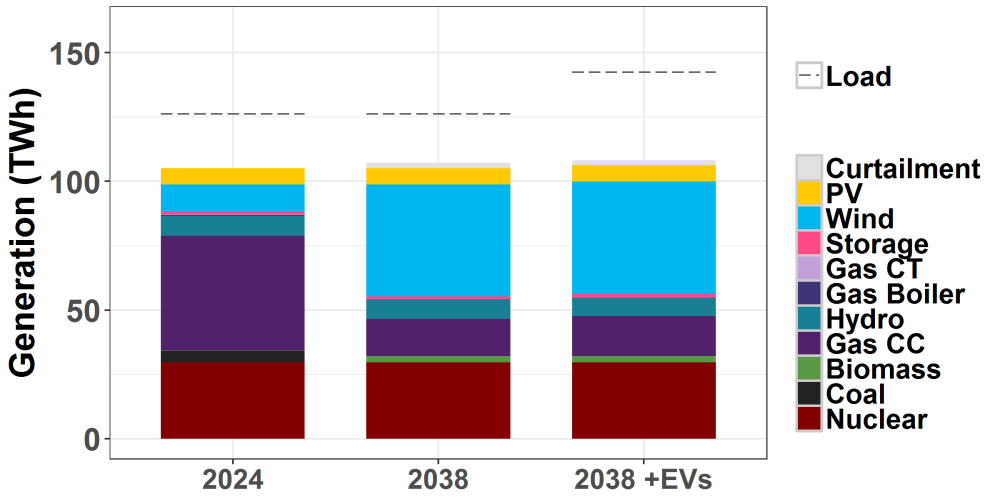

Figure 10. Annual generation in three models of possible future ISO-NE systems: the SEAMS 2024 model, the SEAMS 2038 model (without EV load), and the model used in this study—SEAMS 2038 plus TEMPO 2038 Immediate charging for the All EV Sales by 2035 scenario.

As implied above, we find that additional within-ISO generation resources beyond those included in the ISO-NE PCM isolated from the SEAMS 2038 PCM are not required to support additional EV charging loads in ISO-NE, because the model is able to make more use of available net-imports and gas combined cycle capacity. However, additional intra-regional transmission capacity is warranted. These findings are the end result of a significant model construction and validation effort that started with isolating the ISO-NE subnetwork from the SEAMS model, approximating imports and exports from the full SEAMS model, and turning on the option to model linearized power flow (i.e., DC optimal power flow [DCOPF]; SEAMS used a pipe flow model). Early work with this model exported to the Probabilistic Resource Adequacy Suite confirmed low loss of load expectation (LOLE) even after EV loads were added, which indicated that the model, including fixed import and export schedules, has sufficient generation available to serve all load. However, transmission line limits, which we only enforce on lines at 115 kV and above, were often binding in the 2038 model even before adding EV load.

Because the transmission congestion is attributable to the fact that SEAMS was a national-scale study that used a pipe flow transmission model and only captured inter-regional line limits, we adjust our transmission assumptions to represent a future ISO-NE transmission system upgraded to support new generation and loads. Specifically we increase the transmission capacity of six heavily congested high-voltage transmission lines (115 kV and above) by a total of 658 MW-miles. Via personal correspondence, ISO-NE transmission planners confirmed that all but one of the line increases is realistic, especially in light of ISO-NE's current efforts to rebuild many lines. The one increase in capacity that we apply but might be unrealistic is underground capacity into Boston, which we approximately double to support SEAMS study plant retirements (see additional discussion in Appendix C). Alternative approaches to adding transmission capacity, such as increased efficiency or energy storage resources located in load pockets, could be feasible at lower cost, but are not explored in this study.

We use PLEXOS medium-term (MT) and short-term (ST) optimization horizons to chronologically solve the entire year of day-ahead (DA) and real-time (RT) unit commitment (UC)

and dispatch problems on an hourly basis. In the DA model, MT steps determine daily target volumes for storage and ST steps optimize each day's hourly operations incorporating 6 days of look-ahead at lower temporal resolution (6-hour instead of 1-hour time steps). (We chose 6 days of look ahead for the ST problems to provide satisfactory scheduling of "within-week" EVMC.) Compared to the DA problems, the RT problems fix the commitment status of longer start time thermal generators, and fix the dispatch of pumped hydropower and EV loads. Because of these simplifications, the RT does not require MT solve steps and also does not incorporate look-ahead.[12]

All production costs, including fuel, variable operating and maintenance (VO&M), startup and shutdown costs, and emissions come from SEAMS and are in real 2016 dollars. Burnertip natural gas prices for New England are $8.87/MMBtu based on regionalized 2038 values from the 2017 Annual Energy Outlook (AEO) (EIA 2017). Other fuel prices in are uranium/nuclear ($0.83/MMBtu), wood/biomass ($4/MMBtu), diesel oil ($14.47/MMBtu in New England), and coal ($3.32/MMBtu in New England). A carbon dioxide emissions price of $45/metric ton is applied to all fossil fuel units (Figueroa-Acevedo et al. 2020). Load, wind and solar profiles are time synchronized and use 2012 weather patterns. Days of the week therefore also follow the 2012 calendar, so we show timeseries results using 2012 time stamps. In addition to the marginal costs of generation units, prices in the model are impacted by various penalties that discourage but do not prohibit undesirable conditions such as dump energy, unserved energy (USE), unserved reserves (USR), and violations of thermal line limits. Dump energy penalizes unused generation (e.g., fixed imports) that cannot otherwise be dispatched down nor curtailed at $20/MWh, the penalty for USE (value of lost load in PLEXOS) is $1,000,000/MWh, USR are penalized at $1,500/MWh, and the penalty for violating thermal line limits is $5,000/MWh. Transmission congestion also impacts the dispatch of generators–to the extent that congestion causes higher cost generators to displace lower cost generators both production costs and locational marginal prices (LMPs) are impacted. For example, a line at its thermal limit will have different LMPs at either end as the lower cost generation that is serving marginal load at one node is inaccessible to the node at the other end of the congested line.

To analyze transmission congestion, we compile a "congestion index" by adding up the hourly line flows (in MWh) each multiplied by the absolute difference in hourly price across the line ($/MWh) for an entire year and dividing by 1 million. A higher congestion index thus indicates more value for additional transmission capacity between congested nodes. Although this number technically has units of millions of dollars, it is not an actual cost or revenue, so we report this value as a unit-less index as a basic way to compare degree of congestion across cases.

[12] Although dynamically scheduling hydropower and allowing both hydropower and EVMC to be re-dispatched in the RT could be considered more realistic and economically efficient, in practice storage and demand flexibility dispatch in RT ISO markets and PCMs is challenging given the need to track energy constraints–without some combination of long look-ahead times, accurate energy targets, or lost opportunity cost bidding there is a risk of chasing short-term profit at the expense of long-term feasibility. Because these modeling strategies are either not currently available in our PCM (e.g., accurate RT energy targets, lost opportunity cost bidding) or are computationally expensive and unrealistic (e.g., long RT look-ahead times), we choose to fix storage and storage-like dispatch in the RT and simply use the RT to determine how the rest of the system, excluding hydropower, would respond to accommodate load profiles modified by EVMC.

A final complication in our modeling is the geographic location of both the added EV load and the EVMC resource. TEMPO provides EV charging load at the county level. We map this load to the ISO-NE geography by finding the closest load node to each county's population-weighted centroid. The PCM then provides the mapping from these load nodes to their corresponding dispatch zone and load region (shown in Figure 9). EV baseline load (Immediate charging) is assigned to each load region and then distributed to all load nodes pro-rata with native (non-EV) load. All RT EVMC profiles are also evaluated at this level, that is, regional changes in EV load due to managed charging are computed, added to the original (non-EV plus Immediate charging) regional load, then distributed to all of the load nodes based on load participation factors (fraction of the region's load assigned to each load node within the region). Only when PLEXOS dispatches the aggregate EVMC flexibility resource directly in the DA do the other geographies come into play. In this case, the EVMC resource is represented in PLEXOS as pseudo-storage units at either the per-county node (67 units), the largest load node in each ISO-NE-defined dispatch zone (19 units), or the largest load node in each ISO-NE-defined load region (8 units). In this study, we typically choose to represent PLEXOS-dispatched EVMC at the dispatch zone level (at the locations shown by the stars in Figure 9) because having higher numbers of resources representing EVMC increases computational complexity without meaningfully changing results.

Table 2 summarizes various statistics for the Reference scenario to describe system size, operations, reliability, and costs. Further modeling details are available in Appendix B.

Table 2. Summary of Reference PCM for this Study. Possible future ISO-NE system isolated from the SEAMS 2038 model, with fixed import-export schedule, additional transmission capacity, linearized power flow, and TEMPO 2038 All EV Sales by 2035 Immediate EV charging load.

Category	Metric	Value	Units
Capacity	Generation	46.7	GW
	Pumped Hydropower Storage	858	MW
	Pumped Hydropower Storage	8,460	MWh
Generation	Annual Load[a]	142.7	TWh
	Annual Generation	106.3	TWh
	Annual Storage Losses	0.5	TWh
	Annual Net Imports	36.4	TWh
	Annual VG[b]	50.0	TWh
	Annual RE Generation[c]	59.6	TWh
	Annual Clean Generation[d]	89.3	TWh
	Annual Curtailment	5.0	TWh
	Peak Load[e]	28.9	GW
	Time of Peak Load	July 17 5p.m.–6 p.m. ET	
	Net-Peak Load[f]	20.8	GW
	Time of Net-Peak Load	Aug 24 7 p.m.–8 p.m. ET	
Reliability	Congestion Index[g]	158.9	
	Unserved Reserves (USR)	10.9	MWh
	Unserved Energy (USE)	0	MWh
Costs	Annual System Cost (incl. \$45/ton CO_2)	1.933	billion \$2016
	Annual System Cost (excl. emissions)	1.647	billion \$2016
	Annual Fuel Cost	1.437	billion \$2016
	Annual VO&M Cost	0.117	billion \$2016
	Annual Start & Shutdown Cost	0.092	billion \$2016
	Emissions	6.37	million metric tons CO_2
	Average Load-weighted LMP	46.5	\$/MWh
	Peak Load-weighted LMP	1477.2	\$/MWh
	Time of Peak Load-weighted LMP	Jan 5 8 p.m.–9 p.m. ET	\$/MWh

[a] ISO-NE load, including EV charging load and storage losses. Excludes exports.
[b] VG includes wind and PV.
[c] RE generation includes wind, PV, hydropower, and biomass.
[d] Clean generation includes wind, PV, hydropower, biomass, and nuclear
[e] Peak load is the maximum hourly load considering ISO-NE native load (inclusive of unmanaged EV charging) and storage losses
[f] Net-peak load is the maximum hourly value of load as defined for peak load minus VG
[g] Congestion Index is calculated by adding up the hourly line flows (in MWh) each multiplied by the absolute difference in hourly price across the line (\$/MWh) for an entire year and dividing by 1 million. Line limits are only enforced on lines $\geq$115kV, thus those are the only lines that can induce price differences between connected nodes.

4 Managed Charging

Scheduling EV charging can reduce bulk power system capacity, generation, and transmission costs by better aligning electricity load with electricity supply in both time and space. In this study, we estimate the value of these services under the assumptions of ubiquitous charging (EVs are plugged in whenever they are not driving) and fixed mobility service (all trips completed on time and with maximum electricity miles for PHEVs). We first develop charging flexibility models for individual vehicles and then aggregate them to create MW-scale, battery-like *flexibility resources* suitable for large-scale bulk power system models. In the end, the amount of resource available to provide grid services depends on the number of participating vehicles and whether a grid operator directly dispatches an aggregate, MW-scale resource (DLC) or individual vehicles respond to time-varying prices (RTP or TOU).

4.1 Individual Vehicle Charging Flexibility

We parameterize vehicle-level EVMC based on charging strategies that bound when each sample vehicle can charge while respecting charger capacity limits and preserving mobility service (i.e., all trips can be completed as long as actual charging falls "between" that of the two bounding cases and during times when the vehicle is idle). The Immediate charging strategy consists of plugging in immediately after every trip and charging until the battery is full or the next trip begins, whichever comes first. This strategy maximizes state of charge (SOC) and vehicle range at all times. Because this strategy maximizes the potential for mobility service and minimizes range anxiety, this is the strategy we use to create the unmanaged charging profile (Figure 8) that is included in the Reference scenario (chapter 3). The Immediate strategy is also the charge-as-early-as-possible bounding case for both within-session and within-week charging flexibility. To form the as-late-as-possible bounding case for within-session flexibility, the Delayed charging strategy is simulated for each sample vehicle. This strategy delivers the same amount of energy to each vehicle during each charging session (every time the vehicle is parked) as the Immediate strategy, but it delays the start of charging as long as possible. Creating an as-late-as-possible bounding case for within-week charging flexibility is more complex. Again we ensure that the same amount of energy is delivered, this time over the course of a week, and that each EV has sufficient SOC to complete all prespecified trips, but instead of using all possible charging sessions, a minimum number of charging sessions are selected and the energy delivered during those sessions is delayed as long as possible using a linear programming formulation (details available in Appendix A). The three major charging strategies implemented in TEMPO and used in this study are summarized in Table 3.

Table 3. Charging Strategies that Bound Flexibility while Preserving Mobility Service

Charging Strategy	Representative of	Timing	Frequency	Typical Occurrence	SOC
Immediate	Unmanaged charging; Bound that describes earliest charging (P_1)	Start charging as soon as car is parked	Every time the car is parked after a trip	Immediately after each trip	Charge to maximum or until next trip, whichever is first
Delayed	As-late-as-possible bound for within-session managed charging ($P_{2,S}$)	Maximum delay of charging constrained to deliver the same energy as Immediate during each charging session	Every time the car is parked after a trip	Immediately before each trip	Same SOC as Immediate at end of session
Min Charges and Delayed	As-late-as-possible bound for within-week managed charging ($P_{2,W}$)	Fewest charging sessions over the week holding mobility service constant; Charging delayed to end of selected sessions	Minimum charging sessions per week	Before and after long trips	Determined by a linear program; same energy delivered per week as Immediate

Figure 11 depicts an example set of charging profiles for a single vehicle over a single week. Focusing first on the Immediate and Delayed profiles we see that the SOC for this vehicle stays fairly high (above 80%), and flexibility in timing only appears when an Immediate charging session results in 100% SOC prior to the next trip. Moving to the EV charging flexibility envelope created by Immediate paired with Min Charges & Delayed, that combination results in a much larger set of possible vehicle SOCs over the week, represented by the area between the blue and teal lines. Min Charges & Delayed drops to below 20% SOC for roughly a day during the week. Nevertheless, the vehicle gets back to its initial SOC by the end of the week, fulfilling the Min Charges & Delayed constraint that all energy used during travel is replenished each week.

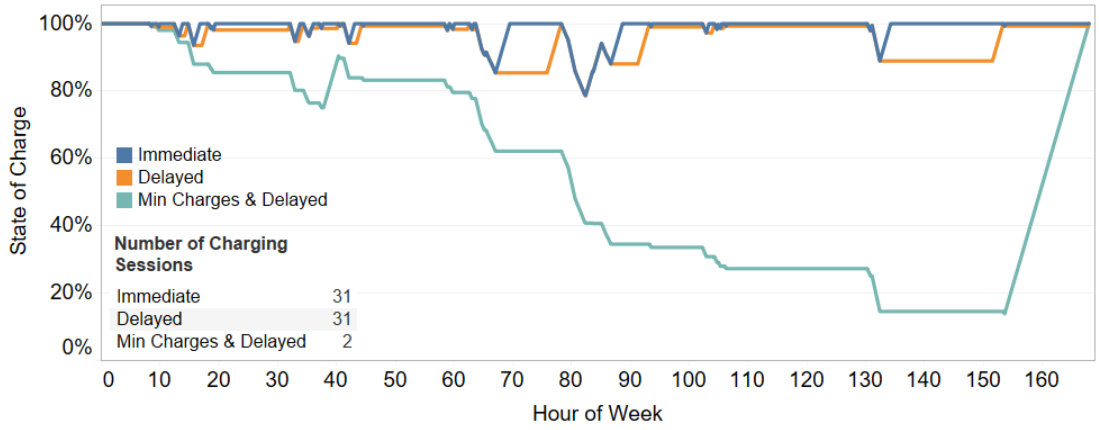

Figure 11. Example of all charging strategies for a single vehicle-week. Trips are indicated by falling SOC; increasing SOC indicates charging. There are 31 charging sessions under the Immediate and Delayed strategies and 2 under Min Charges & Delayed.

Given two charging profiles, $P_1(t)$ and $P_2(t)$, that describe the earliest and latest possible charging, respectively, along with the maximum charging capacity profile, $\overline{P}(t)$, that is zero when the vehicle is not plugged in and equal to the charger power otherwise, we construct a battery-like model of charging flexibility for each vehicle modeled by TEMPO. In general, the battery SOC

$S(t)$ evolves as

$$S(t) = S(t-1) + P(t)\delta t - E(t)\delta t \tag{4.1}$$

where we are assuming a right-hand rule time discretization with time step δt, $P(t)$ is the charging power, and $E(t)$ is the energy lost through driving. (Note that to be fully realistic we would also track the charging efficiency over time, because the conversion rate between electricity consumed and increased vehicle SOC varies by charger type and even within charging sessions. However, in this study we make the simplifying assumption that all chargers are equally efficient and only track electricity consumption.) Taking $P_1(t)$, the earliest possible charging profile, as the baseline, we model charging flexibility as the difference between what actually happens and this baseline charging assumption. That is, $E(t)$ is fixed, the baseline SOC is

$$S_1(t) = S_1(t-1) + P_1(t)\delta t - E(t)\delta t \tag{4.2}$$

and we define

$$\Delta P(t) = P(t) - P_1(t) \tag{4.3}$$
$$\Delta S(t) = S(t) - S_1(t). \tag{4.4}$$

Subtracting Equation 4.2 from Equation 4.1 we obtain the evolution equation for an individual vehicle's charging flexibility:

$$\Delta S(t) = \Delta S(t-1) + \Delta P(t)\delta t. \tag{4.5}$$

However, vehicle charging is not infinitely flexible. We must set bounds on $\Delta P(t)$ and $\Delta S(t)$. The power bounds are derived from

$$0 \leq P(t) \leq \overline{P}(t), \tag{4.6}$$

that is,

$$\underline{\Delta P}(t) = -P_1(t) \leq \Delta P(t) \leq \overline{P}(t) - P_1(t) = \overline{\Delta P}(t). \tag{4.7}$$

The energy bounds are derived from

$$S_2(t) \leq S(t) \leq S_1(t), \tag{4.8}$$

where $S_1(t)$ is defined in Equation 4.2 and $S_2(t)$ is likewise defined as

$$S_2(t) = S_2(t-1) + P_2(t)\delta t - E(t)\delta t, \tag{4.9}$$

where $P_2(t)$ is the as-late-as-possible charging profile. We then see that

$$\underline{\Delta S}(t) = S_2(t) - S_1(t) \leq \Delta S(t) \leq 0 \tag{4.10}$$

and $\underline{\Delta S}(t)$ evolves as

$$\underline{\Delta S}(t) = \underline{\Delta S}(t-1) + (P_2(t) - P_1(t))\delta t, \tag{4.11}$$

which is sufficient to set the $\underline{\Delta S}(t)$ profile as soon as its value is fixed for one specific time. Certainly, any time where $S_2(t) = S_1(t)$ is convenient for this purpose. In our modeling, this occurs at the end of every TEMPO-modeled week, such that the flexibility dispatch returns

the fleet to baseline conditions every 168 hours (time step δt=1 hour) and $\underline{\Delta S}$ only needs to be tracked over the course of each week.

To demonstrate this model of individual vehicle charging flexibility, we apply it to the example profiles shown in Figure 11 to create a within-session (S) flexibility model and a within-week (W) flexibility model, and then dispatch those two models to minimize charging costs assuming that energy prices follow the corresponding DA locational marginal price (LMP) profile from our Reference PCM. (Optimal dispatch formulation details are provided in Appendix E.) The resulting SOC profiles are shown along with the as-soon-as-possible and as-late-as-possible bounds in Figure 12.

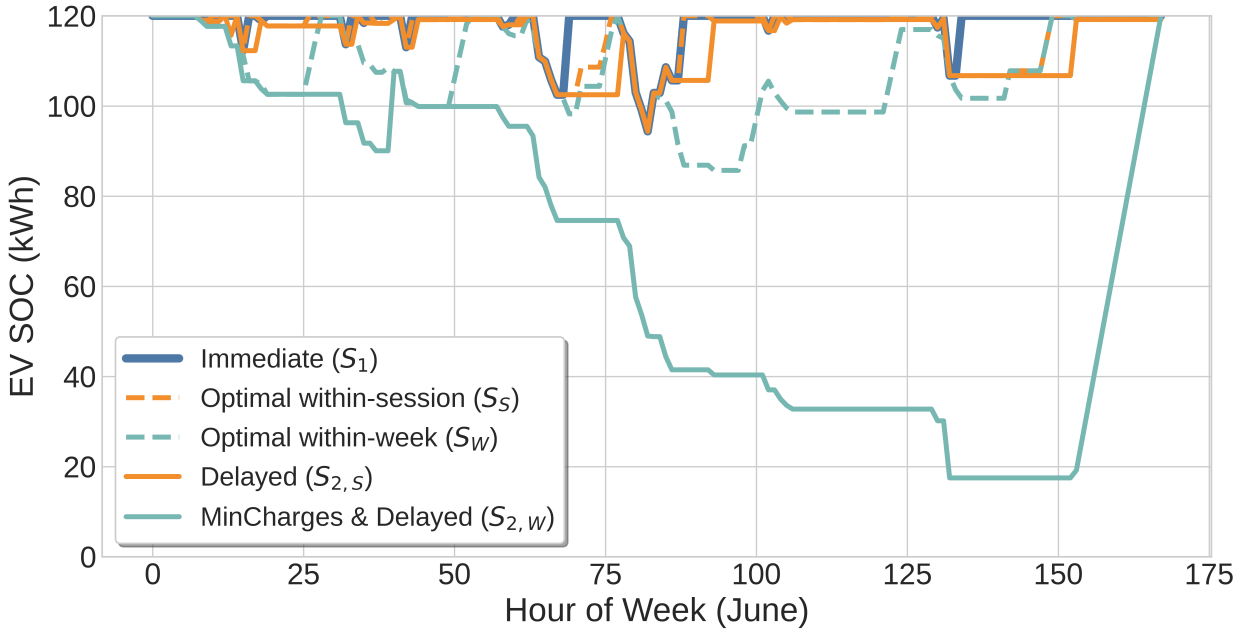

Figure 12. Example optimal and bounding SOC profiles for a single vehicle week. Compared to Figure 11, vehicle charging has been scheduled to minimize costs relative to an RTP. Three types of profiles are shown: baseline (Immediate $= S_1$), delayed (Delayed $= S_{2,S}$; Min Charges & Delayed $= S_{2,W}$), and minimum charging cost (Optimal within-session $= S_S$; Optimal within-week $= S_W$).

By design, the optimal within-session profile still contains 31 charging sessions (as do the Immediate and Delayed profiles), however, the timing of charging is selected to align with lower cost times. For example, the optimal within-session profile charges in the lowest price subset of the 71st-76th hours, with a pause in the middle but still returning to full SOC by the end of the session. The optimal within-week profile avails itself of its larger range of options, engaging in 23 charging events at a total cost of $1.23 for this vehicle-week compared to $7.48 for the optimal within-session profile and $10.24 for the Immediate charging strategy.

4.2 Aggregate Charging Flexibility

The most accurate way to model charging flexibility is to explicitly constrain charging for each EV. However, accuracy comes at a computational cost that is not practical in all situations. Considering least-cost bulk power system UC and dispatch as implemented in, for example, PLEXOS

and software used by ISOs, it is not possible to directly optimize the charging of individual vehicles. The number of vehicles, thousands to millions, is orders of magnitude larger than the tens to hundreds of generating units, and the size of vehicle charging loads, on the order of kW, is orders of magnitude smaller than the injections into and out of transmission buses, which are at the MW scale. Resolving the dispatch of millions of resources of vastly different sizes to the tolerance levels required to give clear instructions to all resources is simply not possible today within reasonable time frames. Furthermore, ISO software typically does not even allow for resource offers in increments smaller than 0.1 MW–the next decimal point of precision is not accepted by the software. In both system operations and our PCM, EV charging flexibility must currently be represented as a storage-like aggregate of hundreds-to-thousands of vehicles, at a MW-scale.

Starting from the model of individual charging flexibility developed in the previous section:

$$\Delta S_k(t) = \Delta S_k(t-1) + \Delta P_k(t)\delta t \tag{4.12}$$

$$\underline{\Delta P_k}(t) = -P_{k,1}(t) \leq \Delta P_k(t) \leq \overline{P_k}(t) - P_{k,1}(t) = \overline{\Delta P_k}(t) \tag{4.13}$$

$$\underline{\Delta S_k}(t) = S_{k,2}(t) - S_{k,1}(t) \leq \Delta S_k(t) \leq 0 \tag{4.14}$$

$$\underline{\Delta S_k}(t) = \underline{\Delta S_k}(t-1) + (P_{k,2}(t) - P_{k,1}(t))\delta t, \tag{4.15}$$

where we have added a subscript k to denote individual vehicles k in the set $\mathbb{K}$ of all participating vehicles, an obvious construction of aggregate flexibility is:

$$\Delta S(t) = \Delta S(t-1) + \Delta P(t)\delta t \tag{4.16}$$

$$\underline{\Delta P}(t) = \sum_{k\in\mathbb{K}} \underline{\Delta P_k}(t) \leq \Delta P_k(t) \leq \sum_{k\in\mathbb{K}} \overline{\Delta P_k}(t) = \overline{\Delta P}(t) \tag{4.17}$$

$$\underline{\Delta S}(t) = \sum_{k\in\mathbb{K}} \underline{\Delta S_k}(t) \leq \Delta S(t) \leq 0, \tag{4.18}$$

which we refer to as the *outer approximation* (OA) of aggregate flexibility.

But how accurate is this outer approximation? If the actual flexibility of the vehicles $\mathbb{K}$ is represented by the set

$$\mathbb{P}_{\mathbb{K}} = \left\{ \sum_{k\in\mathbb{K}} \Delta P_k(t) \,\middle|\, \text{exists } \Delta S_k(t) \text{with (4.12) to (4.15) satisfied for all } k \in \mathbb{K} \right\}, \tag{4.19}$$

how does the set of feasible outer approximation profiles

$$\overline{\mathbb{P}} = \{ \Delta P(t) | \text{exists } \Delta S(t) \text{with (4.16) to (4.18) satisfied} \} \tag{4.20}$$

compare? Extending the work of Hao et al. (2015) we show in Appendix C that $\mathbb{P}_{\mathbb{K}}$ is a subset of $\overline{\mathbb{P}}$, that is, every aggregate trajectory that can feasibly arise from the individual vehicles is feasible for the outer approximation model. Thus the set $\overline{\mathbb{P}}$ is at least as large as $\mathbb{P}_{\mathbb{K}}$ and is likely larger. How much larger? We can develop an intuition by computing an outer approximation for a modest number of vehicles and dispatching both the aggregate and the individual flexibility models against the same hourly prices. Then, we can observe to what extent the sum of the individually-optimized profiles does or does not align with the optimal dispatch of the outer approximation.

Figure 13 depicts such an example analysis created from 475 sample vehicle profiles (totalling 3.02 MW of charging load on average, after sample weights are applied) with within-session flexibility. The top plot shows the price signal against which the individual flexibility models (blue lines) and the outer approximation (OA) aggregate flexibility model (pink lines) are dispatched. The black lines show the bounds for the OA model. As expected, the aggregate model (pink lines) stays within these bounds and is often actively constrained by them. The optimization formulation incentivizes reducing charging load as much as possible when prices are high and satisfying the overall energy demand as much as possible when prices are low. Both power and energy bounds work together to determine exactly what "as much as possible" means at any given time. The sum of the individual dispatch results (blue lines) also stays within these bounds but is not typically hitting them. Because the individual vehicles are optimized using the same cost minimization objective as the aggregate flexibility model and the corresponding annual cost savings for the individual dispatch is only \$494M compared to \$740M for the aggregate dispatch, this implies that while the individual optimal profiles are feasible for the OA aggregate model, the aggregate dispatch is not actually feasible if requested from individual vehicles. That is, we have verified that $\mathbb{P}_{\mathbb{K}} \subset \overline{\mathbb{P}}$ and have also identified a significant feasibility gap ($\overline{\mathbb{P}}$ is strictly larger than $\mathbb{P}_{\mathbb{K}}$) arising from the fact that the aggregate model can unrealistically pair, e.g., one already-fully-charged vehicle's ability to increase load with another already-charging vehicle's ability to accept more charge, effectively requesting a charging rate that is infeasible for the latter vehicle.

Hao et al. (2015) also suggests a way to address this issue of the outer approximation being a strict overestimate of aggregate flexibility. Instead of constructing a model of the form

$$\Delta S(t) = \Delta S(t-1) + \Delta P(t)\delta t \tag{4.21}$$

$$\underline{\Delta P}(t) \leq \Delta P_k(t) \leq \overline{\Delta P}(t) \tag{4.22}$$

$$\underline{\Delta S}(t) \leq \Delta S(t) \leq 0 \tag{4.23}$$

that overestimates actual flexibility, one can determine values of $\underline{\Delta P}(t)$, $\overline{\Delta P}(t)$ and $\underline{\Delta S}(t)$ that allow a proof that the set

$$\underline{\mathbb{P}} = \{\Delta P(t) | \text{exists } \Delta S(t) \text{with (4.21) to (4.23) satisfied}\} \tag{4.24}$$

is an under-approximation of flexibility, that is, that $\underline{\mathbb{P}} \subset \mathbb{P}_{\mathbb{K}}$. Such a model is an *inner approximation*, and any dispatch request made of it is feasible. Therefore, a grid model could safely use such a representation of EVMC and expect the aggregator to be able to fulfill the resulting dispatch request.

Unfortunately, readily constructed inner approximations for time-varying load flexibility (including EVMC) are overly conservative. The construction presented by Hao et al. (2015) assumes that the aggregate dispatch signal will be shared out to all of the contributing resources based on constant fractions β_k and then sets the aggregate bounds in a worst-case sense. That is,

$$\underline{\Delta P_k}(t) \leq \beta_k \underline{\Delta P}(t) \leq \Delta P_k(t) \leq \beta_k \overline{\Delta P}(t) \leq \overline{\Delta P_k}(t) \tag{4.25}$$

$$\underline{\Delta S_k}(t) \leq \beta_k \underline{\Delta S}(t) \leq \Delta S_k(t) \leq 0 \tag{4.26}$$

for all vehicles $k \in \mathbb{K}$ and for all times t. In the case of a time-varying resource like EVMC providing a temporally-linked grid service like energy shifting, this construction generally leads to

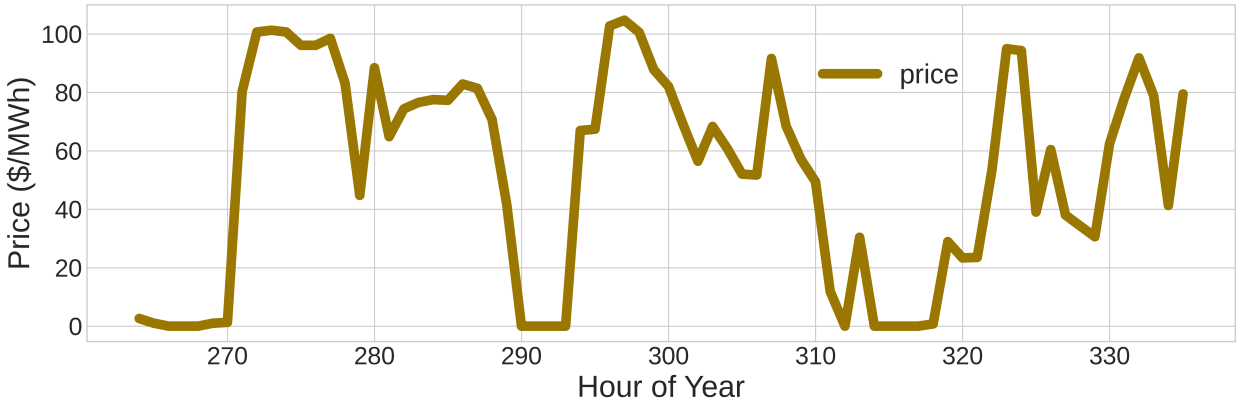

(a) Energy prices

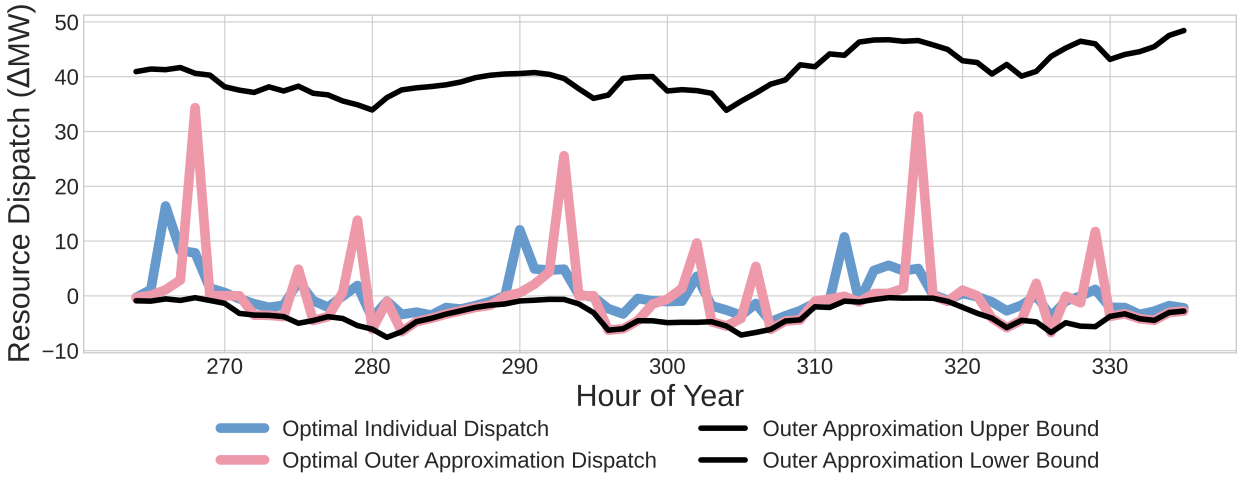

(b) Charging power profile differences from baseline (ΔP)

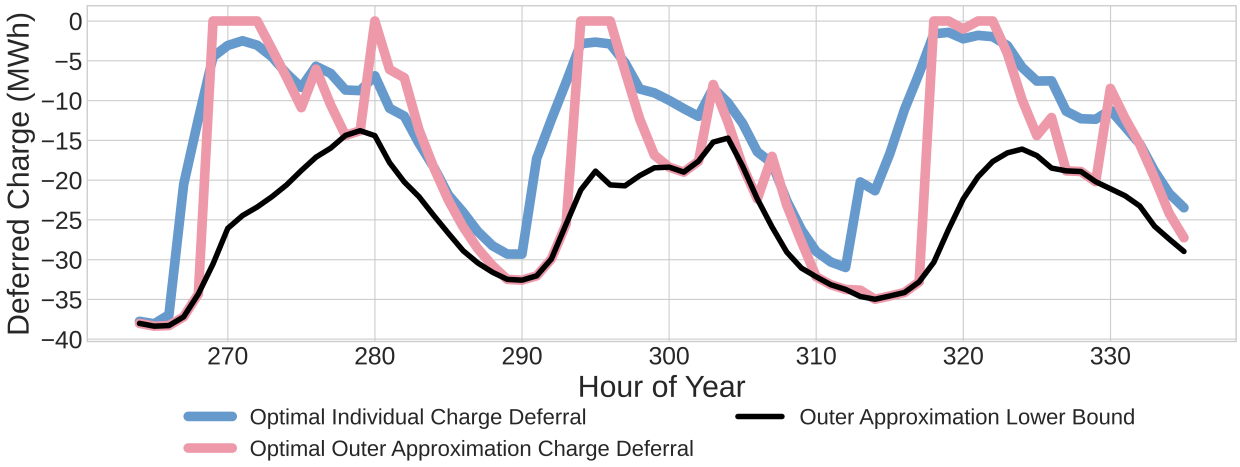

(c) Cumulative delivered charging energy differences from baseline (ΔS)

Figure 13. Optimal dispatch of one outer approximation aggregate resource compared to the aggregated result of optimally dispatching the 475 comprising vehicles individually. This example shows three days of optimal dispatch for one county's TEMPO data.

inner approximations that are too conservative. That is, so much of the flexibility resource is lost to the aggregation process that the gain of provable dispatchability is not sufficient to overcome the loss of potential value (Hale et al. 2022). It might be possible to construct a better type of inner approximation e.g., with time-varying β_k or by relaxing the dispatchability requirement to a high probability of dispatchability rather than an absolute requirement, but as of this writing the authors do not know of such a construction.

We therefore propose to heuristically scale the outer approximation to achieve better outcomes. That is, instead of using the bounds Equation 4.17 and Equation 4.18 directly, we apply scaling factors to the minimum power bound (f_1), the maximum power bound (f_2), and the minimum SOC bound (f_3):

$$f_1 \sum_{k \in \mathbb{K}} \underline{\Delta P_k}(t) \leq \Delta P_k(t) \leq f_2 \sum_{k \in \mathbb{K}} \overline{\Delta P_k}(t) \tag{4.27}$$

$$f_3 \sum_{k \in \mathbb{K}} \underline{\Delta S_k}(t) \leq \Delta S(t) \leq 0, \tag{4.28}$$

and the scaled outer approximation (SOA) model is then defined by Equations 4.16, 4.27, and 4.28.

To define the values of f_1, f_2 and f_3 we perform re-dispatching experiments where, for a set of participating vehicles $k \in \mathbb{K}$ we:

1. Construct a number of SOA models by computing the OA model and then specifying different values for f_1, f_2 and f_3.
2. Compute a dispatch profile for each SOA model by minimizing charging costs using an RTP profile.
3. Dispatch the individual resources $k \in \mathbb{K}$ to minimize the mean absolute error (MAE) between the aggregate dispatch from Step 2 and the aggregated individual resource dispatch, subject to individual vehicle-level constraints (Equation 4.12 to Equation 4.15). (Formulation specified in Appendix E.)
4. Evaluate the quality of the individual dispatch in terms of (a) an error metric and (b) estimated net revenue of managed charging, assuming that the aggregator would have to settle deviations from requested dispatch at the same RTP.

Because it is expensive and computationally challenging to perform Step 3 (optimal disaggregation of individual resources of an aggregate dispatch request), in this study we estimate scaling parameters using a moderately-sized example. Specifically, we analyze the aggregation and dispatch for the same data set used for Figure 13, i.e., 475 sample EVs from a single county representing an annual charging load (including distribution losses) of 26.5 GWh. The SOA aggregate charging flexibility from these vehicles is computed for 125 different combinations of f_1, f_2 and f_3 values–every combination of each parameter being set to 0.2, 0.4, 0.6, 0.8, or 1.0. The SOA models are then dispatched as price-takers against the 8,760-hour DA regional RTP from the Reference scenario and the individual vehicles' dispatch is optimized to fulfill those requests with minimum MAE. The experiment thus consists of 125 pairs of optimal SOA aggregate and disaggregated-and-then-summed individual dispatch profiles to compare in terms of net revenue

(i.e., charging cost savings relative to the Immediate, unmanaged charging strategy, measured using the DA RTP) and MAE.

Figure 14 shows the results of the experiment for within-session flexibility. The left plot (Figure 14a) shows the gross net-revenue achieved by the price-taking dispatch of the SOA models, which are ignorant of the individual vehicle charging constraints, versus the mean absolute error (MAE) between the optimized SOA dispatch and what the individual vehicles are actually able to do when they try to fulfill the aggregate request. The dashed line on that plot depicts the net revenue that results from directly dispatching the individual vehicle flexibility models against the same price profile—the fact that some of the SOA points are above this line indicates that those SOA models are producing infeasible (from an individual vehicle perspective) dispatch requests. That said, just because an SOA point is below the individual net revenue line does not mean that its dispatch is strictly feasible. Indeed, MAE varies from near zero to up to 1.53 MW (about 50% of the average load of 3.02 MW), and high dispatch error is observed for many combinations of scaling factors both above and below the dashed line.

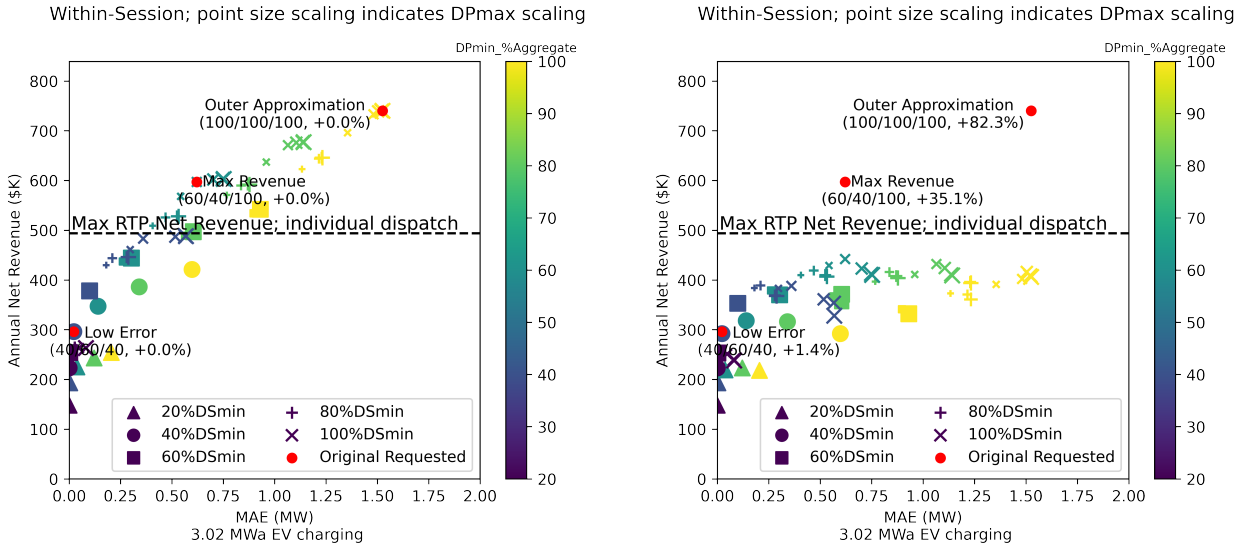

(a) Gross net-revenue for the SOA dispatch profile

(b) Actual net revenue after dispatching individual vehicle charging flexibility to minimize MAE between actual and SOA-requested dispatch

Figure 14. Within-session charging flexibility disaggregation experiment. Both subfigures plot net-revenue versus disaggregation MAE and indicate scaling parameter combinations selected for subsequent analysis with red dots. Annotations list $f_1/f_2/f_3$ multiplied by 100 and the percentage by which gross net-revenues for the annotated points exceed plotted net revenues.

The plot on the right (Figure 14b) shows the net revenue for the aggregation based on the individual charging profiles that result from disaggregating the dispatch requested of the SOA resources. That is, instead of computing net revenue for the SOA dispatch profile, we compute the individual dispatch profiles that best match that aggregate request and then settle out the charging costs based on the price profile. Once we do this, we see that the least-scaled SOA models, by over-promising as an aggregate, produce less revenue than many of the more-scaled SOA models. For the purpose of this study, we draw attention to two specific models on the non-dominated Pareto front of error minimization and net revenue maximization. First, the model with maximum

revenue (MR) for within-session flexibility has $f_1 = 0.6$, $f_2 = 0.4$, and $f_3 = 1.0$. This SOA MR model has significant disaggregation error, around 0.62 MW MAE, but the errors in its favor (i.e., when the vehicles dispatch more in the low price times and less in the high price times than the SOA model predicted) more than make up for the errors that cause it to pay more for charging than expected (i.e., when the vehicles dispatch less in the low price times and more in the high price times than the SOA model predicted), as compared to, e.g., more-scaled models with lower MAE. Second, there are SOAs with very low MAE that achieve net-revenue up to two-thirds of the MR SOA. The highlighted low-error (LE) model has $f_1 = 0.4$, $f_2 = 0.6$, and $f_3 = 0.4$, 0.02 MW MAE, 66% of the MR SOA revenues and 59% of the individually optimized net-revenues. In what follows, we use slightly adjusted versions of these SOA scaling parameters to define within-session MR and LE models. We also estimate "revenue ratios," defined as actual net-revenue divided by gross net-revenue as measured in this experiment, and use them to discount production cost savings results in chapter 5. For example, the revenue ratio we used to adjust OA production cost results for within-session flexibility is 0.55 (gross net-revenue is 82.3% higher than actual net-revenue). The actual scaling parameters and revenue ratios used in what follows are listed in Table 4.

Similar results are presented for within-week flexibility in Figure 15. The results are directionally similar, but the MR and LE SOAs have different optimal scaling factors in this case compared to within-session flexibility. MAE can also be much higher. The scaling parameter for $\underline{\Delta P}$, i.e., f_1 appears to be most important–all of the points that produce gross net revenue estimates above what is achievable by directly dispatching the individual vehicles have f_1 equal to 1.0 or 0.8, and the MR point has $f_1 = 0.8$. The full definition of the MR point is $f_1 = 0.8$, $f_2 = 0.6$, and $f_3 = 0.8$, which has less scaling of $\underline{\Delta P}$ (f_1) and more scaling of $\underline{\Delta S}$ (f_3) as compared to the within-session MR SOA. Figure 15b also shows that many SOA models are able to achieve very low error for within-week flexibility. A common theme of low-error within-week scaling is approximately halving both f_1 and f_3. The specific LE point called out in Figure 15 is $f_1 = 0.6$, $f_2 = 0.2$, and $f_3 = 0.6$, but consistent with within-session, slightly modified values for both MR and LE are chosen for use in chapter 5, see Table 4. For within-week flexibility, the revenue ratio for the OA model is 0.58 (gross net-revenue is 72.7% higher than actual net-revenue).

4.3 Resource Summary and Dispatch Mechanisms

As an upper bound, in this study we consider the case in which all charging other than DCFC for all 5.3 million modeled light-duty passenger vehicles is flexible. That amounts to assuming that up to 12.0% (17.1 TWh with losses) of the system's 142.2 TWh of total load could be shifted in time to occur later than what is simulated by the Immediate charging strategy. Based on our ubiquitous charger assumption, the flexibility in terms of power consumption is the same for within-session and within-week flexibility: only load in the Immediate charging profile can be reduced, and the maximum possible gain in load is equivalent to the amount of charger capacity that is accessible (because a car is parked) but unused (because the car is no longer charging) under the Immediate charging strategy. The ability to delay load, however, differs depending on the flexibility type.

Figure 16 shows what the outer approximation of the flexible resource looks like for one week in June under both within-session and within-week assumptions. Per Figure 16a, the June baseline charging that can potentially be delayed varies between about 300 MW at 4 a.m. to 5 a.m. local

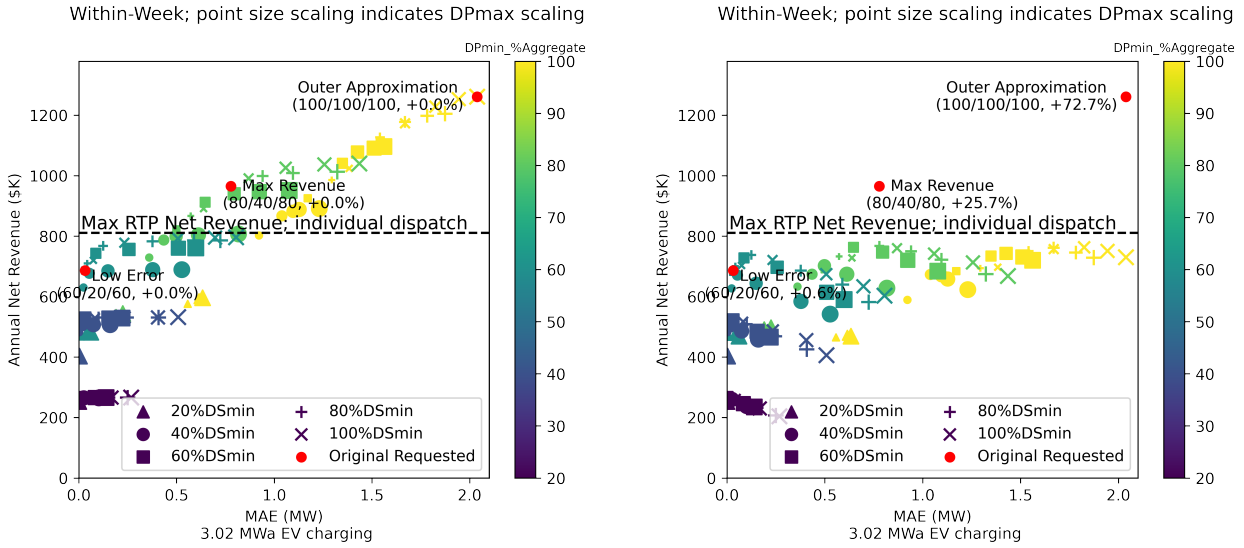

(a) Gross net-revenue for the SOA dispatch profile

(b) Actual net revenue after dispatching individual vehicle charging flexibility to minimize MAE between actual and SOA-requested dispatch

Figure 15. Within-week charging flexibility disaggregation experiment. Both subfigures plot net-revenue versus disaggregation MAE and indicate scaling parameter combinations selected for subsequent analysis with red dots. Annotations list $f_1/f_2/f_3$ multiplied by 100 and the percentage by which gross net-revenues for the annotated points exceed plotted net revenues.

time and 3.4 GW in weekday evening hours. Monthly baseline charging minimums are 300 MW (May) to 380 MW (February) and maximums are 3.2 GW (May) to 4.0 GW (February). On average, passenger vehicles are parked about 95% of the time; this combined with our ubiquitous charger assumption results in available charging capacity being more than 6 times actual charging at all times of day. Figure 16b shows that the Immediate charging strategy keeps the ISO-NE fleet's batteries mostly full all of the time. The aggregate Delayed (within-session) SOC bound at most reduces the fleet's charging level by 21 GWh or 5.5%. The within-week OA flexibility resource provides significantly more energy capacity–up to 114 GWh (30%) at the point of widest difference. The shape of the MinCharges & Delayed SOC (within-week) bound also demonstrates a potential improvement for future work–the gradual loosening and then sudden tightening of the SOC bound at the beginning and end of the week, respectively, is a modeling artifact of the combined TEMPO and dsgrid-flex workflow. In summary, as modeled in this study the EVMC resource is on the order of 0.09 kW/vehicle to 0.66 kW/vehicle (500 MW to 3.4 GW for the 2038 ISO-NE model) in power capacity and up to 4.0 kWh/vehicle to 21.5 kWh/vehicle (21 GWh to 114 GWh for the 2038 ISO-NE model) in energy capacity, the latter depending on whether charging is being scheduled on per-session or weekly timescales.

The resource shown in Figure 16 is an overestimate of flexibility for several reasons, two of which we explore further in the results that follow. First, it is not going to be the case that all vehicles will participate in EVMC programs all the time. In this study we capture that fact through participation rates, which we model by randomly selecting sample vehicles to include in the flexibility modeling until the sum of their sample weights represents a desired percentage of the total number of vehicles. Second, we saw above that not all load profiles that are feasible for the outer

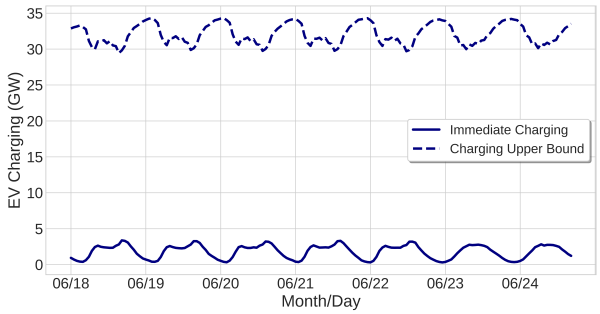

(a) Immediate (baseline) charging and upper bound on hourly EV charging. For the OA model minimum charging is 0 GW in all hours.

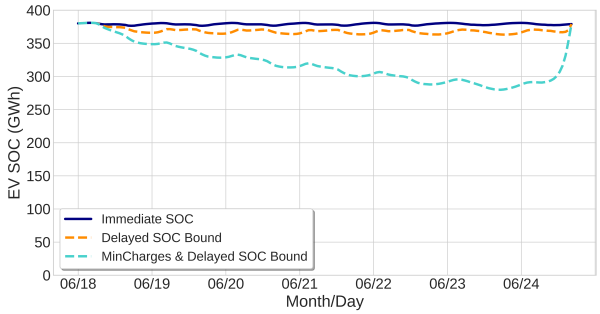

(b) Baseline (Immediate) and minimum SOC bounds for all vehicles for within-session (Delayed) and within-week (MinCharges & Delayed) flexibility

Figure 16. Outer approximation power and SOC bounds for all ISO-NE modeled vehicles (i.e., 5.3 million EVs) for one week in June

approximation are feasible once the individual vehicle constraints are considered. In what follows we address this concern by modeling three different dispatch mechanisms, some of which have additional variants.

The dispatch mechanisms used to schedule managed EV charging in this study are summarized in Table 4. RTP allows individual vehicles to respond directly to the hourly prices forecast by the Reference scenario DA model (with unmanaged EV charging). We dispatch vehicles against an ISO-NE system average RTP, computed as the load-weighted average of the eight regional price profiles. TOU similarly allows individual vehicles to respond directly, but to a much coarser price signal that varies with seasons and time blocks. In this study the TOU rates are designed to match the system-level RTP as well as possible in a least-squares sense, using a specified number of seasons and blocks and subject to the TOU tariff recovering at least as much revenue as RTP under baseline load conditions. Seasons are contiguous sets of days and are subject to a minimum length constraint. Blocks are contiguous hours within days, are also subject to a minimum length constraint, and are defined differently for weekdays and weekend days. As described in more detail in Appendix D, we find the optimal TOU formulation challenging to solve even with commercial solvers and we obtain better objective function values by applying agglomerative clustering[13] to the RTP profile to create TOU rates. In this study we present results for two different TOU rates: TOU-1-2 with one season and two blocks, and TOU-4-4 with four seasons and four blocks (definitions available in Appendix D). Finally, DLC allows EVMC to participate in the DA price formation process by dispatching it directly alongside supply-side resources. We analyze three DLC models with different scaling factors: DLC-OA (unscaled), DLC-MR (scaling factors maximize revenue), and DLC-LE (scaling factors ensure low dispatch error and otherwise maximize revenue), in recognition of the challenges of constructing accurate, MW-scale estimates of EVMC resource.

In the price-taking dispatch mechanisms (RTP, TOU), the full flexibility of the individual vehicles is available because they are dispatched using the individual vehicle constraints, but we represent the worst case from the grid operator point of view in that the DA model does not anticipate that the EVMC that will show up in the actual (RT) load profiles. We simulate this by dispatching

[13] "sklearn.cluster.AgglomerativeClustering," scikit-learn, https://scikit-learn.org/stable/modules/generated/sklearn.cluster.AgglomerativeClustering.html

Table 4. Summary of Dispatch Mechanisms and Defining Parameters

Dispatch Mechanism	Parameter	Within-Session Flexibility	Within-Week Flexibility
RTP	Price profiles	Unmanaged charging DA prices	
	Number of prices in tariff	8,760	
TOU-1-2	Time series to mimic	Unmanaged charging DA prices	
	Number of seasons	1	
	Number of blocks[a]	2	
	Number of prices in tariff	4	
TOU-4-4	Time series to mimic	Unmanaged charging DA prices	
	Number of seasons	4	
	Number of blocks[a]	4	
	Number of prices in tariff	32	
DLC-OA	f_1, f_2, f_3	1.0	
	Revenue ratio[b]	0.55	0.58
DLC-MR	f_1	0.5	1.0
	f_2	0.5	0.5
	f_3	1.0	1.0
	Revenue ratio[b]	0.76	0.63
DLC-LE	f_1	0.5	0.5
	f_2	0.5	0.5
	f_3	0.5	0.5
	Revenue ratio[b]	0.99	0.99

[a] Blocks are defined differently for weekdays and weekends. Therefore, the number of price points in these TOU rates is equal to the number of seasons times the number of blocks times two.
[b] Revenue ratio is the net-revenue from dispatching individual vehicles to match a requested aggregate profile divided by the net-revenue expected based on dispatching the aggregate. In both cases net-revenue is calculated based on the same price profile. The values here come from the disaggregation experiments described at the end of Section 4.2, but computed specifically for the listed points.

the individual vehicles against an RTP or TOU price that reflects the DA, unmanaged charging Reference conditions, and then inserting the resulting load changes into the RT model with Reference (unmanaged charging) unit-commitment patterns. Thus, these stylized price-taking dispatch mechanisms show what value EVMC can provide even if charging flexibility is not anticipated by grid operators nor the price formation process. Similar to other research (Roozbehani, Dahleh, and Mitter 2012; Cole et al. 2014; McKenna and Keane 2016; Ruth, Lunacek, and Jones 2017) we find these dispatch mechanisms can on-net increase system costs at high participation rates because large unanticipated deviations of actual load from forecast can cause the very types of grid stress that price-responsiveness is supposed to mitigate. This study counters those effects by muting the aggregate managed EV charging response with a penalty on hour-to-hour changes (ramps) in aggregate charging. This approach produces lower bound results for the capabilities of price-taking (RTP or TOU) approaches at high participation rates, because in practice the impact of these mechanisms would likely be represented in DA operational models (and thus DA RTPs) via load forecasts or approximate representations of inter-temporal charging flexibility (similar to the DLC models described herein) to better align prices and UC patterns with actual price-taking EVMC response. To the best of our knowledge, the academic literature does not contain much on those exact approaches, but the coordination problem is well known and a number of authors have addressed it by either iterating between power system dispatch and load scheduling or by computing prices that will induce loads to meet specific objectives such as peak load reduction or valley-filling (David and Li 1993; Corradi et al. 2013; Cole et al. 2014; Ma, Callaway, and Hiskens 2013; Xi and Sioshansi 2014).

The DLC dispatch mechanism presents aggregate flexibility to the grid operator in the DA model, but the amount of flexibility is reduced from what is accessible through the individual vehicles by scaling factors (LE and MR cases) or is significantly infeasible (OA and MR cases). The flexibility is also not accurately located in the DA model–it is aggregated into pseudo-storage flexibility resources at 19 (dispatch zone resolution) nodes. We evaluate overall outcomes in terms of dispatch and system cost savings by fixing the EVMC profiles determined in the DLC DA model in the RT model formulated from the DLC DA UC results. The unscaled DLC-OA represents an upper bound on the bulk power system value of EVMC, because it strictly overestimates charging flexibility and is able to modify unit-commitment decisions in the DA. Narrowing EV charging power and energy bounds with scaling factors to create the DLC-LE and DLC-MR resources yields more realistic descriptions of what coordinated EVMC dispatched in DA markets could look like if the aggregate resource is scaled either to have few infeasible dispatch requests (-LE) or to maximize revenue after accounting for buying back infeasible dispatch at the clearing price (-MR). Unfortunately, it was not within the scope of this study to take the DA dispatch requests for these aggregates and then compute feasible vehicle-level charging profiles to best fulfill those requests. This study is therefore not able to fully analyze, but can only approximate, the bulk system value of the DLC-LE and DLC-MR dispatch mechanisms. Because of this deficiency, we often analyze DLC-LE results that are expected to be close to feasible, rather than DLC-MR results that are expected to have more inaccuracies but produce more system and aggregator value if deviations from expected dispatch are settled against the final RT prices.

5 Bulk Power System Value of Managed Charging

We explore the value of EVMC in an envisioned 2038 ISO-NE bulk power system based on the scenario framework shown in Table 5. Rather than running all possible combinations of scenarios, we select specific runs that help us answer a series of four questions, culminating in, "What is the trade-off between per-vehicle value, total system cost reductions, and dispatch mechanism complexity?" In all cases, the unmanaged, Immediate EV charging scenario serves as a reference condition against which we measure the value of EVMC. We also explore the differences between within-session and within-week charging flexibility throughout. Different combinations of participation rate and dispatch mechanism are selected as we progress, and by the end, in addition to answering the posed questions we also grapple with some DER aggregation challenges: "If we ask for demand flexibility, how much will actually show up?" and "When does price responsive flexibility break down if it is not factored into the price formation process?"

Table 5. Scenario Framework for Exploring the Value of EVMC in the ISO-NE Bulk Power System

	Charging Strategy	Flexibility Type	Participation in Managed Charging	Managed Charging Mechanism
Value	Unmanaged vs. Managed	Within-session versus Within-week	5%, 10%, …, 100%	DLC, RTP, TOU
What does it represent?	Cost savings if the timing of EV charging is managed (V1G)	Value of choosing charging times daily or weekly	Depth of need for EVMC services	Value of more precision in EVMC dispatch
What does it not represent?	Impact of different charging infrastructure scenarios; V2G or V2X	Impact of place-based differentiated pricing	Trade-offs between utility costs and/or program design and participation rates	Dispatch to maximize value across multiple grid services, trade-offs with distribution system costs

5.1 What system cost savings could EVMC provide if all personal passenger light-duty EVs participated?

Because DLC-OA simply sums individual charging bounds to estimate aggregate resource size and thus overstates actual charging flexibility by potentially infeasible combinations of charging and energy capacity, we can calculate an upper bound for the total bulk system production cost savings of EVMC by applying the DLC-OA dispatch mechanism with 100% participation. This lets the Reference DA UC model shift up to 12.0% of load, all 17.1 TWh of generation needed to serve the charging load of 5.3 million vehicles, to reduce system costs by avoiding unit starts and shut downs, reducing fuel and VO&M costs, and reducing transmission congestion. The result of this shifting, calculated in the DA at the dispatch zone level (19 pseudo-storage units) and realized at all of the ISO-NE load nodes in the RT model, is shown in terms of system costs (excluding emissions costs) in Figure 17. If the vehicles present within-session flexibility to the system operator, production costs are reduced by 6.7% or $20.9/vehicle-year. The corresponding results for within-week flexibility are 8.2% production cost savings or $25.5/vehicle-year.

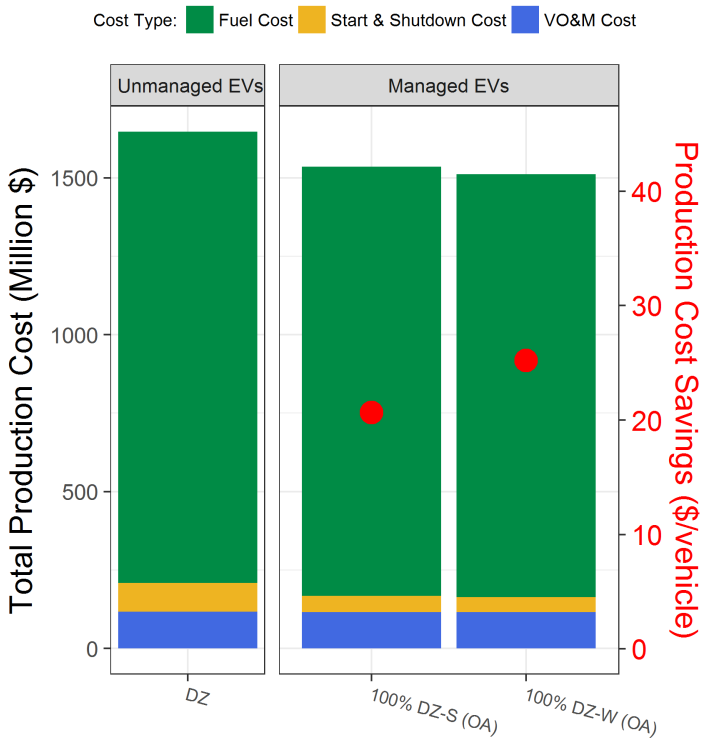

Figure 17. Annual production costs with within-session (-S) and within-week (-W) DLC-OA EVMC with 100% participation compared to annual production costs with unmanaged EV charging. As shown in Section 4.2, DLC-OA is an overestimate of aggregate flexibility such that these results are an upper bound on total production cost savings.

If we factor in the analysis of Section 4.2 and estimate total production cost savings for DLC-OA (unscaled), DLC-LE (scaling factors ensure low dispatch error and otherwise maximize revenue), and DLC-MR (scaling factors maximize revenue) assuming that production cost savings would be reduced by the revenue ratios in Table 4, we end up with production cost savings estimates of 3.7% to 4.7% for within-session and 4.4% to 6.4% for within-week flexibility (Figure 18). Certainly the Table 4 revenue ratios are not the right discount factors for capturing the impact of DLC-LE, DLC-MR and DLC-OA dispatch infeasibilities on production costs. It would be best to directly compute dispatch profiles for the 101,031 sample vehicles that in total minimize the error between the actual and requested aggregate dispatch and then calculate production cost savings in the RT for the sum of those individual profiles; it would be an improvement to at least perform those calculations for some cases and then calculate production cost discount factors by comparing the results for requested and actual EVMC dispatch. Regardless, computing disaggregated dispatch at that scale is computationally onerous and out of scope for this study, so we apply the price-taking revenue discount factors in Table 4 as the best available proxies.

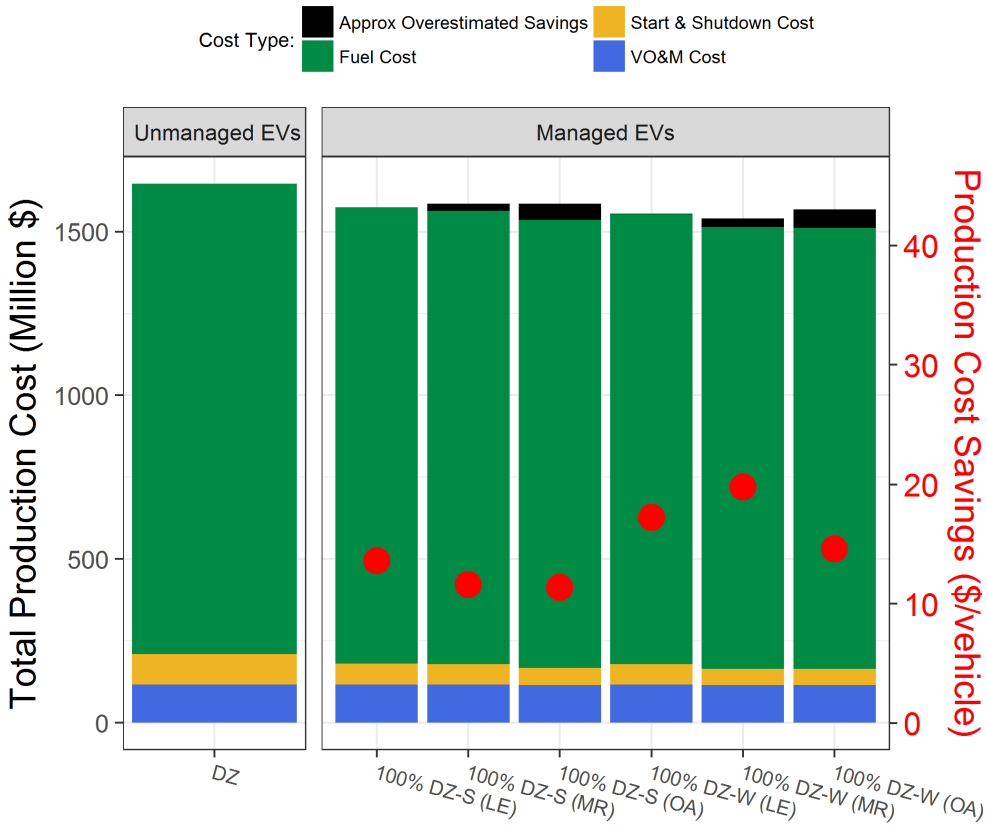

Figure 18. Annual production costs with within-session (-S) and within-week (-W) EVMC with 100% participation using the DLC-LE, DLC-MR, and DLC-OA dispatch mechanisms all compared to annual production costs with unmanaged EV charging. Estimates of how much savings might be overstated by dispatching SOA aggregate resources are shown in black and factored into per-vehicle production cost savings estimates.

The results in Section 4.2 show that DLC-LE is the most conservative aggregate dispatch in the sense that it is more likely to be feasible when implemented with individual vehicles compared to DLC-MR and DLC-OA. For this reason, we predominantly analyze the DLC-LE aggregate models in what follows. That said, the DLC-MR scaling might be more likely in an operational setting, and DLC-LE achieves lower net revenue than optimal dispatch of individual vehicles in Figure 14b and Figure 15b, so the DLC-LE results can be considered an underestimate of maximum achievable EVMC value under DLC.

EVMC can reduce firm capacity requirements by shifting load out of the most expensive to serve hours. A reasonable first-order approximation for the most expensive to serve hours are those with the highest net load. Following Stephen, Hale, and Cowiestoll (2020) and Jorgenson et al. (2021), we estimate the firm capacity contribution of EVMC by calculating the average MW reduction in the top 100 net-load hours based on comparing net-load duration curves with and without EVMC included. For example, Figure 19 shows the first 100 hours of the net-load duration curves, which are load minus VG values for every hour of the year sorted from highest to lowest, for the 2038 PCM without EV load (light grey), the Reference scenario (black), the DLC-LE 100% participation within-session EVMC scenario (yellow), and the DLC-LE 100% participation within-week EVMC scenario (dashed cyan). On average, unmanaged EV load

adds 1,620 MW to the top 100 hours of net-load in this system. DLC-LE EVMC with 100% participation reduces that amount by about half no matter whether the flexibility type is within-session or within-week.

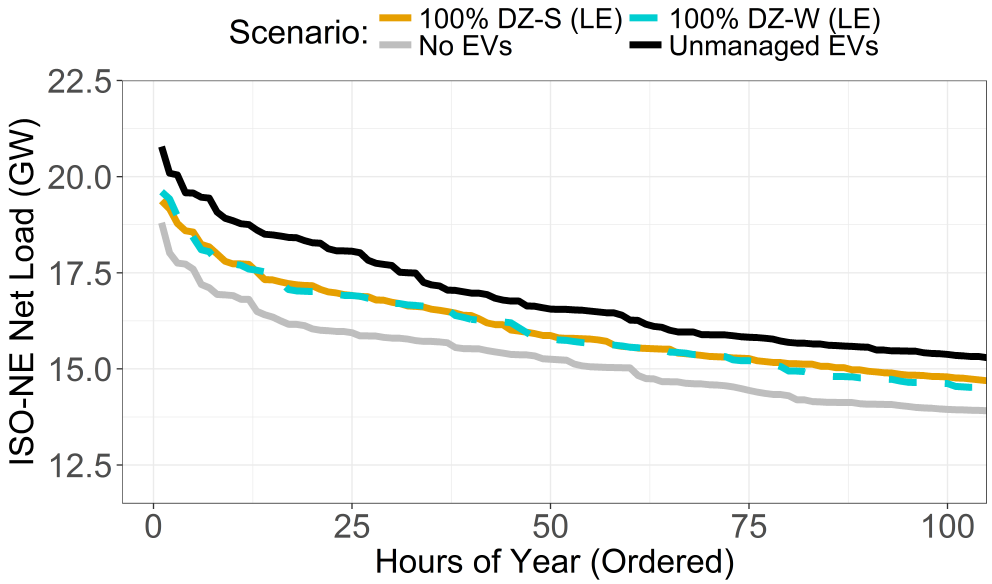

Figure 19. Top 100 hours of the net-load duration curves for the 2038 PCM without EV load (No EVs), the Reference scenario (Unmanaged EVs), and the DLC-LE 100% participation scenarios for within-session (100% DZ-S (LE)) and within-week (100% DZ-W (LE)) flexibility. The firm capacity contribution of EVMC is estimated to be the average net load reduction across these top 100 net-load hours. Capacity value is estimated by multiplying the firm capacity contribution by capacity prices from the Cambium data set (Gagnon et al. 2021).

The firm capacity value for the DLC-LE 100% participation scenarios is shown in Table 6 alongside other key statistics that summarize the overall bulk power system value of this EVMC scenario. We estimate firm capacity value by multiplying firm capacity avoided by an assumed capacity price of $75.62 to $96.81/kW-y in $2016 ($81.55/kW-y to $104.40/kW-y in $2020),[14] which are the ISO-NE 2038 capacity prices of the Mid-case 95% decarbonization by 2035 and Mid-case 95% decarbonization by 2050 scenarios in the 2021 Cambium data set (Gagnon et al. 2021). (The Mid-case capacity price falls within this range at $96.5/kW-y in $2016.) Overall, the per-year monetary value of this EVMC scenario is $147.9 million to $164.4 million for within-session flexibility and $175.9 million to $193.6 million for within-week flexibility ($2016), inclusive of production cost savings, avoided CO_2 emissions valued at $45/ton, and the aforementioned range of firm capacity value. In addition, compared to the Reference scenario 402 GWh (within-session) and 579 GWh (within-week) more within-ISO generation is used locally through a combination of reduced VG curtailment and reduced "dump energy" (unused generation that cannot otherwise be curtailed nor dispatched down costs $20/MWh). These are approximate upper bounds for the system-level value of EVMC in the envisioned ISO-NE system, based on 5.3 million vehicles (45% of the passenger LDV fleet) participating in the 2038 time frame.

[14] Values in $2016 are computed from the $2020 values in the Cambium data set using an annual simple average of the monthly Consumer Price Index for all urban consumers (CPI-U, https://fred.stlouisfed.org/series/CPIAUCSL).

Table 6. Summary of EVMC Bulk System Value if All Vehicles Participate Using the DLC-LE Dispatch Mechanism

Metric	Within-Session Flexibility	Within-Week Flexibility
Production cost savings (million $/yr)	73.9	92.4
Production cost savings (%)	4.4	5.6
Production cost savings ($/vehicle-yr)	13.9	17.5
Emissions avoided (million metric tons)	0.33	0.44
Emissions avoided (%)	5.2	6.9
Emissions avoided (kg/vehicle-yr)	59	75
Increased use of within-ISO generation[a] (GWh)	402	579
Increased use of within-ISO generation[a] (kWh/vehicle-yr)	76	109
Firm capacity avoided (MW)	781	834
Firm capacity avoided (kW/vehicle-yr)	0.15	0.16
Firm capacity value (million $/yr)	59.1 - 75.6	63.1 - 80.7
Firm capacity value ($/vehicle-yr)	11.1 - 14.3	11.9 - 15.2
Transmission congestion index	174.9	170.3
Transmission congestion index reduction	-16.0	-11.4

[a] EVMC increases the use of within-ISO generation by avoiding VG curtailments (with a $0/MWh cost) and reducing net imports. Exactly which type of non-use of within-ISO generation occurs in a given scenario is a complex function of system DCOPF dispatch, but we do observe a clear trend of EVMC enabling more use of within-ISO generation.

Table 6 also reports the transmission congestion index for the DLC-LE 100% participation within-session flexibility and within-week flexibility scenarios. Contrary to our expectations, EVMC actually increases transmission congestion in the high-voltage ISO-NE network (115 kV and above) in these scenarios. The values reported in the table are for the RT models. The values for the DA models, in which EVMC shows up at 19 nodes, show congestion reduction for within-session flexibility (172.1 compared to 174.0 in the Reference scenario DA model) but a significant increase in transmission congestion (237.4) for within-week flexibility, suggesting potential difficulty in scheduling of EVMC with heavier reliance on the coarser beyond-day look-ahead for the longer within-week time horizon. This finding also suggests that the value of using EVMC to reduce fuel, start & shutdown, VO&M and emissions costs can be worth an additional amount of transmission congestion. More work is required to fully understand how EVMC impacts trade-offs between congestion on the distribution and transmission systems, costs to upgrade the distribution and transmission systems, and the value streams EVMC can provide to bulk power systems.

Figure 20 shows annual generation in the DLC-LE 100% scenarios minus the Reference scenario annual generation. Within-session and within-week EVMC reduce wind, solar, and hydropower curtailment (shown as increased generation from those resources); reduce use of pumped hydropower energy storage (thus avoiding some of the round-trip losses experienced in the Reference scenario); increase biomass generation and reduce gas combined cycle generation. The

magnitude of the changes differs depending on EVMC type. Within-session EVMC produces annual generation by type changes on the order of 1 TWh in either direction, whereas within-week EVMC avoids over 3 TWh of curtailments. In the latter case, the additional VG is balanced by a larger reduction in gas combined cycle generation and by a sizable reduction in net imports (i.e., increased exports that cost ISO-NE $20/MWh).

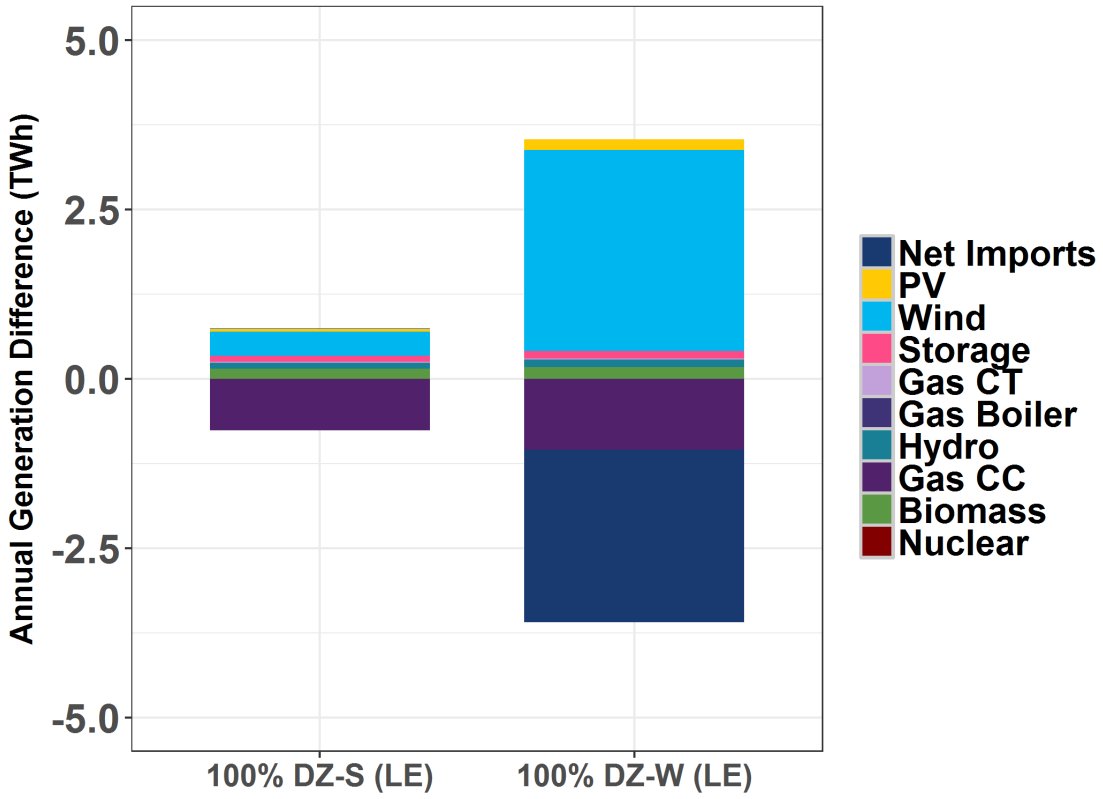

Figure 20. Annual generation by type for the 100% DLC-LE scenarios for within-session (-S) and within-week (-W) flexibility minus annual generation by type for the unmanaged EV charging Reference scenario

Figure 21 shows the within-week EVMC pattern of trading off reduced curtailments for increased exports during some hours as well as the more general pattern—seen for both types of flexibility—of shifting load from evening hours to early morning, midmorning, and early afternoon hours. Such load shifts can be especially valuable during peak and near-peak days, when the most expensive units in the system are called on to help meet peak demand. Because Figure 21 shows such peak and near-peak days (the middle day, July 17, is the gross peak load day), we also see that within-week EVMC is on net able to shift some load out of these days entirely, whereas within-session EVMC is constrained to use approximately the same amount of energy as the Reference scenario across these three days.

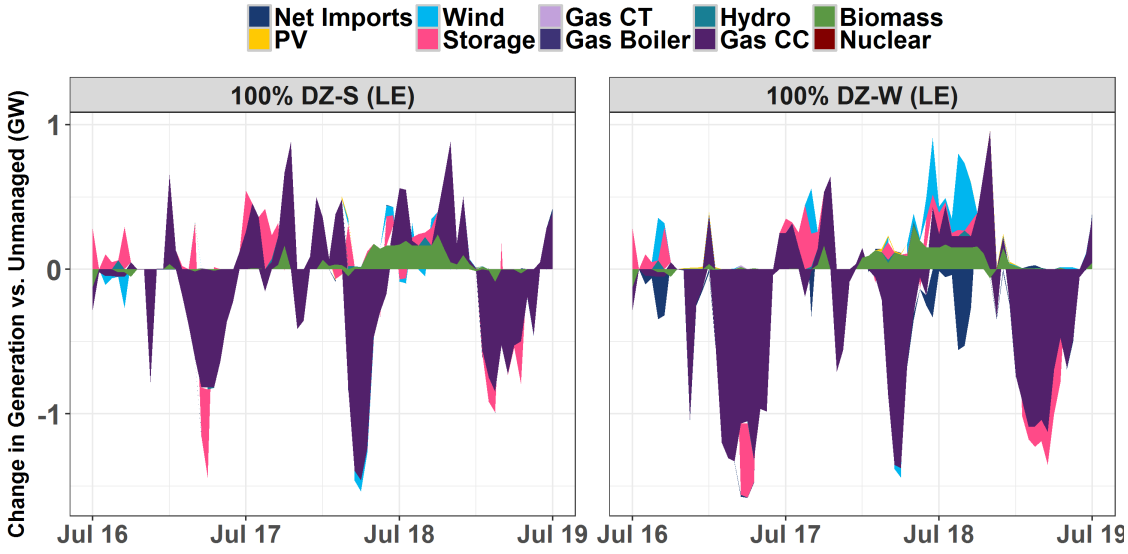

Figure 21. Hourly generation by type for three days of the 100% DLC-LE within-session and within-week EVMC scenarios minus the corresponding hourly generation by type profiles for the unmanaged EV charging Reference scenario. The three days shown contain the peak load day, July 17.

5.2 What is the value of the first increment of EVMC participation?

Though EVMC provides the most overall value to the bulk power system at 100% participation (Section 5.1), the first increment of EVMC provides the most per-vehicle value. We estimate the value of this first increment by analyzing scenarios with 5% participation rates, which is small enough to be considered a first increment but large enough to mostly avoid numerical issues caused by trying to resolve the effect of a very small resource in a large system. Figure 22 shows the production cost savings for the DLC-LE 5% scenarios. Total production costs are only reduced by 0.5% for both within-session and within-week flexibility in this case; considerably lower than the 4.4% and 5.6% observed for 100% participation (Table 6). However, as expected, per vehicle-year production cost savings are higher than in the 100% participation DLC-LE scenario: $28.4/vehicle-yr for within-session and $28.0/vehicle-yr for within-week, compared to $13.8/vehicle-yr and $17.4/vehicle-yr, respectively. Unexpectedly, within-week flexibility is somewhat less valuable than within-session flexibility, however, this appears to be an optimization issue–it was significantly more difficult for the PLEXOS mixed-integer program to resolve the dispatch of this small quantity of within-week flexibility compared to either a similar quantity of within-session flexibility or larger quantities of within-week flexibility.

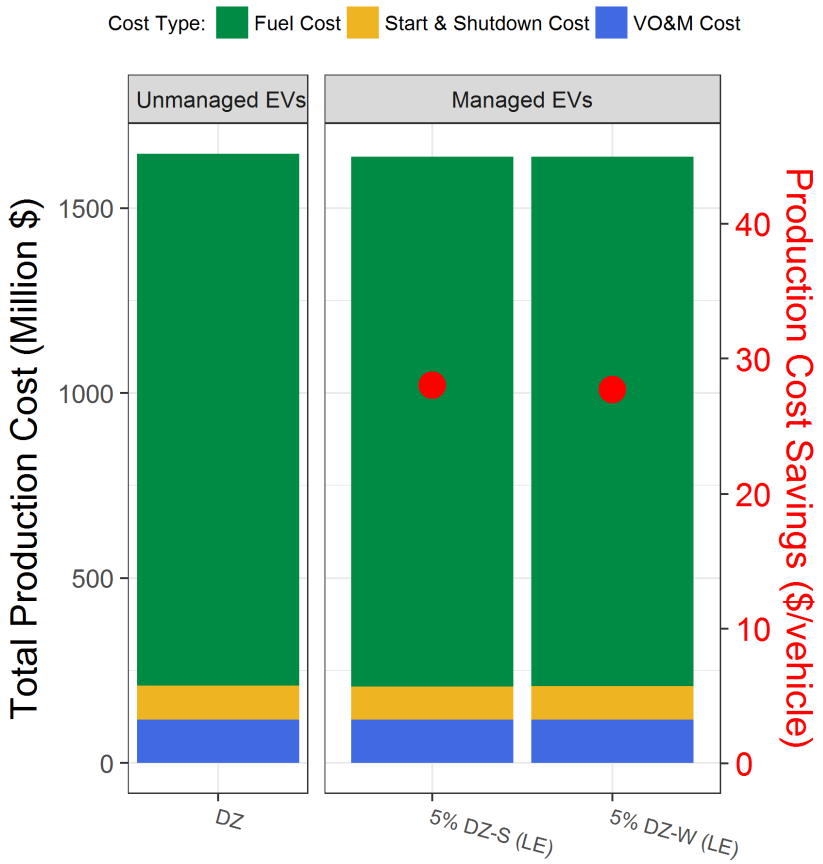

Figure 22. Annual production costs with within-session (-S) and within-week (-W) EVMC for the DLC-LE dispatch mechanism with 5% participation compared to annual production costs with unmanaged EV charging

Price-taking dispatch mechanisms like RTP or TOU can also be used to manage EV charging at low participation rates. Figure 23 shows the production cost savings for DLC-LE, RTP, TOU-1-2, and TOU-4-4, for both within-session and within-week flexibility, all at 5% participation. At this level of participation, individual vehicles responding to an RTP reduces production costs the most: $30.2/vehicle-yr for within-session flexibility and $37.7/vehicle-yr for within-week flexibility. RTP outperforming DLC-LE demonstrates that at low participation rates the additional savings from being able to fully schedule all vehicles' charging individually outweighs the inefficiency of dispatching bulk system resources with no anticipation of the EVMC flexibility resource.

TOU rates can also provide production cost savings at low levels of participation. Somewhat surprisingly, of the two TOU rates described in Appendix D, the simpler one-season, two-block (TOU-1-2) rate produces more production cost savings than the four-season, four-block (TOU-4-4) rate. One would generally expect the TOU-4-4 rate's 32 prices to produce production cost savings that fall between those induced by the TOU-1-2 rate's 4 prices and the RTP's 8,760 prices. However, the TOU-4-4 rate described in Appendix D underperforms relative to this expectation because of a poor transition between winter weekdays and winter weekends. In particular, winter Friday evenings have energy prices of 6.0 cents/kWh until 11 p.m., 0.8 cents/kWh until midnight, 5.2 cents/kWh until 3 a.m. Saturday morning, and then 1.4 cents/kWh until 8 a.m. This

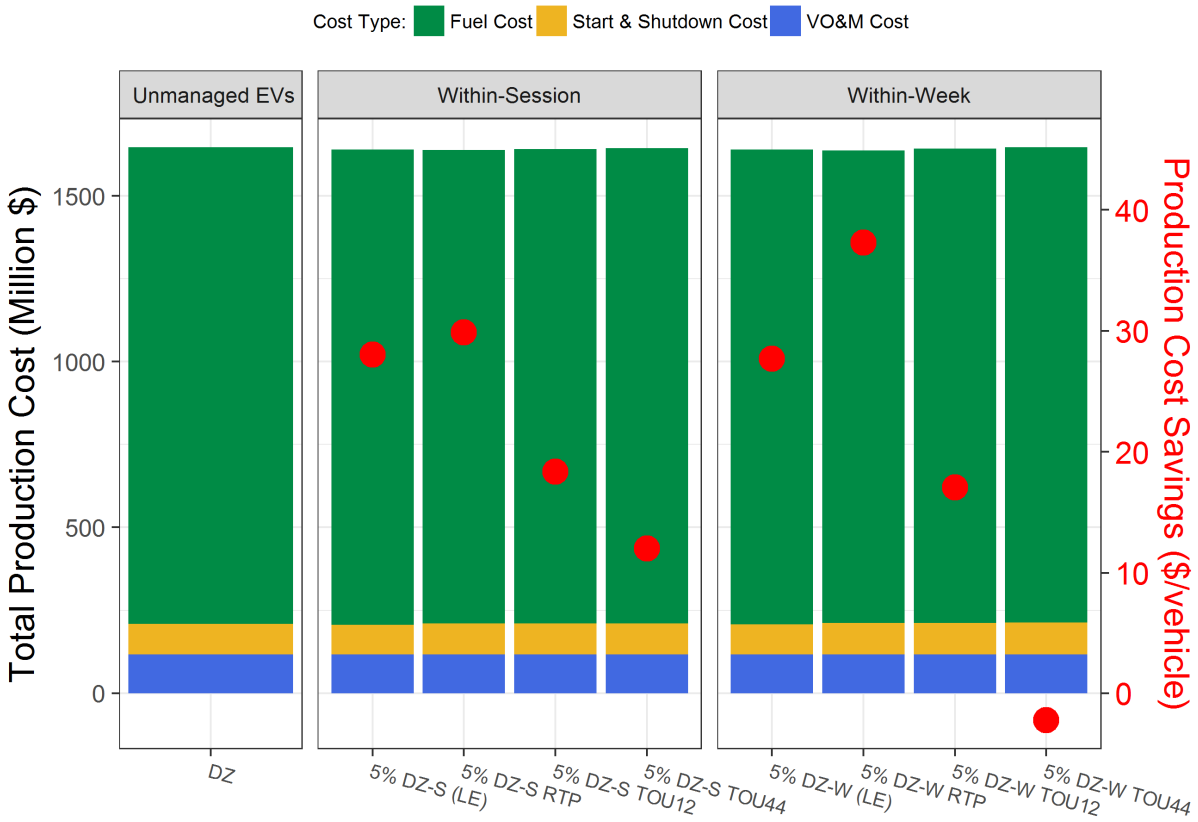

Figure 23. Annual production costs with within-session (-S) and within-week (-W) EVMC at 5% participation for all dispatch mechanisms (DLC-LE, RTP, TOU-1-2, and TOU-4-4) compared to annual production costs with unmanaged EV charging

price profile, with a one-hour lowest-price from 11 p.m.-midnight, encourages maximizing EV charging during this hour, producing unexpectedly high charging load during that hour that is difficult for committed and fast-start resources to dispatch upward to accommodate in the RT. Resulting production cost increases suggest weekday and weekend time blocks should not be designed independently. The TOU-1-2 rate simply charges less for energy overnight (midnight to either 7 a.m. or 9 a.m.) than at other hours, and the EVMC dispatch patterns generated by this rate at 5% participation can achieve 61.3% and 45.7% of the RTP savings for within-session and within-week flexibility respectively.

5.3 What is the trade-off between per-vehicle value and system cost savings as participation rates increase?

The DLC-LE results depicted in Figure 24 show how system-level production cost savings and per-vehicle production cost savings change with participation level. Both within-session and within-week flexibility show the clear "declining marginal value" pattern that has been well-established for all resource types, as the per-vehicle value is highest at the lowest participation level, is smallest at 100% participation, and monotonically decreases in between. As expected, within-week flexibility is generally more valuable than within-session flexibility. Excluding the 5% participation point, within-week flexibility is 22% to 26% more valuable than within-session flexibility, as measured by DLC-LE production costs alone. We suspect PLEXOS had a hard

time resolving the optimal dispatch for within-week flexibility at 5% participation. It is generally challenging to get PLEXOS to compute optimal dispatch for (a) small resources and (b) within-week resources relying on longer look-ahead—this particular point combines both characteristics. We also see in Section 5.2 that the per-vehicle value for this point dispatched using RTP is much higher: $37.7/vehicle-yr instead of the $28.0/vehicle-yr shown here.

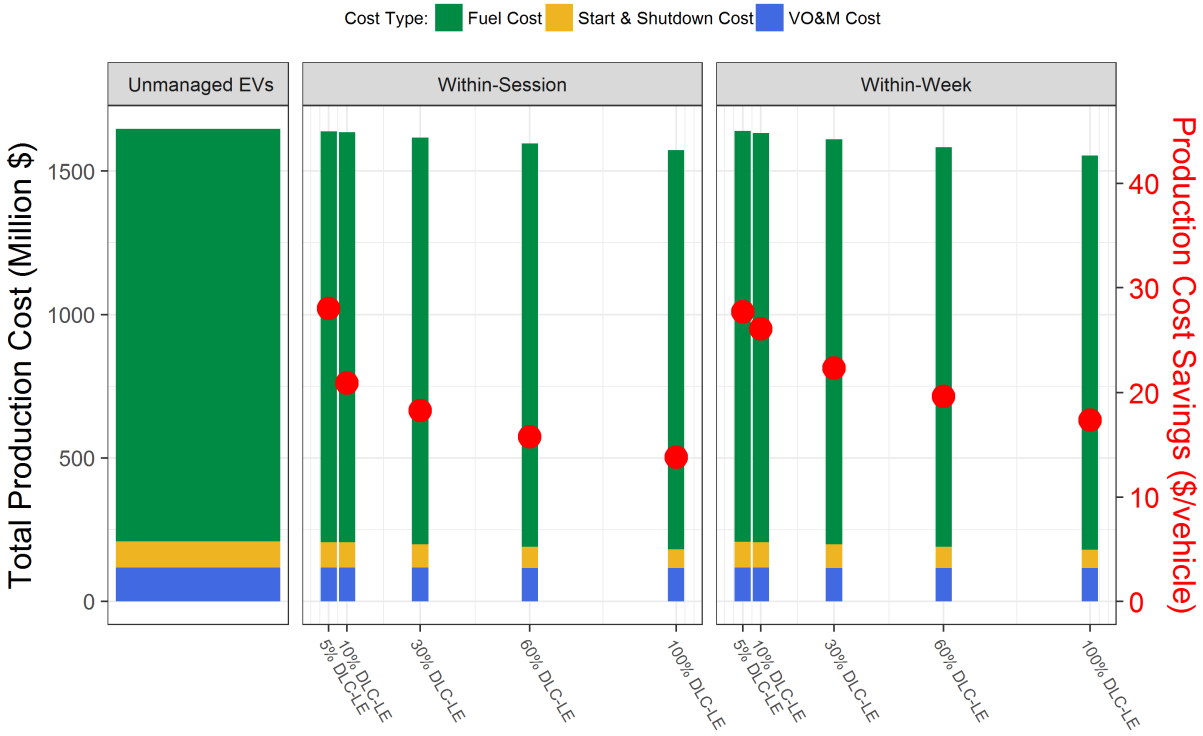

Figure 24. Annual production costs with within-session (-S) and within-week (-W) EVMC for the DLC-LE dispatch mechanism and varying participation levels compared to annual production costs with unmanaged EV charging

Capacity value follows a similar declining marginal value pattern (Figure 25). In this case, within-week flexibility is again about 25% more valuable than within-session flexibility but only at lower participation rates. At 100% participation within-week flexibility is only about 6% more valuable than within-session flexibility: $12/vehicle-yr to $15/vehicle-yr for within-week flexibility compared to $11/vehicle-yr to $14/vehicle-yr for within-session flexibility. In terms of overall capacity resource, at 5% participation, the resource is on the order of tens of megawatts, growing to hundreds of megawatts for 30% to 60% participation, and reaching 780 MW (within-session flexibility) to 830 MW (within-week flexibility) at 100% participation.

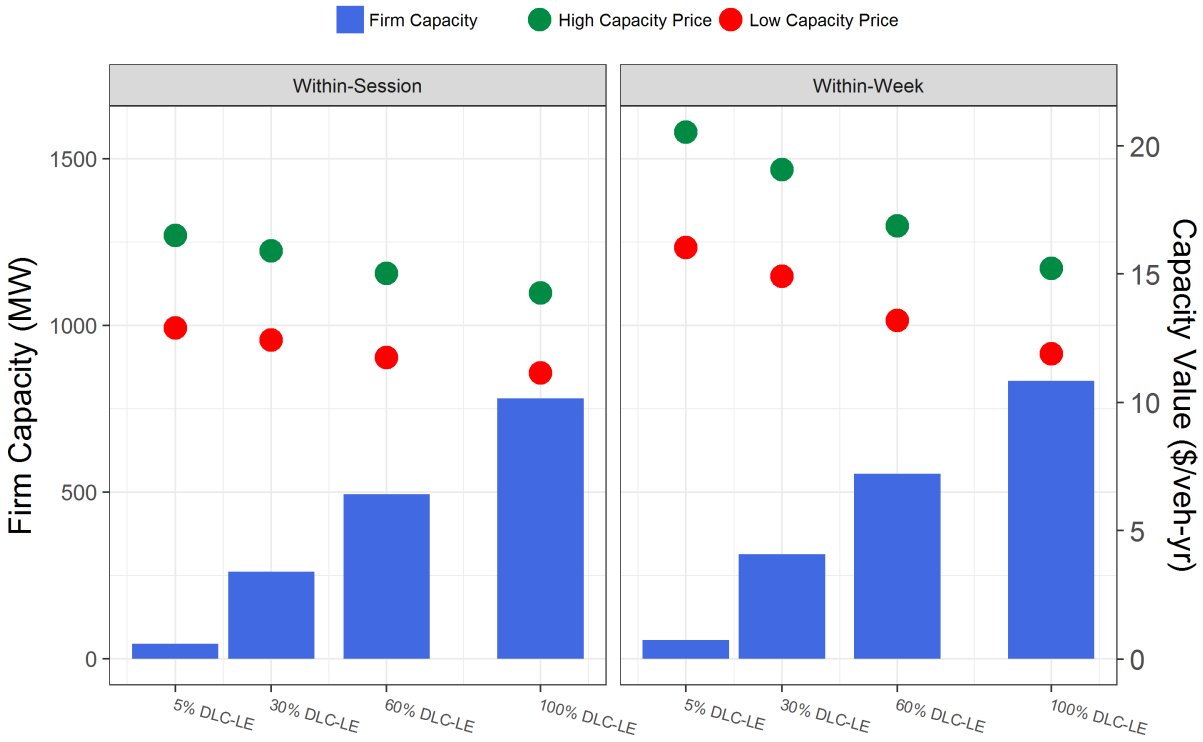

Figure 25. Firm capacity supplied by DLC-LE EVMC with within-session (-S) and within-week (-W) flexibility.
Dots on secondary axis use capacity prices from Cambium (in $2016) to convert firm capacity to capacity value.

Increasing amounts of EVMC also support increasing use of within-ISO generation realized through either reduced VG curtailment or reduced exports or both. Although in our study the curtailment and net import trends are not perfectly steady on their own, the trends in the sum of reduced curtailments and reduced exports are steady and show that within-week flexibility can increase use of within-ISO generation by about 25% to 45% more than within-session flexibility (Figure 26) across all participation rates. For all but one run, both curtailment and exports are reduced modestly to produce the overall increases in within-ISO use of within-ISO generation shown in the figure. In the 100% participation, within-week scenario large curtailment reductions (3.1 TWh) are balanced by increased exports (2.5 TWh), but as shown, the net increase in within-ISO use of within-ISO generation is in line with the other scenarios.

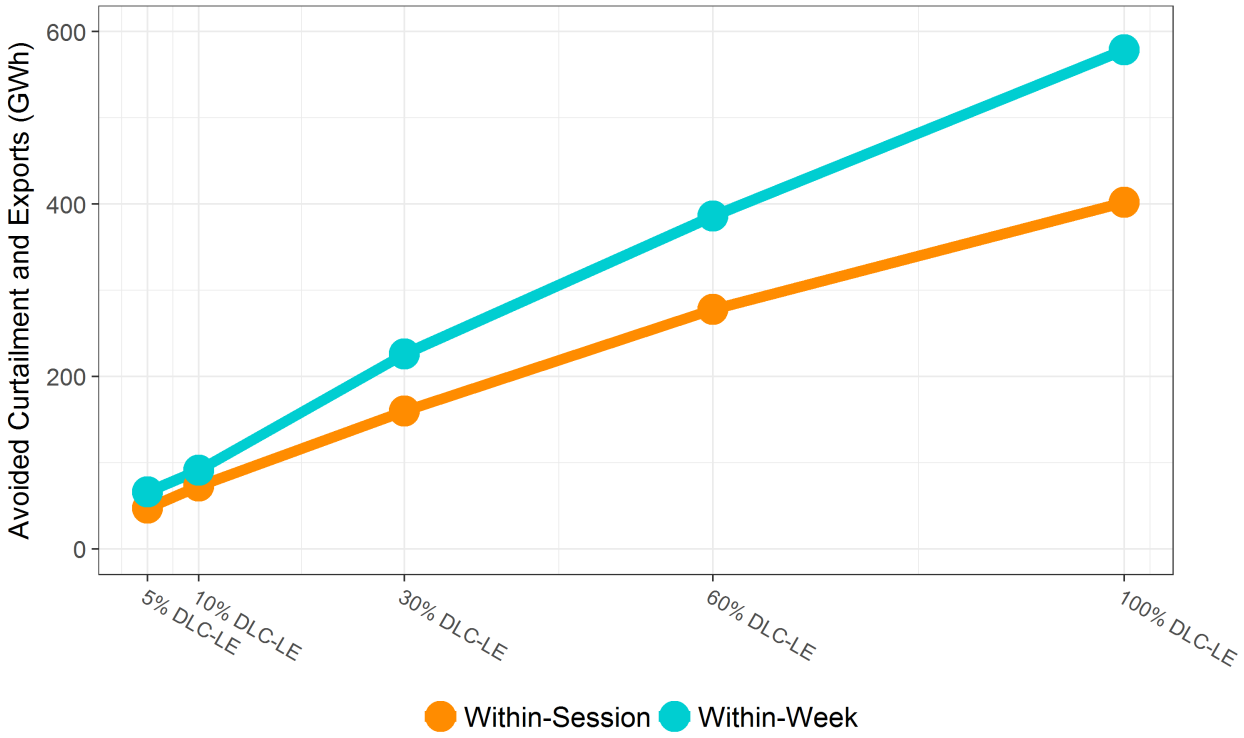

Figure 26. Increased use of available within-ISO generation for the DLC-LE EVMC scenarios. Compared to the Reference scenario with unmanaged charging, DLC-LE reduces VG curtailment, reduces exports, or both.

5.4 What is the trade-off between per-vehicle value, system cost savings, and dispatch mechanism complexity?

Section 5.3 demonstrates that the DLC-LE dispatch mechanism works reasonably well across all participation levels and shows the expected trade-off between more participation yielding more system-level benefits but with less value per vehicle than at low participation. Section 5.2 demonstrates that at low participation levels, individual vehicles responding to a real-time price can provide more value than an aggregate dispatched with the DLC-LE mechanism, and that vehicles responding to a simple two-block TOU tariff (with lower prices overnight) can provide a significant fraction of the DLC-LE value. That is, at low participation levels dispatch mechanisms that are much simpler than DLC, because they only require communicating prices annually, weekly, or daily to individual vehicles, can provide similar levels of value as DLC. It is well known that the effectiveness of price-taking methods deteriorates as participation levels increase. What does that deterioration look like for this particular case study?

First, RTP, with price-responsive EVMC unanticipated in the DA UC, produces detrimental system outcomes at 100% participation. Figure 27 demonstrates this for three example days in January. Based on the hourly prices from the DA UC model, almost all vehicles charge during just a few lowest price overnight hours—only those vehicles that require daytime charging to complete trips charge during the day when prices are higher. In the most extreme case, this increases the daily EV charging load peak from about 4 GW in the evening to over 14 GW in the early morning hours (Figure 27a). Such a large change in load causes the price-taking assumption to break down in a system with a peak load of 28.9 GW and a net-peak load of 20.8 GW (Table 2). The resulting RT price profile demonstrates that rather than benefiting the

system, enough unanticipated load materializing due to RTP response can be highly detrimental (Figure 27b).

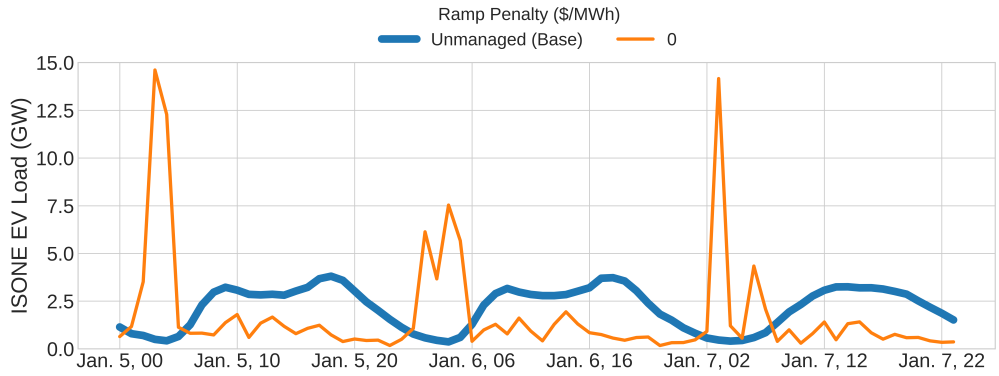

(a) EV Charging Profiles

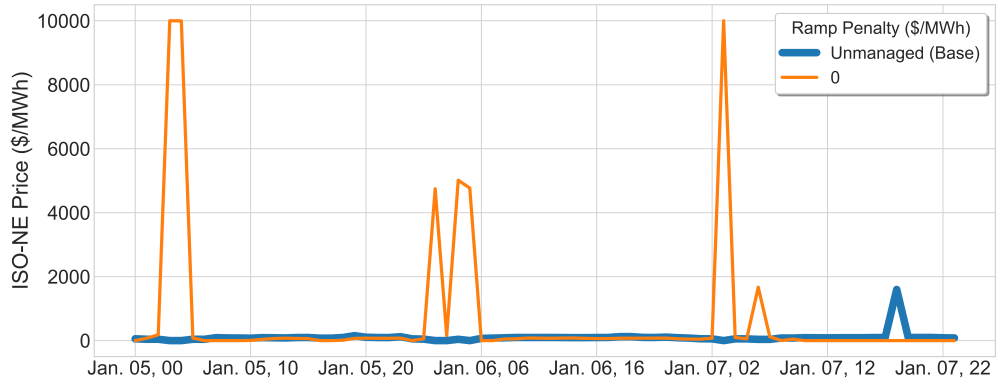

(b) Price Profiles

Figure 27. With all 5.3 million vehicles participating, EVMC implemented with RTP eliminates the price spikes in the DA UC model but creates even larger price spikes at other times because of the dramatic EV load shape changes induced by responding to the RTP in an uncoordinated fashion.

There should be ways to inform the DA UC of potential load flexibility and then reflect desired behavior back to vehicles in terms of prices (David and Li 1993; Corradi et al. 2013; Cole et al. 2014; Ma, Callaway, and Hiskens 2013; Xi and Sioshansi 2014); see Section 4.3. In this study we make the simplifying assumption that price-taking response is coordinated based on a penalty on aggregate hourly change in EV load. That is, a group of vehicles' charging profiles are simultaneously optimized to minimize their individual charging costs, but we also add a ramp penalty (in $/MW) on the aggregate hourly change in EV load compared to the unmanaged baseline EV load in either direction (up or down) in the objective function (Section E.1) to mute the overall response. EV load profiles for the same three example days as Figure 27 are shown in Figure 28, this time with additional curves for RTP with nonzero ramp penalties. As expected, higher ramp penalties push the RTP response closer and closer to the baseline profile. In this particular example, a $500/MW penalty still produces some load shape change but the load profile computed with a $1,000/MW penalty is nearly identical to that of the unmanaged case.

To compare across dispatch mechanisms, we select optimal ramp penalties for each combination of price-taking dispatch mechanism (i.e., RTP, TOU-1-2, and TOU-4-4) and participation level.

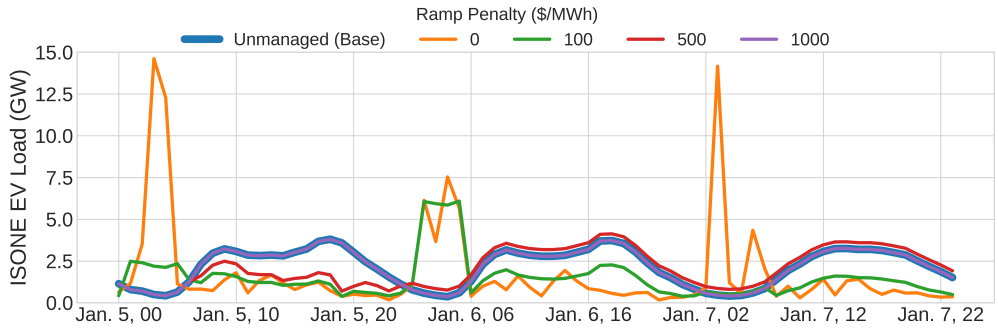

Figure 28. Adding a penalty on the aggregate response ramp to the RTP dispatch formulation mutes the overall response. In this 100% participation scenario and for these particular example days, a ramp penalty of $500/MW is sufficient to bring actual EV load peaks back down below 150% of the unmanaged charging EV load peaks.

For simplicity, we analyze just four participation levels: 5%, 30%, 60%, and 100%, and a few ramp penalties: $0/MW, $1/MW, $10/MW, $50/MW, $100/MW, $500/MW, and $1,000/MW; and we choose the ramp penalties that maximize production cost savings.

Figure 29 shows a limited number of results for the RTP dispatch mechanism applied to within-session flexibility. As shown earlier, at 5% participation, production cost savings of $30.2/vehicle-yr can be obtained using plain (ramp penalty of $0/MW) RTP dispatch. However, muting that response slightly, with a $1/MW ramp penalty, actually saves about $33.1/vehicle-yr, implying that some coordination of EVMC is desirable even at this level of participation. Our results for 30%, 60%, and 100% participation suggest that simply muting aggregate RTP response is not an effective strategy at high levels of participation—though it avoids cost increases, it provides little cost savings. For example, at 30% participation and with a $100/MW aggregate ramp penalty the production cost savings per vehicle are $4.0/vehicle-yr, which compares poorly to the $18.5/vehicle-yr obtained with the DLC-LE dispatch mechanism (Figure 24).

Per Figure 30, even more coordination is required for within-week flexibility. At 5% participation, RTP with a ramp penalty of $10/MW produces the highest per-vehicle production cost savings for all of the RTP variants: $65.0/vehicle-yr compared to $37.7/vehicle-yr with no ramp penalty. RTP for within-week flexibility does not produce significant production cost savings at 30% participation and above, even when response is coordinated through significant ramp penalties.

The TOU rates paired with aggregate ramp penalties perform similarly. As shown in Table 7—which does not report ramp penalties for combinations of dispatch mechanism and participation rate with maximum production cost savings less than $1/vehicle-yr—in no case do the price-taking dispatch mechanisms analyzed in this study produce significant per-vehicle production cost savings at participation rates of 60% or above. For within-week flexibility, even 30% participation is too high for all three price-taking dispatch mechanisms. We also find similar optimal ramp penalties for RTP and the more complex TOU rate (TOU-4-4), while TOU-1-2 performs best at 5% participation with a $1/MW ramp penalty for both flexibility types: within-session and within-week.

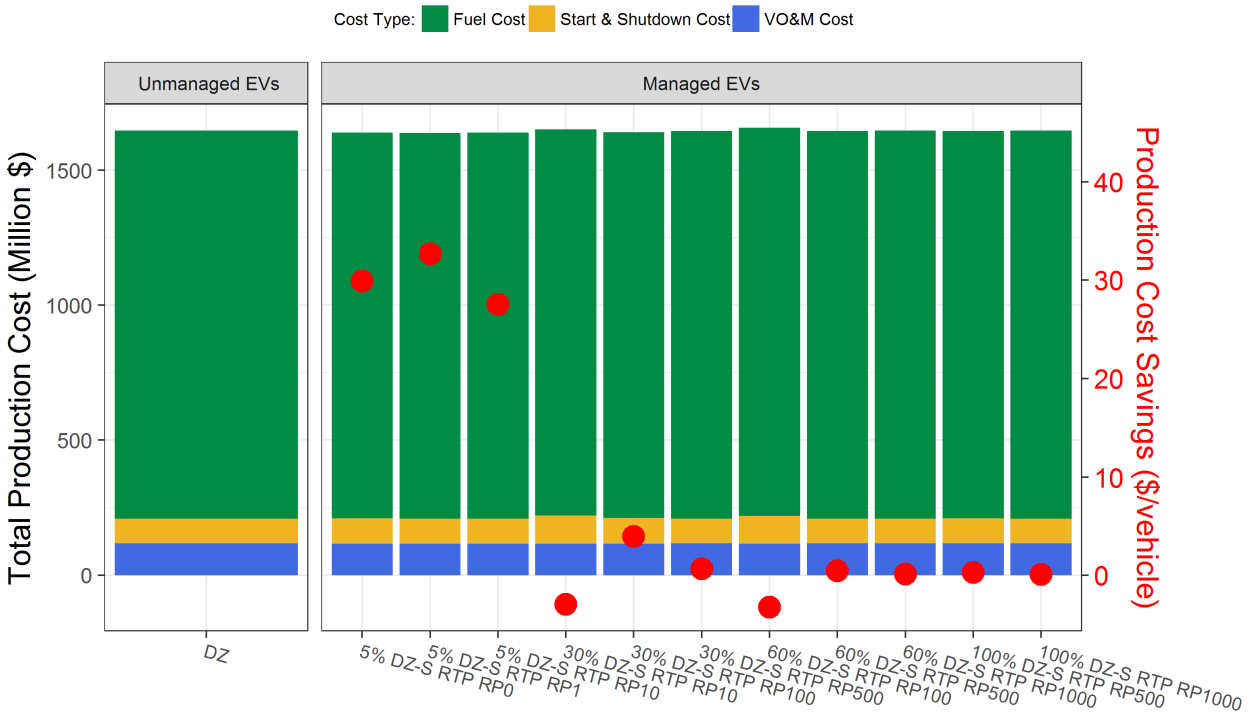

Figure 29. Annual production costs for within-session EVMC realized through RTP response muted with penalties applied to hourly aggregate ramps compared to annual production costs with unmanaged EV charging. Two or three ramp penalties are depicted for each of four participation rates. For example, the three points for 5% participation have ramp penalties of $0/MW, $1/MW, and $10/MW, which are indicated in the figure as RP0, RP1, and RP10. Only two ramp penalties are displayed for 100% participation, because lower ramp penalties have significantly negative savings.

Figure 31 shows the per-vehicle and total production cost savings for DLC-LE at four participation levels (5%, 30%, 60%, and 100%) and for both flexibility types alongside the eight non-null dispatch mechanisms listed in Table 7. As can be seen by examining the 5% participation rate results, both within-session and within-week flexibility demonstrate the same ordering of dispatch mechanisms: RTP produces the most savings, followed by DLC-LE, TOU-1-2, and TOU-4-4; however, the amount of difference across mechanisms is much more pronounced for within-week flexibility than within-session flexibility. For example, for within-week flexibility, RTP produces 132% more and TOU-4-4 produces 68% less production cost savings than DLC-LE, but for within-session flexibility, RTP produces only 16% more and TOU-4-4 produces only 50% less production cost savings than DLC-LE. For higher participation rates, DLC-LE clearly reduces production costs the most and within-week flexibility reduces production costs 20%–25% more than within-session flexibility.

To complete our analysis, we estimate two more value streams for these 16 points: avoided firm capacity and CO_2 emission reductions. We estimate the firm capacity avoided by EVMC using the top 100 hours of net-load heuristic described in Section 5.1, and we estimate its monetary value using the capacity price range from Gagnon et al. (2021), which is also described in that section. Emissions are an output of each scenario's RT model. We then provide two estimates of bulk system all-in savings of EVMC. The Low estimate uses the lower $75.62/kW-yr ($2016)

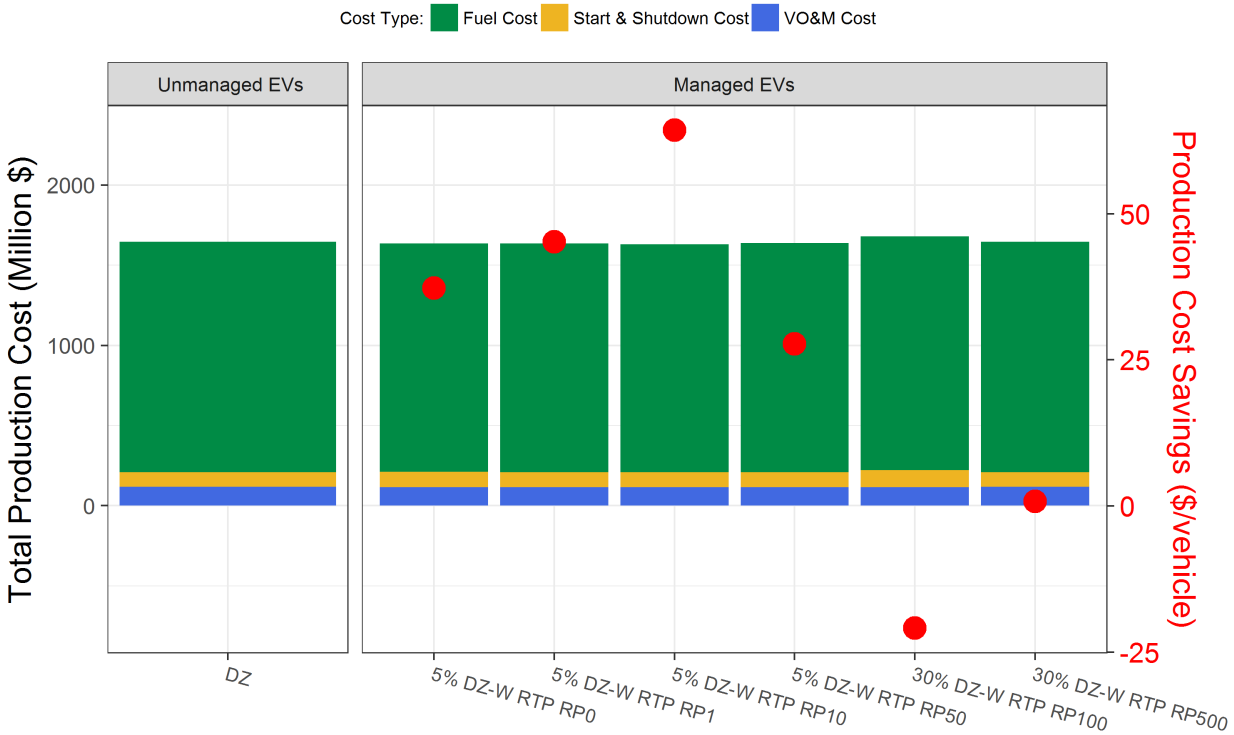

Figure 30. Annual production costs for within-week EVMC realized through RTP response muted with penalties applied to hourly aggregate ramps compared to annual production costs with unmanaged EV charging Multiple ramp penalties are depicted for two participation levels. For example, the four points for 5% participation have ramp penalties of $0/MW, $1/MW, $10/MW, and $50/MW, which are indicated in the figure as RP0, RP1, RP10, and RP50.

capacity price and sets the carbon price to $0/ton. The High estimate uses the higher, $96.81/kW-yr capacity price and sets the carbon price to $45/ton (per Figueroa-Acevedo et al. 2020, also in $2016). These results, along with the production cost savings, are shown in Figure 32 and are summarized along with other key metrics in Table 8.

The highest per-vehicle value is achieved at 5% participation with within-week flexibility and the RTP dispatch mechanism: $92.8/vehicle-yr to $119.6/vehicle-yr. The High estimate includes $65.0/vehicle-yr for production cost savings, $35.9/vehicle-yr for capacity savings, and $18.7/vehicle-yr for emissions reductions. Of course, realizing these savings in practice would require the publication of week-ahead energy price forecasts, to enable week-ahead scheduling of EV charging, which to the authors' knowledge is not a current practice of any U.S. utility or ISO. The optimal within-week, 5% participation RTP dispatch mechanism also assumes a $10/MW aggregate ramp penalty, which implies some coordination or randomization across vehicles is required for this scenario to meet its full potential. The RTP mechanism for within-session flexibility at 5% participation would be easier to implement, as only DA prices are needed and the optimal ramp penalty is $1/MW, but total per-vehicle value in that case is about 58% of the value of within-week flexibility.

At 100% participation and absent price formation processes that both anticipate and incent beneficial price-responsiveness, only the DLC mechanism provides significant bulk power system

Table 7. Optimal Ramp Penalties for the Price-taking Dispatch Mechanisms that Reduce Production Costs by at Least $1/vehicle-yr. Combinations that do not yield sufficient production cost savings for any value of ramp penalty are indicated with dashes.

Participation (%)	Within-session			Within-week		
	RTP	TOU-4-4	TOU-1-2	RTP	TOU-4-4	TOU-1-2
5	1	10	1	10	10	1
30	100	100	—	—	—	—
60	—	—	—	—	—	—
100	—	—	—	—	—	—

value. In this case, the per-vehicle value is only 30% (within-week) to 45% (within-session) of the 5% participation RTP per-vehicle value, but it is still significant: $25.1/vehicle-yr to $36.5/vehicle-yr. The total system benefits assuming within-session flexibility are 4.4% production cost savings, 5.2% emissions savings, and 781 MW of firm capacity. The total system benefits assuming within-week flexibility are 5.6% production cost savings, 6.9% emissions savings, and 834 MW of firm capacity.

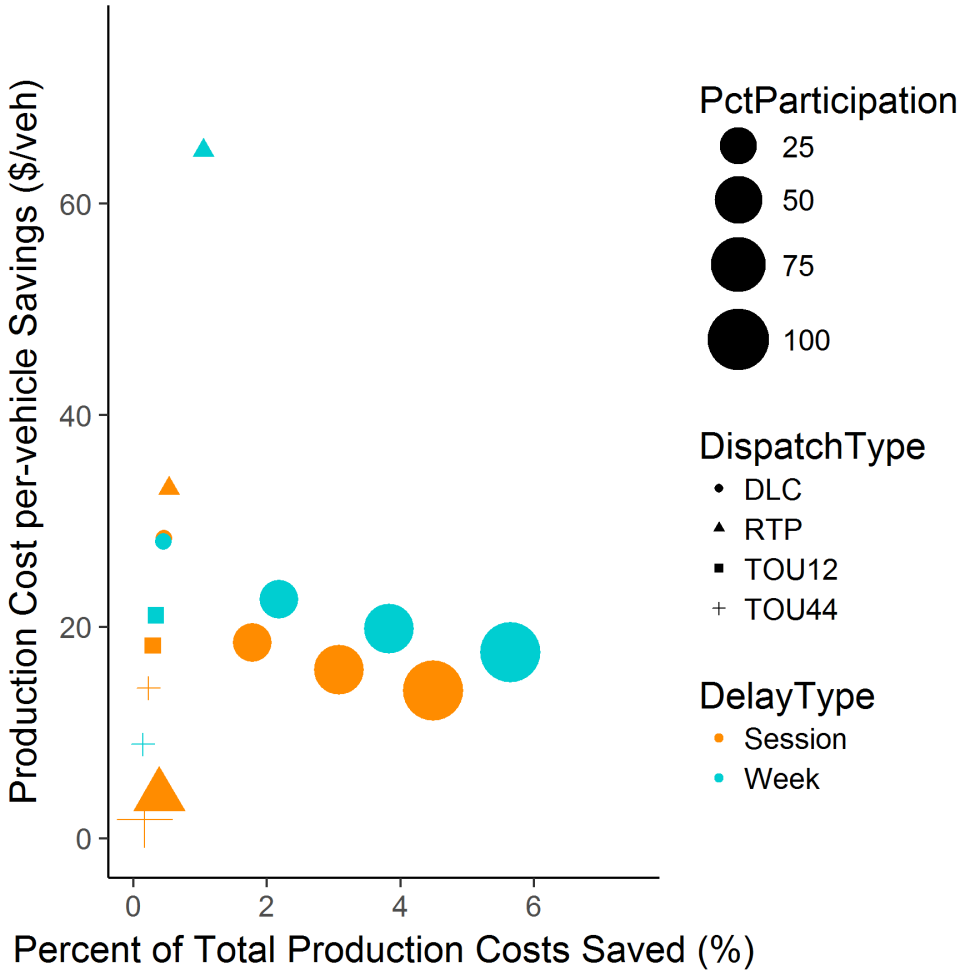

Figure 31. Production cost savings per vehicle and as a percentage of total production costs for 16 combinations of flexibility type, participation rate, and dispatch mechanism. DLC-LE results are provided for all combinations of 5%, 30%, 60% and 100% participation and both flexibility types (within-session and within-week). The other eight points correspond to the non-null ramp penalties listed in Table 7.

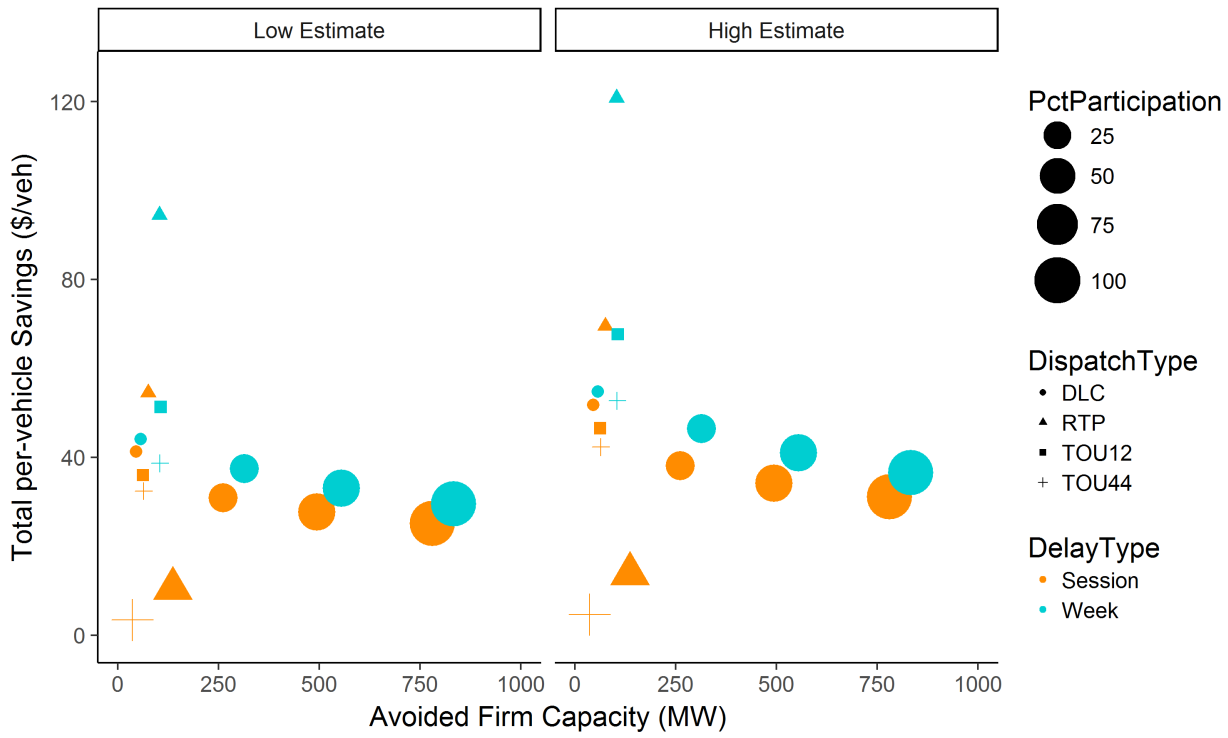

Figure 32. Low and high estimates of total bulk power system cost savings per vehicle for 16 combinations of flexibility type, participation rate, and dispatch mechanism. The Low estimate uses a capacity price of $75.62/kW-yr and values emissions at $0/metric ton CO_2. The High estimate uses a capacity price of $96.81/kw-yr and values emissions at $45/metric ton CO_2. DLC-LE results are provided for all combinations of 5%, 30%, 60% and 100% participation and both flexibility types (within-session and within-week). Results are also reported for the non-null dispatch mechanism and ramp penalty combinations from Table 7.

Table 8. Annual Production Costs, Emissions, Avoided Firm Capacity, and Related Savings Metrics for 16 Combinations of Flexibility Type and Dispatch Mechanism

Participation Rate (%)	Dispatch Mechanism	Production Costs (million $)	Production Cost Savings (million $)	Production Cost Savings ($/vehicle)	Emissions (million metric tons CO_{2e})	Avoided Capacity (MW)	All-In Savings ($/vehicle) Low[a]	All-In Savings ($/vehicle) High[b]
Reference Scenario								
0	Unmanaged	1,646	0	0	6.37	0	0	0
Within-Session Flexibility								
5	DLC-LE	1,639	7.5	28.4	6.33	45.2	42.3	52.6
	RTP, RP1	1,638	8.8	33.1	6.32	75.2	54.7	69.0
	TOU-4-4, RP10	1,643	3.8	14.2	6.34	63.9	32.6	42.6
	TOU-1-2, RP1	1,642	4.8	18.2	6.34	62.3	35.6	45.8
30	DLC-LE	1,617	29.4	18.5	6.24	261.3	31.2	38.3
	RTP, RP100	1,640	6.3	4.0	6.32	136.1	10.8	14.0
	TOU-4-4, RP100	1,644	2.8	1.8	6.34	35.8	3.5	4.8
60	DLC-LE	1,596	50.6	15.9	6.14	493.7	27.7	34.3
100	DLC-LE	1,573	73.9	14.0	6.04	780.9	25.1	31.0
Within-Week Flexibility								
5	DLC-LE	1,639	7.4	28.0	6.33	56.2	45.5	56.6
	RTP, RP10	1,630	17.2	65.0	6.26	103.2	92.8	119.6
	TOU-4-4, RP10	1,644	2.4	8.9	6.34	104.5	40.4	53.7
	TOU-1-2, RP1	1,641	5.6	21.1	6.33	105.9	52.1	67.2
30	DLC-LE	1,611	35.9	22.6	6.20	313.4	37.4	46.4
60	DLC-LE	1,584	63.1	19.8	6.07	554.5	32.9	40.9
100	DLC-LE	1,554	92.9	17.5	5.93	833.6	29.4	36.5

[a] Low all-in savings includes production cost savings and avoided firm capacity valued at $75.62/kW-yr.

[b] High all-in savings includes production cost savings, avoided firm capacity valued at $96.81/kW-yr, and emissions savings valued at $45/ton.

6 Discussion

In this study, we explore how the bulk power system value of EVMC (V1G) changes with participation rate, dispatch mechanism, and flexibility type while keeping the total number of EVs and the composition of the power system fixed. Our context is a future ISO-NE power system with 84% clean, within-ISO generation, 26% of load served by net imports, and a passenger LDV fleet that is 45% electrified. On a per-vehicle basis, we find production cost savings of $14–$65 per vehicle-yr, CO_2 emissions reductions of 0.1–0.4 metric tons CO_2 per vehicle-yr, net-peak load reductions of 0.1–0.4 kW/vehicle-yr, and increases in use of within-ISO generation of 76–249 kWh/vehicle-yr. These metrics largely fit within the review findings of Anwar et al. (2022) of "cost savings between $15-$360 per EV per year, CO_2 emissions of -0.1 to 2.5 metric tons CO_2 per EV per year, peak load reductions of 0.2-3.3 kW per EV, and VRE curtailment reduction of 23-2400 kW h per EV per year." Unsurprisingly, our ranges are also tighter than those of Anwar et al. (2022), because this study only examines a single power system with a single EV build-out assuming V1G and examining only personal passenger LDVs.

Unique to our study, we examine EVMC value starting from heterogeneous, vehicle-level simulations of household vehicle adoption and use, and we compare within-session to within-week charging flexibility while preserving EV mobility service. This approach lets us illustrate the benefits and limitations of price-taking dispatch mechanisms like RTP and TOU, the implementation challenges of operating a DLC program, and the additional value that could be unlocked by scheduling charging over several days to a week rather than simply shifting charging times during fixed charging sessions. We generally find that:

- Price-taking dispatch mechanisms can provide similar amounts to, or more value than, DLC at low participation rates (e.g., 5% of study vehicles, which corresponds to active participation by 2% of the passenger LDV fleet).
- Even at low participation levels, price-taking dispatch mechanisms provide more value when paired with some sort of coordination or muting of response (i.e., in our study, it was helpful to partially coordinate RTP and TOU responses via a small ramp penalty on the aggregate flexibility profile even at 5% participation).
- Simple price-taking dispatch in which the EVMC response is unanticipated by the price formation process and DA UC decisions breaks down at fairly modest participation rates (e.g., at less than 30% of study vehicles, which corresponds to active participation by 14% of the passenger LDV fleet).
- In contrast, DLC works well over the full range of participation rates, with the caveat that naïve aggregation of vehicle-level flexibility significantly overestimates megawatt-scale flexibility (DLC-OA).
- Simple scaling of aggregate flexibility parameters can yield megawatt-scale resources for which the requested dispatch is likely to be approximately feasible (low, but nonzero expected mean absolute error, DLC-LE), but in our study this requires approximately halving the capability of the naive "outer approximation."
- Less-aggressive scaling of key parameters (i.e., ability to delay charging energy for within-session flexibility and ability to delay charging energy and ability to reduce charging power

for within-week flexibility) can yield megawatt-scale resources whose realized dispatch is likely to differ significantly from the initial request but is also likely to maximize expected revenue on net (DLC-MR).

- Depending on the metric, within-week flexibility can be 70%–100% more valuable than within-session flexibility at low participation rates (5%, RTP), but the effect is muted at higher participation rates, dropping to 15%–25% at moderate (30%, DLC-LE) and higher (100%, DLC-LE) participation rates.

Some of the challenges we identify with these dispatch mechanisms are likely straightforward for aggregators, utilities, and ISOs to overcome through actual operation of gradually implemented EVMC programs. Charging patterns induced by TOU rates can be learned and then anticipated in operational load forecasts. Aggregators can bid their flexibility into ISO markets and learn how they should interface with both individual vehicles and the markets to maximize revenues. Various stakeholders can think through which devices (e.g., vehicles, chargers, smart phones, utility meters) should take measurements, communicate signals, compute charging schedules, and actuate charging, and all the data that are collected can be used to guide, troubleshoot, and improve EVMC systems. However, some of the phenomena documented in this study represent fundamental issues aggregators, utilities, and ISOs should be aware of, namely:

- Responses to RTP and TOU rates may need to be dampened or smoothed in some way, even at low participation rates.
- At low participation rates, allowing vehicles to respond directly to RTPs could be the simplest and most valuable approach to implementing EVMC, but we are unaware of clear guidance on how to effectively design and operate an RTP program (for any form of demand flexibility) at high participation rates.
- The dispatch profiles requested of megawatt-scale aggregations of vehicle charging flexibility cannot in general be exactly fulfilled by the individual vehicles in the aggregation even with perfect foresight and control, but through experimentation and experience, it is possible to learn and productively work with error rate distributions.
- Megawatt-scale aggregations can be tuned to be low error or maximum revenue. If insufficient care is taken, they can produce both high error rates and low revenue.
- It is possible to dispatch pseudo-storage resources representing EVMC alongside utility-scale resources in UC and economic dispatch models, but doing so can be computationally challenging, especially for small resources or resources like within-week EVMC that require longer look-ahead times than those currently used in ISO markets.

The modeling we did for this study could be improved or extended in several ways:

- Instead of assuming all EVs can plug in whenever they are parked (i.e., ubiquitous charging) and there are no distribution-level constraints on the amount of EV charging that can occur in any one place at any one time, we would like to construct realistic infrastructure scenarios and directly examine the trade-offs between charger, distribution, and transmission infrastructure costs, including enablement costs for different EVMC dispatch mechanisms, and the bulk power system value of EVMC. In general, the more charging,

distribution, and transmission capacity there is, the more flexible EV charging can be; but as we have seen, EVMC can bring only so much value to the bulk power system. Given this, what are near-optimal amounts of charger capacity, grid build-out, and communications, controls, and program administration for EVMC from the perspective of balancing costs across the combined EV service equipment (EVSE) and power systems?

- To ensure comparability between runs and generally simplify the modeling tasks, in our PCM, we captured imports, exports, and hydropower dispatch as fixed time series in both the DA and RT models; and we fixed pumped hydropower storage and EVMC dispatch in the RT in all cases. In practice, all these resources are dynamic and to the extent possible should be actively scheduled in both the DA and RT time frames. Our study results are also limited to one power system—a single region and a single model year. A future study could examine more regions or more grid scenarios, or it could examine the interplay of EV adoption, grid build out, and EVMC at a national scale over a decadal time horizon using a capacity expansion model.
- Finally, related to our EV flexibility modeling, as mentioned earlier, we would like to adjust our within-week envelope creation method to be less asymmetric. The data created for this study tends to overly limit flexibility early in the week relative to later in the week. We would also like to study disaggregation and price formation processes in more detail. Perhaps by studying a smaller system we could fully simulate the aggregation and disaggregation processes and quantify the impact of different SOA aggregates in terms of production costs, revenues, and dispatch error statistics, fully accounting for both DA and RT UC and dispatch processes. A study setting like this could also be used to explore whether there are straightforward ways to compute and respond to RTP and TOU prices that work even at high participation rates.

7 Conclusions

This report presents a new methodology for evaluating the value of EVMC in bulk power systems as well as results for an envisioned 2038 New England power system with 84% clean, within-ISO generation. The new methods start from detailed and heterogeneous simulations of EV adoption, use, and charging for each county in New England. An All EV Sales by 2035 scenario generates vehicle adoption results out to 2050. The charging flexibility (V1G) of the projected 2038 New England EV fleet of 5.3 million vehicles (45% of all personal passenger LDVs) is then analyzed in detail with the help of three simulated charging profiles that, in pairs, describe mobility-preserving vehicle-level within-charging session and within-week flexibility. Simple dynamic models of individual vehicle flexibility are directly dispatched against hourly RTP and season-block TOU price signals and are aggregated into megawatt-scale, battery-like flexibility resources suitable for direct inclusion in large-scale grid models. The value of EVMC in terms of reducing production costs, avoiding firm capacity, reducing emissions, and reducing transmission congestion is evaluated in a nodal, DCOPF production cost model of an envisioned 2038 New England power system developed from the SEAMS study's national-scale PLEXOS model.

As expected, per-vehicle value is highest at low participation rates, system cost and emissions savings are highest at high participation rates, within-week flexibility is more valuable than within-charging session flexibility, and price-taking by individual vehicles can work as well or better than direct load control at low participation rates. Less expected was that in some cases within-week flexibility is only about 10%–20% more valuable than within-session flexibility, but this may be due in part to modeling challenges, and to RTP and TOU responses needing to be anticipated in the DA UC model at modest EVMC participation rates (e.g., by the time 14% of all vehicles are actively participating). In this technical potential study, the value of EVMC to the bulk power system is significant: up to $119.6/vehicle-yr at low participation rates and up to $36.5/vehicle-yr at 100% participation, inclusive of production cost savings, capacity value, and emissions savings value, assuming a 2016 dollar-year, a capacity price of $96.81/kW-yr, and an emissions reduction value of $45/metric ton CO_2. Nonetheless, that value is modest when considered as an upper bound on a potential monthly incentive payment ($3–$10 per vehicle-month) for participation in an EVMC program that does not yet factor in enablement costs, assumes a charger is always available, and assumes perfect foresight of mobility needs. That said, the potential benefits to the overall system are significant: up to 5.6% of production costs and 6.9% of emissions could be avoided by effective EVMC programs operated at scale in this particular example.

References

Anwar, M. B., M. Muratori, P. Jadun, E. Hale, B. Bush, P. Denholm, O. Ma, and K. Podkaminer. 2022. "Assessing the value of electric vehicle managed charging: a review of methodologies and results" [in en]. *Energy & Environmental Science:* 10.1039.D1EE02206G. ISSN: 1754-5692, 1754-5706, accessed February 4, 2022. doi:10.1039/D1EE02206G. http://xlink.rsc.org/?DOI=D1EE02206G.

Biden, J. 2021. *Executive Order on Strengthening American Leadership in Clean Cars and Trucks,* August. https://www.whitehouse.gov/briefing-room/presidential-actions/2021/08/05/executive-order-on-strengthening-american-leadership-in-clean-cars-and-trucks/.

Black, D., J. MacDonald, N. DeForest, and C. Gehbauer. 2018. *Los Angeles Air Force Base Vehicle-to-Grid Demonstration* [in en]. Technical report. Lawrence Berkeley National Laboratory, California Energy Commission, October. https://ww2.energy.ca.gov/2018publications/CEC-500-2018-025/CEC-500-2018-025.pdf.

Bloom, A., J. Novacheck, G. Brinkman, J. McCalley, A. Figueroa-Acevedo, A. Jahanbani-Ardakani, H. Nosair, et al. 2022. "The Value of Increased HVDC Capacity Between Eastern and Western U.S. Grids: The Interconnections Seam Study." Conference Name: IEEE Transactions on Power Systems, *IEEE Transactions on Power Systems* 37, no. 3 (May): 1760–1769. ISSN: 1558-0679. doi:10.1109/TPWRS.2021.3115092.

CEC. 2019. *Distribution System Constrained Vehicle-to- Grid Services for Improved Grid Stability and Reliability* [in en]. Technical report CEC-500-2019-027. California Energy Commission (CEC), March. https://ww2.energy.ca.gov/2019publications/CEC-500-2019-027/CEC-500-2019-027.pdf.

Cochran, J., P. Denholm, M. Mooney, D. Steinberg, E. Hale, G. Heath, B. Palmintier, et al. 2021a. *LA100: The Los Angeles 100% Renewable Energy Study - Executive Summary.* Technical report. National Renewable Energy Laboratory, March. Accessed March 29, 2021. https://www.nrel.gov/docs/fy21osti/79444-ES.pdf.

———. 2021b. *The Los Angeles 100% Renewable Energy Study (LA100)* [in English]. Technical report NREL/TP-6A20-79444. National Renewable Energy Lab. (NREL), Golden, CO (United States), March. Accessed January 5, 2022. doi:10.2172/1774871. https://www.osti.gov/biblio/1774871.

Cohen, S. M., J. Becker, D. A. Bielen, M. Brown, W. J. Cole, K. P. Eurek, A. Frazier, et al. 2019. *Regional Energy Deployment System (ReEDS) Model Documentation: Version 2018* [in English]. Technical report NREL/TP-6A20-72023. National Renewable Energy Lab. (NREL), Golden, CO (United States), April. Accessed January 5, 2022. doi:10.2172/1505935. https://www.osti.gov/biblio/1505935/.

Cole, W. J., J. D. Rhodes, W. Gorman, K. X. Perez, M. E. Webber, and T. F. Edgar. 2014. "Community-scale residential air conditioning control for effective grid management" [in en]. *Applied Energy* 130 (October): 428–436. ISSN: 0306-2619, accessed June 24, 2022. doi:10.1016/j.apenergy.2014.05.067. https://www.sciencedirect.com/science/article/pii/S0306261914005728.

Conference of the New England Governors and Eastern Canadian Premiers. 2017. *2017 Update of the Regional Climate Change Action Plan: Building on Solid Foundations.* Technical report. Charlotteetown, Prince Edward Island: Eastern Canadian Secretariat, Coalition of Northeastern Governors, August. Accessed June 24, 2022. https://www.coneg.org/wp-content/uploads/2019/01/2017-rccap-final.pdf.

Corradi, O., H. Ochsenfeld, H. Madsen, and P. Pinson. 2013. "Controlling Electricity Consumption by Forecasting its Response to Varying Prices." Conference Name: IEEE Transactions on Power Systems, *IEEE Transactions on Power Systems* 28, no. 1 (February): 421–429. ISSN: 1558-0679. doi:10.1109/TPWRS.2012.2197027.

Das, S., and D. Sanchari. 2020. *Vehicle-Grid Integration: A New Frontier for Electric Mobility in India.* Technical report. New Delhi: Alliance for an Energy Efficient Economy, October. Accessed December 14, 2020. https://aeee.in/wp-content/uploads/2020/10/Full-Report-Vehicle-Grid-Integration-AEEE.pdf.

David, A., and Y. Li. 1993. "Effect of inter-temporal factors on the real time pricing of electricity." Conference Name: IEEE Transactions on Power Systems, *IEEE Transactions on Power Systems* 8, no. 1 (February): 44–52. ISSN: 1558-0679. doi:10.1109/59.221247.

Denholm, P., Y. Sun, and T. Mai. 2019. *Introduction to Grid Services: Concepts, Technical Requirements, and Provisions from Wind.* Technical report NREL/TP-6A20-72578. National Renewable Energy Laboratory (NREL), January. https://www.nrel.gov/docs/fy19osti/72578.pdf.

EIA. 2017. *Annual Energy Outlook 2017 with projections to 2050.* Technical report. Washington, D.C.: U.S. Energy Information Association (EIA), January. Accessed October 17, 2017. https://www.eia.gov/outlooks/aeo/.

Figueroa-Acevedo, A. L., A. J. Ardakani, H. Nosair, A. Venkatraman, J. D. McCalley, A. Bloom, D. Osborn, et al. 2020. "Design and Valuation of High-Capacity HVDC Macrogrid Transmission for the Continental US." Conference Name: IEEE Transactions on Power Systems, *IEEE Transactions on Power Systems:* 1–1. ISSN: 1558-0679. doi:10.1109/TPWRS.2020.2970865.

Gagnon, P., W. Frazier, W. Cole, and E. Hale. 2021. *Cambium Documentation: Version 2021* [in English]. Technical report NREL/TP-6A40-81611. Golden, CO (United States): National Renewable Energy Laboratory (NREL), December. Accessed June 3, 2022. doi:10.2172/1835075. https://www.osti.gov/biblio/1835075.

Guo, J., J. Yang, Z. Lin, C. Serrano, and A. M. Cortes. 2019. "Impact Analysis of V2G Services on EV Battery Degradation -A Review." In *2019 IEEE Milan PowerTech,* 1–6. June. doi:10.1109/PTC.2019.8810982.

Hale, E., M. Leach, B. Cowiestoll, Y. Lin, and D. Levie. 2022. *Physically Realistic Estimates of Electric Water Heater Demand Response Resource: Methods and a Case Study.* Technical Report NREL/TP-6A40-82315. Golden, CO (United States): National Renewable Energy Laboratory (NREL).

Hao, H., B. M. Sanandaji, K. Poolla, and T. L. Vincent. 2013. "A generalized battery model of a collection of thermostatically controlled loads for providing ancillary service." In *Communication, Control, and Computing (Allerton), 2013 51st Annual Allerton Conference on,* 551–558. IEEE.

———. 2015. "Aggregate Flexibility of Thermostatically Controlled Loads." *IEEE Transactions on Power Systems* 30, no. 1 (January): 189–198. ISSN: 1558-0679. doi:10.1109/TPWRS.2014.2328865.

ISO-NE. 2022. *2021 Net Energy and Peak Load by Source.* Accessed June 29, 2022. https://www.iso-ne.com/isoexpress/web/reports/load-and-demand/-/tree/net-ener-peak-load.

Jacobsen, M. R., and A. A. van Benthem. 2015. "Vehicle Scrappage and Gasoline Policy" [in en]. *American Economic Review* 105, no. 3 (March): 1312–1338. ISSN: 0002-8282, accessed May 10, 2022. doi:10.1257/aer.20130935. https://www.aeaweb.org/articles?id=10.1257/aer.20130935.

Jorgenson, J., S. Awara, G. Stephen, and T. Mai. 2021. *Comparing Capacity Credit Calculations for Wind: A Case Study in Texas* [in English]. Technical Report NREL/TP-5C00-80486. Golden, CO (United States): National Renewable Energy Laboratory (NREL), September. Accessed June 21, 2022. doi:10.2172/1823456. https://www.osti.gov/biblio/1823456.

Kaluza, S., D. Almeida, and P. Mullen. 2016. *BMW i ChargeForward: PG&E's Electric Vehicle Smart Charging Pilot.* Technical report. A cooperation between BMW Group, Pacific Gas, and Electricity Company. Accessed March 18, 2019. http://www.pgecurrents.com/wp-content/uploads/2017/06/PGE-BMW-iChargeForward-Final-Report.pdf.

Ma, Z., D. S. Callaway, and I. A. Hiskens. 2013. "Decentralized Charging Control of Large Populations of Plug-in Electric Vehicles." Conference Name: IEEE Transactions on Control Systems Technology, *IEEE Transactions on Control Systems Technology* 21, no. 1 (January): 67–78. ISSN: 1558-0865. doi:10.1109/TCST.2011.2174059.

Mai, T., P. Jadun, J. Logan, C. McMillan, M. Muratori, D. Steinberg, L. Vimmerstedt, B. Haley, R. Jones, and B. Nelson. 2018. *Electrification Futures Study: Scenarios of Electric Technology Adoption and Power Consumption for the United States.* Technical Report NREL/TP-6A20-71500. Golden, Colorado: National Renewable Energy Laboratory. https://www.nrel.gov/docs/fy18osti/71500.pdf.

McKenna, K., and A. Keane. 2016. "Residential Load Modeling of Price-Based Demand Response for Network Impact Studies." *IEEE Transactions on Smart Grid* 7, no. 5 (September): 2285–2294. ISSN: 1949-3053. doi:10.1109/TSG.2015.2437451.

Muratori et al. 2021. "The Rise of Electric Vehicles – 2020 Status and Future Expectations." *Progress in Energy* 3, no. 2 (March): 022002. https://iopscience.iop.org/article/10.1088/2516-1083/abe0ad.

Muratori, M. 2018. "Impact of uncoordinated plug-in electric vehicle charging on residential power demand." Publisher: Nature Publishing Group, *Nature Energy* 3 (3): 193–201.

Muratori, M., P. Jadun, B. Bush, D. Bielen, L. Vimmerstedt, J. Gonder, C. Gearhart, and D. Arent. 2020. "Future integrated mobility-energy systems: A modeling perspective" [in en].

Renewable and Sustainable Energy Reviews 119 (March): 109541. ISSN: 1364-0321, accessed February 4, 2022. doi:10.1016/j.rser.2019.109541. https://www.sciencedirect.com/science/article/pii/S136403211930749X.

Muratori, M., P. Jadun, B. Bush, C. Hoehne, L. Vimmerstedt, A. Yip, J. Gonder, E. Winkler, C. Gearhart, and D. Arent. 2021. "Exploring the future energy-mobility nexus: The transportation energy & mobility pathway options (TEMPO) model" [in en]. *Transportation Research Part D: Transport and Environment* 98 (September): 102967. ISSN: 1361-9209, accessed February 4, 2022. doi:10.1016/j.trd.2021.102967. https://www.sciencedirect.com/science/article/pii/S1361920921002650.

Muratori, M., and T. Mai. 2020. "The shape of electrified transportation." Publisher: IOP Publishing, *Environmental Research Letters* 16 (1): 011003.

Murphy, C., T. Mai, Y. Sun, P. Jadun, M. Muratori, B. Nelson, and R. Jones. 2021. *Electrification futures study: Scenarios of power system evolution and infrastructure development for the united states.* Technical report. National Renewable Energy Lab.(NREL), Golden, CO (United States).

Noel, L., G. Zarazua de Rubens, J. Kester, and B. Sovavool. 2019. *Vehicle-to-Grid: A Sociotechnical Transition Beyond Electric Mobility* [in en]. Energy, Climate and the Environment (ECE). Palgrave Macmillan. ISBN: 978-3-030-04863-1, accessed May 10, 2022. https://link.springer.com/book/10.1007/978-3-030-04864-8.

Roozbehani, M., M. A. Dahleh, and S. K. Mitter. 2012. "Volatility of Power Grids Under Real-Time Pricing." Conference Name: IEEE Transactions on Power Systems, *IEEE Transactions on Power Systems* 27, no. 4 (November): 1926–1940. ISSN: 1558-0679. doi:10.1109/TPWRS.2012.2195037.

Ruth, M. F., M. S. Lunacek, and B. Jones. 2017. *Impacts of Using Distributed Energy Resources to Reduce Peak Loads in Vermont* [in English]. Technical Report NREL/TP-6A20-70312; DOE/GO-102017-5057. Golden, CO (United States): National Renewable Energy Laboratory (NREL), November. Accessed June 24, 2022. doi:10.2172/1411137. https://www.osti.gov/biblio/1411137.

Seel, J., and A. D. Mills. 2021. *Integrating Cambium Marginal Costs into Electric Sector Decisions: Opportunities to Integrate Cambium Marginal Cost Data into Berkeley Lab Analysis and Technical Assistance* [in English]. Technical report. Berkeley, CA (United States): Lawrence Berkeley National Laboratory (LBNL), November. Accessed June 3, 2022. doi:10.2172/1828856. https://www.osti.gov/biblio/1828856/.

SEPA. 2021. *The State of Managed Charging in 2021.* Technical report. Smart Electric Power Alliance (SEPA), November. https://go.sepapower.org/l/124671/2021-11-16/lv5djl?email=paige.jadun%40nrel.gov&first=Paige&last=Jadun&Company=NREL&Title=researcher&&Organization%20Type=Government%2C+Non-Profit+%26+Education.

Stephen, G., E. Hale, and B. Cowiestoll. 2020. *Managing Solar Photovoltaic Integration in the Western United States: Resource Adequacy Considerations.* Technical Report NREL/TP-6A20-72472. Golden, CO: National Renewable Energy Laboratory.

Szinai, J. K., C. J. Sheppard, N. Abhyankar, and A. R. Gopal. 2020. "Reduced grid operating costs and renewable energy curtailment with electric vehicle charge management." Publisher: Elsevier, *Energy Policy* 136:111051.

Wood, E., C. Rames, M. Muratori, Sesha Raghavan, and M. Melaina. 2017. "NATIONAL PLUG-IN ELECTRIC VEHICLE INFRASTRUCTURE ANALYSIS" [in en]. Accessed February 22, 2022. doi:10.13140/RG.2.2.25881.93280. http://rgdoi.net/10.13140/RG.2.2.25881.93280.

Xi, X., and R. Sioshansi. 2014. "Using Price-Based Signals to Control Plug-in Electric Vehicle Fleet Charging." *IEEE Transactions on Smart Grid* 5, no. 3 (May): 1451–1464. ISSN: 1949-3061. doi:10.1109/TSG.2014.2301931.

Yip, A., C. Hoehne, P. Jadun, C. Ledna, E. Hale, and M. Muratori. n.d. *Spatially and temporally resolved household electric vehicle charging load scenarios for the United States.* Technical Report NREL/TP-5400-83916. Golden, CO (United States): National Renewable Energy Laboratory.

Zhang, C., J. B. Greenblatt, P. MacDougall, S. Saxena, and A. Jayam Prabhakar. 2020. "Quantifying the benefits of electric vehicles on the future electricity grid in the midwestern United States" [in en]. *Applied Energy* 270 (July): 115174. ISSN: 0306-2619, accessed December 12, 2020. doi:10.1016/j.apenergy.2020.115174. http://www.sciencedirect.com/science/article/pii/S0306261920306863.

Zhou, E., and T. Mai. 2021. *Electrification Futures Study: Operational Analysis of US Power Systems with Increased Electrification and Demand-Side Flexibility.* Technical report. National Renewable Energy Lab.(NREL), Golden, CO (United States).

Appendix A. EV Charging Strategy Details

Charging profiles were estimated using the TEMPO model under the scenario assumptions described in chapter 2. The TEMPO model generates trips by household vehicle for a representative week (including 5 weekdays and 2 weekend days) for a sample of households in each model year. Trip data for all EVs are passed to the TEMPO BEV module for processing and estimating charging profiles.

TEMPO trip data are aggregated into nine periods (2–6 hours long) for each day. The BEV module preprocesses these data to add information and enforce a level of realism needed for estimating charging profiles, including:

- Assign trips to a continuous time within the period according to within-period distributions derived from the National Household Travel Survey[15]
- Calculate dwell times between trips that can be used for charging
- Wrap trips that exceed beyond the end of the week to complete at the beginning of the week
- Adjust trip times to avoid simultaneous trips on the same vehicle
- Add dwell times for required DCFC stops for trips that exceed the vehicle range (the monetized time of these charging stops is modeled in TEMPO, but the explicit impact on trip timing/duration is not).

The preprocessing also generates a set of arrays for each vehicle to pass as parameters to the charging strategy formulation described below.

The TEMPO BEV module includes multiple charging strategies to achieve different objectives. Charging profiles are computed in two steps: optimization and postprocessing. During optimization, either the Greedy or Min Charges strategy is specified. In postprocessing, charging can be shifted toward the beginning (Immediate) or the end (Delayed) of each selected charging session. The charging strategies described in the report map to the TEMPO BEV module as follows. The Immediate charging strategy is computed using the Greedy optimization formulation postprocessed under Immediate charging assumptions. The Delayed charging strategy also uses the Greedy optimization formulation but postprocessed for Delayed charging. The Min Chargees and Delayed strategy uses the Min Charges optimization formulation and the Delayed charging postprocessing step.

A.1 Optimization

The Greedy strategy is formulated as a linear program, and it maximizes the SOC over the modeled week. The Min Charges strategy minimizes the number of charges required to complete all trips, and it is formulated as a mixed integer program. Min Charges only applies to BEVs, as minimizing PHEV charging events would result in no charging. In addition to the primary objective of the charging strategies, the formulation includes constraints to maximize PHEV electricity use and to adjust trips to accommodate additional charging stops if consecutive trips results in a negative SOC due to insufficient dwell time for charging.

[15] https://nhts.ornl.gov/

A.1.1 Primary Formulation

This section details the model sets, parameters, variables, constraints, and objective functions for the TEMPO charging strategies applied at the individual vehicle level.

Table A.1. Set and Element Symbols

Symbol	Description
E	Set of all vehicle events (events include both trips and dwell times for the vehicle, where dwell times allow for charging opportunities)
e	Event

Table A.2. Index Sets

Symbol	Description
$e \in E$	Events, indexed from 1...|E|, the number of events

Table A.3. Subsets

Symbol	Description
$N \subset E$	Subset of vehicle events excluding the final event, |E|
$T \subset E$	Subset of vehicle events when trips occur

Table A.4. Parameters

Symbol	Description
c_e	Energy consumption of event e, which is positive only for trip events (kWh)
p_e	Power available for charging at event e, which is positive only for dwell time events (kW)
t_e	Start time of event e (hours)
d_e	Duration of event e (hours)
f	final hour of modeled time horizon
$\overline{b}$	maximum battery capacity of modeled vehicle (kWh)
$\underline{b}$	minimum desired state of charge of battery for modeled vehicle (kWh)
$\|E\|$	Number of events

Table A.4. Continued

Symbol	Description
W^{def}	Weighting parameter to penalize a charge deficit below $\underline{b}$
W^{phev}	Weighting parameter to maximize electricity consumption for PHEVs

Table A.5. Variables

Symbol	Description
σ_e	(continuous) State of charge of vehicle battery at start of event e (kWh)
δ_e	(continuous) Change in battery state of charge for event e due to charging (kWh)
μ_e	(continuous) Difference between σ_e and $\underline{b}$ at the start of event e (kWh)
ρ_e	(continuous) Electricity consumption of PHEV vehicle of event e (kWh)
χ_e	(binary) Specifies if a charge session occurred during event e (only used in Min Charges strategy)

Constraints

General constraints applicable to all vehicles and charging strategies enforce bounds on vehicle SOC, positive vehicle charging events, and the same beginning and ending vehicle SOC. The μ_e decision variable is used to enforce a soft constraint to maintain vehicle SOC above $\underline{b}$ unless required to complete a trip, where μ_e is only positive if $\sigma_e < \underline{b}$:

$$\sigma_e \leq \overline{b},\ \forall e \in E \tag{A.1}$$

$$\sigma_e \geq 0,\ \forall e \in E \tag{A.2}$$

$$\mu_e \geq 0,\ \forall e \in E \tag{A.3}$$

$$\mu_e \geq \underline{b} - \sigma_e,\ \forall e \in E \tag{A.4}$$

$$\delta_e \geq 0,\ \forall e \in E \tag{A.5}$$

$$\sigma_1 = \sigma_{|E|} \tag{A.6}$$

For the Greedy strategy, charging is constrained by available charger power capacity over the duration of the event:

$$\delta_e \leq p_e \cdot d_e,\ \forall e \in E. \tag{A.7}$$

For the Min Charges strategy, charging is additionally constrained by whether there is an active charging session, specified by χ_e:

$$\delta_e \leq p_e \cdot d_e \cdot \chi_e,\ \forall e \in E. \tag{A.8}$$

For BEVs, the difference in the state of charge from one event to the next equals the reduction from energy consumption (c_e) of the event plus the increase from charging (δ_e), and no PHEV electricity use (ρ_e) occurs:

$$\sigma_{e+1} = \sigma_e + \delta_e - c_e, \ \forall e \in N \tag{A.9}$$

$$\rho_e = 0, \ \forall e \in E. \tag{A.10}$$

For PHEVs, the difference in the state of charge from one event to the next equals the increase from charging (δ_e) minus electricity consumption (ρ_e), which must be greater than zero and less than both the total battery capacity ($\overline{b}$) and the event's total energy consumption (c_e):

$$\rho_e \leq \overline{b}, \ \forall e \in E \tag{A.11}$$

$$\rho_e \leq c_e, \ \forall e \in E \tag{A.12}$$

$$\rho_e \geq 0, \ \forall e \in E \tag{A.13}$$

$$\sigma_{e+1} = \sigma_e + \delta_e - \rho_e, \ \forall e \in N \tag{A.14}$$

Greedy Objective Function

The Greedy objective function maximizes accumulated state of charge (σ_e) and amount of PHEV travel served by electricity (ρ_e) while minimizing extent to which battery charge is less than the desired minimum level (μ_e):

$$\max \sum_{e \in E} \sigma_e - \mu_e \cdot W^{def} + \rho_e \cdot W^{phev} \tag{A.15}$$

Min Charges Objective Function

The basic Min Charges objective function minimizes the number of charging events (χ_e) and the extent to which battery charge is less than the desired minimum level (μ_e):

$$\min \sum_{e \in E} \chi_e + \mu_e \cdot W^{def} \tag{A.16}$$

In this analysis, the Min Charges objective function also includes a term to maximize the initial state of charge, σ_1, for additional consistency with the Greedy strategy. We subtract σ_1 from the objective function, which can be weighted more or less heavily than χ_e, depending on the goal of the strategy (e.g., should an additional charge occur in order to maximize SOC at the beginning of the week).

A.1.2 Adjustments for Infeasible Trip Sequences

This analysis estimates aggregate flexibility resources based on individual vehicle profiles, as described in chapter 4, requiring realistic and feasible vehicle-level charging profiles. The core TEMPO model does not represent detailed charging behavior when estimating trip choices; thus in some cases, TEMPO could project infeasible sequences of trips for a modeled BEV (e.g., if too many trips are selected in a given period without sufficient charging time), resulting in an infeasible model given the formulation above. To adjust for this, we add the formulation below

to allow for the shifting of trips and dwell times to achieve feasible trip behavior (trip duration is not adjusted). The shifting of trips is highly penalized in the objective function, and it only occurs if the model is otherwise infeasible. This formulation requires binary variables; thus, the Greedy strategy becomes a mixed integer program instead of linear.

Table A.6. Additional Variables for Infeasible Trip Adjustments

Symbol	Description
τ_e	(continuous) Adjusted start time of event e (hours)
λ_e	(continuous) Adjusted duration of event e (hours)
ψ_e	(binary) Value specifying whether trip event e was adjusted to accommodate additional charging
γ_e	(continuous) Modified adjusted duration variable dependent on the value of χ_e for event to avoid a quadratic formulation e (hours)

Table A.7. Additional Parameters for Infeasible Trip Adjustments

Symbol	Description
f	Final time of the modeling horizon
L	Large constant used to assign a binary value of 1 for each adjusted trip
W^{time}	Weighting parameter to penalize the change in start times of adjusted trips
W^{trip}	Weighting parameter to the number of trips adjusted

Constraints

$$\lambda_e \geq 0,\ \forall e \in E \tag{A.17}$$

$$\lambda_e = d_e,\ \forall e \in T \tag{A.18}$$

$$\tau_{e+1} = \tau_e + \lambda_e,\ \forall e \in N \tag{A.19}$$

$$\tau_{e+1} \geq t_e,\ \forall e \in E \tag{A.20}$$

$$\psi_e \cdot L \geq \lambda_e - d_e,\ \forall e \in E \tag{A.21}$$

For the sake of simplicity in the current analysis, we do not allow shifting of trips past the end of the week, as enforced with the following constraints:

$$f \geq \tau_e + \lambda_e,\ \forall e \in N \tag{A.22}$$

$$f = \tau_{|E|} + \lambda_{|E|} \tag{A.23}$$

For Min Charges, to avoid a quadratic model formulation when replacing d_e with λ_e in equation A.8, we calculate a new variable, γ_e, which equals 0 if $\chi_e = 0$ (no charge session occurred during event e) and equals λ_e if $\chi_e = 1$ (a charge session occurred during event e):

$$\gamma_e \leq f \cdot \chi_e, \ \forall e \in E \tag{A.24}$$

$$\gamma_e \leq \lambda_e, \ \forall e \in E \tag{A.25}$$

To account for the adjusted dwell time duration, equation A.7 is then changed to equation A.26 for the Greedy strategy, and equation A.8 is changed to equation A.27 for Min Charges:

$$\delta_e \leq p_e \cdot \lambda_e, \ \forall e \in E \tag{A.26}$$

$$\delta_e \leq p_e \cdot \gamma_e, \ \forall e \in E \tag{A.27}$$

Finally, the following parameters are added to the summations in the respective objective functions to penalize both the time that trips may be shifted and the number of trips shifted: $-(\tau_e - t_e) \cdot W^{time}$, $-\psi_e \cdot W^{trip}$.

A.2 Additional Processing

Following the optimization, the BEV module adjusts the charging time within a dwell session to reflect Immediate or Delayed charging specifications. Under Immediate assumptions, the charging session begins at the beginning of the dwell session, and under Delayed assumptions, the charging session is postponed to as late as possible to reach the maximum SOC allowed by the dwell time. When the maximum SOC cannot be reached in the given dwell time, Immediate and Delayed are equivalent and charging occurs throughout the entire session. Charging energy requirements are also adjusted to reflect the efficiency of EV chargers, resulting in higher energy use than that used onboard the vehicle. The result of the BEV module is a vehicle-level, time-series data set of trips, charging sessions, and associated energy use, for each scenario and charging strategy specification.

Appendix B. Bulk Power System Modeling Details

Fixed imports and exports are estimated from the full 2024 and 2038 SEAMS models aggregated import/export power flow at the boundary nodes. Imports and exports are incorporated as fixed generation and load, respectively, in PLEXOS at interfaces between ISO-NE and neighboring power systems (including DC ties to Quebec). During the early modeling stages, we experienced transmission flow-related infeasibilities due to the large quantity of fixed imports and exports at boundary nodes. We alleviated this issue with a set of 20 300-MW high cost pseudo-generators at the boundary nodes to provide imports/exports flexibility. These pseudo-generators are intended to be used sparingly, and they are not dispatched in any final scenarios except some of the RTP and TOU cases with insufficient ramp penalties (and negative EVMC value). The pseudo-generators are assigned a VO&M cost of $5,000/MWh and start cost of $20,000. The purpose of these values is to ensure pseudo-generators are only used to overcome fixed import/export-related infeasibilites, not to avoid lower-cost penalties like congestion and unserved reserves.

Transmission line limits, which we only enforce on lines at 115 kV and above, are often binding in the 2038 DCOPF model, even before adding EV load. This is because SEAMS is a national-scale study with pipe flow transmission that only captures interregional line limits, large quantities of fixed imports and exports, wind and solar capacity additions located based on resource quality as opposed to transmission availability, and retirements of 77 coal, oil, and gas units totaling 5,448 MW of nameplate capacity. Adding EV load pro rata with existing regional load participation factors increases ISO-NE total load by 13% and exacerbates congestion.

We adjust transmission capacity with a 2038 transmission expansion scenario designed to reduce high price spikes set by thermal limit violation penalties. We increase the transmission capacity of six heavily congested high-voltage (115 kV and above) transmission lines by a total of 658 MW-miles. These additions reduce thermal violation-related price spikes from $1500/MWh to $180/MWh. To determine whether these modeling changes were realistic, we corresponded with ISO-NE transmission planners who said all but one of the line increases was realistic, especially in light of ISO-NE's current efforts to rebuild many lines, a number of which are over a century old. The one increase in capacity that we apply but which might be unrealistic is underground capacity into Boston, which we approximately double to support plant retirements (1,118 MW of the 5,448 MW of retirements in the SEAMS 2038 model compared to the 2024 model are in the Northeast Massachusetts and Boston Load Zone). This detail indicates future grid planners might have to contend with a dynamic similar to what was seen in the LA100 study concerning "in-basin" versus "out-of-basin" resources Cochran et al. 2021b as they decide how to serve this critical load center with 100% clean electricity Conference of the New England Governors and Eastern Canadian Premiers 2017. In the meantime, this is another source of uncertainty in our Reference scenario model of a possible future ISO-NE system.

Appendix C. Aggregation Details

Hao et al. (2013) has demonstrated methods for creating generalized battery models that represent aggregates of thermostatically controlled loads. Here we apply their methods to the simpler case of EVMC, explicitly account for the storage characteristics of DER resources, and discuss the possibility of using these aggregation methods for longer-duration grid services than their context, which was frequency regulation. To do this, we start with a collection of individual charging flexibility models with individual EVs identified with indices $k \in \mathbb{K}$ and express their individual shiftability as:

$$\frac{d\Delta S_k(t)}{dt} = \eta_k(t)\Delta P_k(t) \tag{C.1}$$

$$\underline{\Delta S_k}(t) \leq \Delta S_k(t) \leq \overline{\Delta S_k}(t) \tag{C.2}$$

$$\underline{\Delta P_k}(t) \leq \Delta P_k(t) \leq \overline{\Delta P_k}(t) \tag{C.3}$$

Then, we seek a similar model formulation to represent their aggregate flexibility:

$$\frac{d\Delta S(t)}{dt} = \eta(t)\Delta P(t) \tag{C.4}$$

$$\underline{\Delta S}(t) \leq \Delta S(t) \leq \overline{\Delta S}(t) \tag{C.5}$$

$$\underline{\Delta P}(t) \leq \Delta P(t) \leq \overline{\Delta P}(t) \tag{C.6}$$

Following Hao et al. (2013), the general procedure for estimating the parameters $\eta(t)$, $\underline{\Delta S}(t)$, $\overline{\Delta S}(t)$, $\underline{\Delta P}(t)$, and $\overline{\Delta P}(t)$ required to define the aggregate model is fairly straightforward in the Laplace domain, not in an exact sense, but in the sense of being able to create bounding models. Because we are most concerned with the flexibility realized in terms of the aggregate shifted energy:

$$\sum_k w_k \Delta P_k(t), \tag{C.7}$$

where w_k is a sample weight for individual resource k, the model construction focuses on defining allowable shifting profiles at both the individual and aggregate levels. That is, if we define the sets of possible realizations at the individual level to be:

$$\mathbb{P}_k = \{\Delta P_k(t) \,|\, \exists \Delta S_k(t) \text{ with individual model (C.1) - (C.3) for device } k \in \mathbb{K} \text{ satisfied}\}, \tag{C.8}$$

and the possible realizations for the aggregate to be

$$\mathbb{P}_{\mathbb{K}} = \left\{ \sum_k w_k \Delta P_k(t) \,\middle|\, \Delta P_k(t) \in \mathbb{P}_k, \forall k \in \mathbb{K} \right\}, \tag{C.9}$$

we can work to define pairs of generalized storage model parameters for which the resulting models define sets of allowable power profiles $\Delta P(t)$ that are either strictly smaller or strictly larger than $\mathbb{P}_{\mathbb{K}}$.

To this end, let:

$$\Phi = \left(\eta(t), \underline{\Delta S}(t), \overline{\Delta S}(t), \underline{\Delta P}(t), \overline{\Delta P}(t)\right) \tag{C.10}$$

be any realization of the aggregate storage model and:

$$\mathbb{P}_{\Phi} = \{\Delta P(t) \,|\, \exists \Delta S(t) \text{ with the aggregate model (C.4) - (C.6) defined by } \Phi \text{ satisfied}\}. \quad \text{(C.11)}$$

Then, we seek $\underline{\Phi}$ and $\overline{\Phi}$ such that:

$$\mathbb{P}_{\underline{\Phi}} \subset \mathbb{P}_{\mathbb{K}} \subset \mathbb{P}_{\overline{\Phi}}. \quad \text{(C.12)}$$

Thus, $\underline{\Phi}$ represents a lower-bound, inner-approximation, sufficient estimate of $\mathbb{P}_{\mathbb{K}}$; whereas $\overline{\Phi}$ represents an upper-bound, outer-approximation, necessary estimate of $\mathbb{P}_{\mathbb{K}}$, and the size of the difference between them is a metric of estimate tightness.

C.1 Aggregation of Individual Flexibility Models with Constant Charging Efficiency

The techniques of Hao et al. (2013) are easily applied when η is constant.

Theorem 1. ***Outer Approximation When η is Constant***

Assume η_k in (C.1) is time-invariant for all individual devices $k \in \mathbb{K}$. Then, with an arbitrarily chosen constant η, the aggregate model represented by (C.4) - (C.6) with

$$\underline{\Delta S}(t) = \sum_k w_k \frac{\eta}{\eta_k} \underline{\Delta S_k}(t), \quad \overline{\Delta S}(t) = \sum_k w_k \frac{\eta}{\eta_k} \overline{\Delta S_k}(t), \quad \text{(C.13)}$$

$$\underline{\Delta P}(t) = \sum_k w_k \underline{\Delta P_k}(t), \quad \overline{\Delta P}(t) = \sum_k w_k \overline{\Delta P_k}(t), \quad \text{(C.14)}$$

defines an outer-approximation, necessary model $\mathbb{P}_{\overline{\Phi}}$ for $\mathbb{P}_{\mathbb{K}}$. That is,

$$\overline{\Phi} = \left(\eta, \underline{\Delta S}(t), \overline{\Delta S}(t), \underline{\Delta P}(t), \overline{\Delta P}(t)\right), \quad \text{(C.15)}$$

with $\underline{\Delta S}(t)$ and $\overline{\Delta S}(t)$ defined in (C.13), and $\underline{\Delta P}(t)$ and $\overline{\Delta P}(t)$ defined in (C.14) constitutes an outer bound such that $\mathbb{P}_{\mathbb{K}} \subset \mathbb{P}_{\overline{\Phi}}(t)$.

Proof of Theorem 1. First, we take the Laplace transform of (C.1) after dropping the time-dependence of η_k:

$$s\Delta S_k(s) = \eta_k \Delta P_k(s). \quad \text{(C.16)}$$

We then similarly transform (C.4):

$$s\Delta S(s) = \eta \Delta P(s). \quad \text{(C.17)}$$

To connect these individual and aggregate models, we define:

$$\Delta P(t) = \sum_k w_k \Delta P_k(t), \quad \text{(C.18)}$$

such that:

$$\Delta P(s) = \sum_k w_k \Delta P_k(s). \quad \text{(C.19)}$$

This allows us to bring the individual models into (C.17) by first using (C.19):

$$\Delta S(s) = \frac{\eta}{s} \sum_k w_k \Delta P_k(s) \quad \text{(C.20)}$$

and then substituting in (C.16) solved for $\Delta P_k(s)$:

$$\Delta S(s) = \frac{\eta}{s}\sum_k w_k \frac{s}{\eta_k}\Delta S_k(s). \tag{C.21}$$

Rearranging, we arrive at:

$$\Delta S(s) = \sum_k w_k \frac{\eta}{\eta_k}\Delta S_k(s). \tag{C.22}$$

The upper-bound, necessary estimate $\overline{\Phi}$ is constructed by specifying energy, charging, and discharging capacities that envelop all possible realizations of the individual devices' shiftability. Thus, we construct upper and lower bounds on charging capacity:

$$\underline{\Delta P}(t) = \sum_k w_k \underline{\Delta P_k}(t) \leq \Delta P(t) \leq \sum_k w_k \overline{\Delta P_k}(t) = \overline{\Delta P}(t). \tag{C.23}$$

To bound energy capacity, we simply specify a value for η and then construct upper and lower bounds on change in energy level:

$$\underline{\Delta S}(t) = \sum_k w_k \frac{\eta}{\eta_k}\underline{\Delta S_k}(t) \leq \Delta S(t) \leq \sum_k w_k \frac{\eta}{\eta_k}\overline{\Delta S_k}(t) = \overline{\Delta S}(t). \tag{C.24}$$

□

Theorem 2. ***Inner Approximations When η is Constant***

Choose a β_k for each $k \in \mathbb{K}$ such that $0 \leq w_k\beta_k \leq 1$ and $\sum_k w_k\beta_k = 1$. Then, with:

$$\eta = \sum_k w_k\beta_k\eta_k \text{ and } \Delta P_k(t) = \beta_k \Delta P(t), \tag{C.25}$$

we see that:

$$\Delta P(t) = \sum_k w_k \Delta P_k(t) \tag{C.26}$$

and we can show that $\mathbb{P}_{\underline{\Phi}} \subset \mathbb{P}_{\mathbb{K}}$, where $\mathbb{P}_{\mathbb{K}}$ is defined by (C.9) and:

$$\underline{\Phi} = \left(\sum_k w_k\beta_k\eta_k, \max_k \frac{\eta}{\eta_k}\frac{\underline{\Delta S_k}(t)}{\beta_k}, \min_k \frac{\eta}{\eta_k}\frac{\overline{\Delta S_k}(t)}{\beta_k}, \max_k \frac{\underline{\Delta P_k}(t)}{\beta_k}, \min_k \frac{\overline{\Delta P_k}(t)}{\beta_k} \right). \tag{C.27}$$

Proof of Theorem 2. Taking the Laplace transform of the expression for ΔP_k in (C.25) and substituting into (C.16) yields:

$$\Delta S_k(s) = \beta_k \frac{\eta_k}{s}\Delta P(s). \tag{C.28}$$

Rearranging (C.17) to solve for $\Delta P(s)$ and substituting in yields:

$$\Delta S_k(s) = \beta_k \frac{\eta_k}{\eta}\Delta S(s). \tag{C.29}$$

Then, to ensure (C.2) is always satisfied we simply set:

$$\underline{\Delta S}(t) \geq \frac{\eta}{\eta_k}\frac{\underline{\Delta S_k}(t)}{\beta_k} \text{ and } \overline{\Delta S}(t) \leq \frac{\eta}{\eta_k}\frac{\overline{\Delta S_k}(t)}{\beta_k} \quad \forall k \in \mathbb{K} \tag{C.30}$$

and similarly require:

$$\underline{\Delta P}(t) \geq \frac{\underline{\Delta P_k}(t)}{\beta_k} \text{ and } \overline{\Delta P}(t) \leq \frac{\overline{\Delta P_k}(t)}{\beta_k} \quad \forall k \in \mathbb{K} \tag{C.31}$$

to satisfy (C.3). □

C.2 Discussion

Though the construction of outer approximations is not negatively affected by time-varying parameters $\underline{\Delta S_k}(t)$, $\overline{\Delta S_k}(t)$, $\underline{\Delta P_k}(t)$, or $\overline{\Delta P_k}(t)$, the proof of Theorem 2 essentially says the inner approximation bounds should be set by the most constrained individual resource for every time t. Thus, in practice, such inner approximations can only present nonzero resource if every device in the aggregation can move in the same direction at the same time. This constraint can be accommodated somewhat by grouping similar resources, but in this study, we instead choose to pursue a heuristic approach of scaling the outer approximation bounds by constant fractions. We select fractions to apply to the right-hand sides of (C.13) and (C.14) based on moderate-scale experiments where we optimally schedule individual vehicle charging to fulfill aggregate dispatch requests.

Appendix D. Time-of-Use Rates

D.1 Rates Used in the Study

As described in detail below, we construct TOU rates that attempt to mimic RTP patterns as closely as possible while enforcing the user-specified season and block structure. While the formulation is general and could be used to construct any number of rates with different numbers of seasons, blocks, and restrictions on season and block length, in this study, we analyze two rates: one with season and two blocks (TOU-1-2) and another with four seasons and four blocks (TOU-4-4).

In all cases, the rates we construct are only intended to represent the energy portion of a typical retail tariff. Other common tariff components include distribution, transmission, and line items to cover specific utility programs (e.g., efficiency, or clean energy). Seasons are defined as groups of contiguous days that can wrap around the first day of the year (i.e., December 31 and January 1 can be in the same season). Blocks are defined separately for weekdays and weekend days, but in both cases, they consist of groups of contiguous hours that can wrap around at midnight (i.e., 11 p.m.–2 a.m. and 12 a.m.–1 a.m. can be in the same block). Seasons must persist for a minimum number of days; blocks must be at least as long as a minimum number of hours.

The rates for TOU-1-2 are listed in Table D.1 and shown in Figure D.1. As expected, the rates are lower overnight than in daytime and on lower on the weekend than weekdays. For both day types, lower rates start at midnight. The transition to daytime prices happens at 7 a.m. on weekdays and at 9 a.m. on weekends. Overall, the prices range from 2.9 cents/kWh overnight on weekends to 5.5 cents/kWh during the day on weekdays.

Table D.1. TOU Tariff with 1 Season and 2 Blocks (TOU-1-2)

Season	Day Type	Block	Rate (cents/kWh)	Qualitative Description
1	Weekday	1	4.2	Early morning/overnight (midnight to 7 a.m.)
		2	5.5	Daytime through evening (7 a.m. to midnight)
	Weekend	1	2.9	Early morning/overnight (midnight to 9 a.m.)
		2	4.8	Daytime through evening (9 a.m. to midnight)

The rates for TOU-4-4 are listed in Table D.2 and shown in Figure D.2. In this case, 32 prices are in effect over the course of the year. Although it is much more complex than TOU-1-2, TOU-4-4 is still a much coarser price signal than is a full RTP, which has 8,760 different energy prices. TOU-4-4 breaks up the year into a most-expensive winter season, a least-expensive spring season, a long summer season, and a very short fall season. The highest rates occur on winter weekend evenings (9.6 cents/kWh) and fall weekday evenings (7.5 cents/kWh). In general, daytime and evening prices are higher than overnight and early morning prices. Overall, the TOU-4-4 tariff is less intuitive than the TOU-1-2 tariff but it better reflects patterns evident in the DA energy prices from the Reference scenario PCM. Seasonal patterns include lower gross load in shoulder seasons, which is reflected in lower price seasons in March–May (Months 3-5) and October (Month 10). The spring shoulder season has particularly low prices due to a confluence of higher-than-average wind and solar generation with lower-than-average load; April is the month where this pattern is most evident. Winter and summer seasons have higher prices, with blocks following different patterns based on load and availability of variable generation. In the

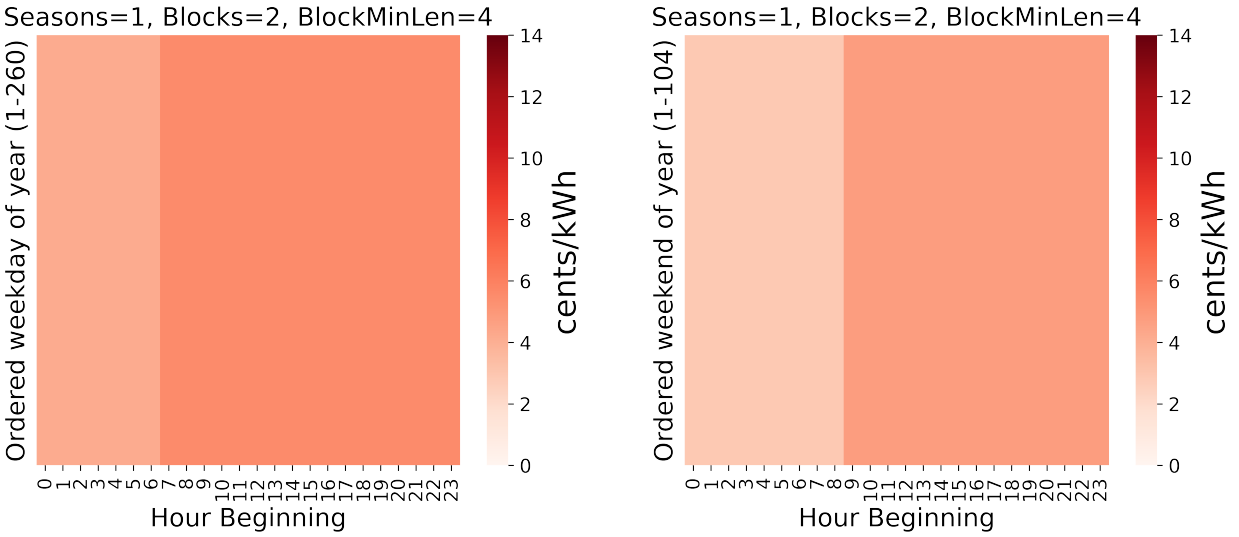

(a) Weekday energy prices **(b) Weekend energy prices**

Figure D.1. TOU tariff with 1 season and 2 blocks (TOU-1-2). The blocks are required to be at least 4 hours long. January is at the top of the y-axes.

summer season, which has lower-than-average wind generation, prices generally follow gross load, which is highest in the afternoon and evening hours and lowest in the early morning hours. In the winter season, wind generation is high, particularly in late-evening to overnight hours; this generally yields a high price period in the early evening when net load is highest, followed by a lower price overnight period, and then a higher-priced early morning period when wind generation decreases (see Figure D.3 and Figure D.4).

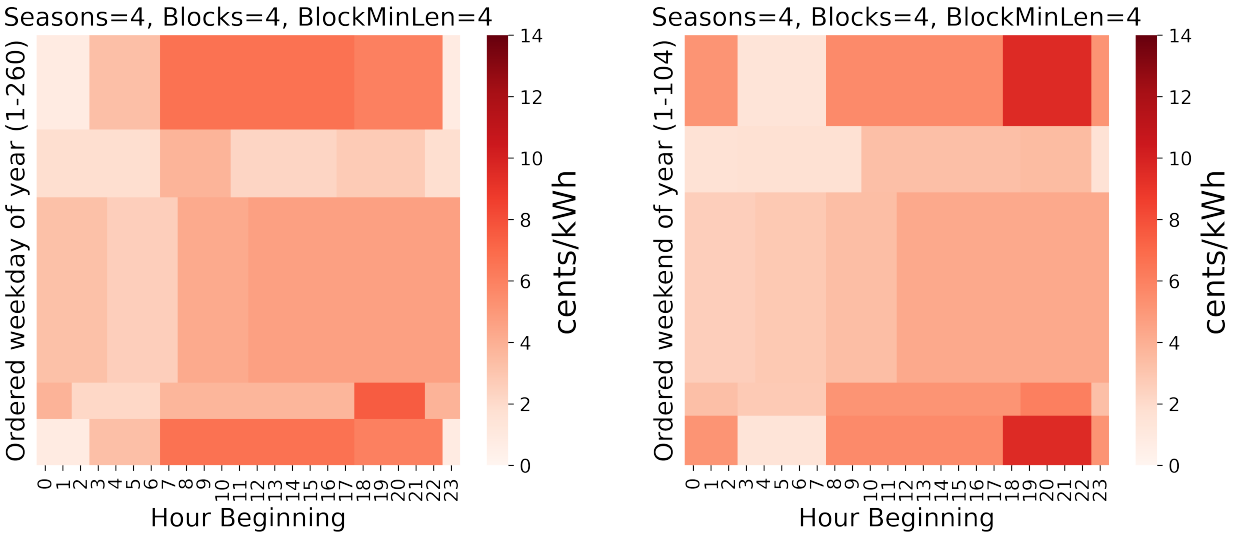

(a) Weekday energy prices **(b) Weekend energy prices**

Figure D.2. TOU tariff with 4 seasons and 4 blocks (TOU-4-4). The seasons are required to be at least 30 days long and the blocks are required to be at least 4 hours long. January is at the top of the y-axes.

Table D.2. TOU Tariff with 4 Seasons and 4 Blocks (TOU-4-4)

Season	Day Type	Block	Rate (cents/kWh)	Description
1	Weekday	1	0.8	Winter very early morning
		2	3.3	Winter early morning
		3	6.6	Winter daytime
		4	6.0	Winter evening
	Weekend	1	5.2	Winter very early morning
		2	1.4	Winter early morning
		3	5.6	Winter daytime
		4	9.6	Winter evening
2	Weekday	1	1.8	Spring overnight/early morning
		2	3.8	Spring morning
		3	2.3	Spring afternoon
		4	2.7	Spring evening
	Weekend	1	1.6	Spring overnight/early morning
		2	1.7	Spring morning
		3	3.3	Spring afternoon/early evening
		4	3.5	Spring evening
3	Weekday	1	3.2	Summer very early morning
		2	2.6	Summer early morning
		3	4.2	Summer morning
		4	4.7	Summer afternoon and evening
	Weekend	1	2.6	Summer very early morning
		2	2.9	Summer early morning
		3	3.4	Summer morning
		4	4.3	Summer afternoon and evening
4	Weekday	1	3.8	Fall overnight/early morning
		2	2.1	Fall early morning
		3	3.7	Fall daytime
		4	7.5	Fall evening
	Weekend	1	3.3	Fall overnight/early morning
		2	2.8	Fall early morning
		3	5.2	Fall daytime
		4	6.1	Fall evening

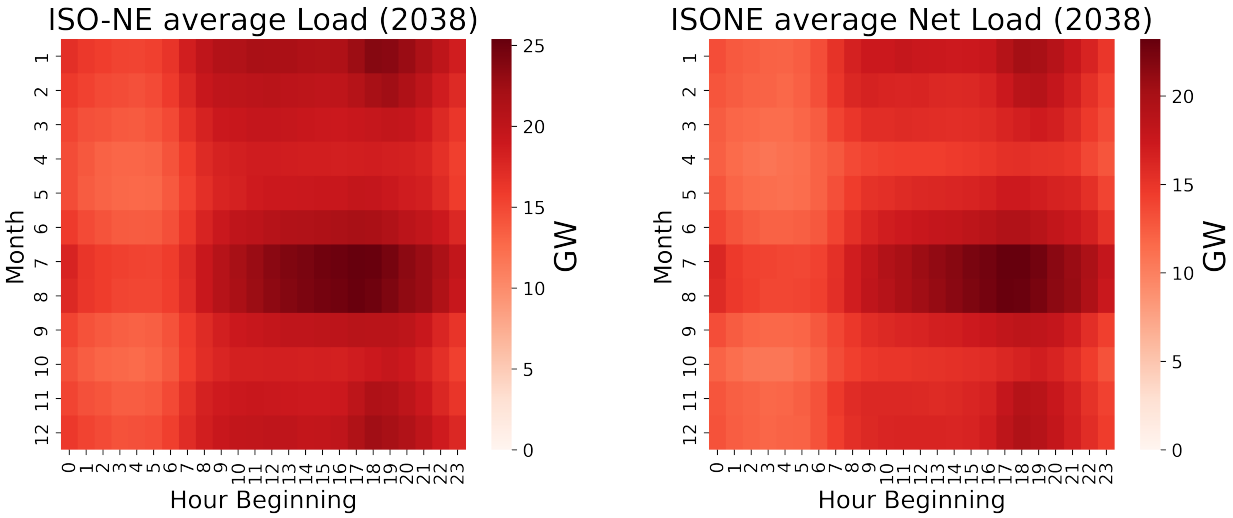

(a) Month-hour average load **(b) Month-hour average net load**

Figure D.3. Average month-hour load and net load for modeled year in ISO-NE.

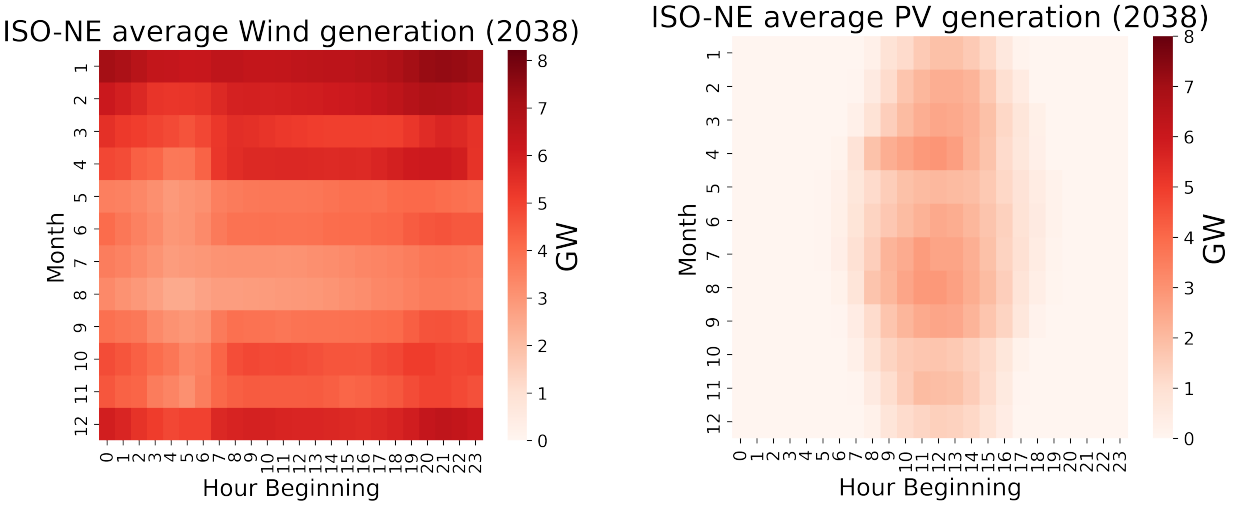

(a) Month-hour average wind generation **(b) Month-hour average solar PV generation**

Figure D.4. Average month-hour Wind and PV Generation for modeled year in ISO-NE.

D.2 Formulation

We compute TOU rates for energy based on the notion that, given a certain number of seasons and blocks, we would like the TOU tariff to mimic actual RTP patterns as closely as possible. Also, the TOU rates need to recover a similar amount of revenue. Lacking a more appropriate target for this study, we require the TOU tariff to recover at least as much revenue as the RTP tariff, assuming load is fixed to the Reference scenario load profile in both cases.

The problem as stated can be written as a mathematical program, which is documented in subsection D.2.2. Unfortunately, as written, the program is a non-convex mixed-integer nonlinear program (MINLP) that we were unable to solve at the required scale (365 days of data) with commercial solvers. We were able to solve moderate-sized problems (30-60 days of data) after replacing bilinear terms (indicated below) with piecewise linear approximations, which transformed the non-convex MINLP into a convex mixed-integer quadratic program (MIQP). As part of working to get the problem to solve, we implemented the ability to compute feasible starting points with an agglomerative clustering approach[16]. It proved to produce better solutions (as measured by our objective function) on its own as than solving the convex formulation from either a simple or the clustered starting point. There might be ways to adjust the formulation to work more cleanly with one or more commercial solvers. In the meantime, the rates described in Section D.1 were essentially computed with agglomerative clustering (described below) and then finalized by solving the optimization problem with season and block structure fixed to the clustering result.

D.2.1 Notation

Table D.3. Set and Element Symbols

Symbol	Description
T	Set of all time stamps
D	Set of all days
W	Set of all weekday types (weekend/holiday and weekday)
H	Set of all hours within a day
S	Set of all TOU tariff seasons
B	Set of all TOU tariff blocks
t	Time stamp
d	Day
w	Weekday type
h	Hour of the day
s	TOU tariff season
b	TOU tariff block

[16] https://scikit-learn.org/stable/modules/generated/sklearn.cluster.AgglomerativeClustering.html

Table D.4. Superscripts

Symbol	Description
TOU	TOU tariff results
ISO	Wholesale market results

Table D.5. Index Sets

Symbol	Description
$t \in T$	Time stamps for which we have wholesale energy prices
$d \in D$	Days of the year
$w \in W$	Weekday types (weekend/holiday and weekday)
$h \in H$	Local time hours of each day
$s \in S$	Seasons defined in the TOU tariff
$b \in B$	Blocks of time defined in the TOU tariff

Table D.6. Subsets

Symbol	Description
$T_{w,d} \subset T$	Time stamps that map to weekday type w and day d
$T_{w,h} \subset T$	Time stamps that map to weekday type w and local time hour h

Table D.7. Parameters

Symbol	Description
l_t	Baseline system load in time stamp t
p_t	Wholesale energy price in time stamp t
$\|S\|$	Number of TOU seasons (compile-time parameter)
$\|B\|$	Number of TOU blocks (compile-time parameter)
$\underline{n}^S$	Minimum season length in days
$\underline{n}^B$	Minimum block length in hours

Table D.8. Variables

Symbol	Description
$\pi_{s,w,b}$	(continuous) TOU tariff price
ρ_t^{TOU}	(continuous) TOU revenue in time t
ρ^{TOU}	(continuous) Total TOU revenue
ρ_t^{ISO}	(continuous) Wholesale market revenue in time t
ρ^{ISO}	(continuous) Total wholesale marekt revenue
$\mu_{s,d}^{\text{S}}$	(binary) Indication of active days d for season s
$\mu_{s,w,b,h}^{B}$	(binary) Indication of active hours h for block b in season s and weekday type w
$\lambda_{s,w,b,t}$	(continuous, positive) Load at time t assigned to season s weekday type w and time block b
$\sigma_{s,d}^{S}$	(binary) Start-up day of season s
$\tau_{s,d}^{S}$	(binary) Shut-down day of season s
$\sigma_{s,w,b,h}^{B}$	(binary) Start-up hour of block b during season s and on weekday type w
$\tau_{s,w,b,h}^{B}$	(binary) Shut-down hour of block b during season s and on weekday type w

D.2.2 Description

The objective is to minimize the difference between TOU and wholesale energy prices:

$$\min \sum_{t \in T} \left(\rho_t^{\text{TOU}} - \rho_t^{\text{ISO}} \right)^2 \tag{D.1}$$

subject to the constraint that the TOU rate should generate enough revenue to cover wholesale market costs under marginal price compensation and baseline load conditions:

$$\sum_{t \in T} \rho_t^{\text{TOU}} \geq \sum_{t \in T} \rho_t^{\text{ISO}}. \tag{D.2}$$

Wholesale market revenue per time period is not a variable, but a parameter precomputed from the load and price parameters l_t and p_t:

$$\rho_t^{\text{ISO}} = l_t \cdot p_t, \; \forall t \in T. \tag{D.3}$$

Load l_t is allocated to the TOU tariff blocks (variable $\lambda_{s,w,b,t} \geq 0$) using indicator variables $\mu_{s,d}^{S}$ and $\mu_{s,w,b,h}^{B}$:

$$\lambda_{s,w,b,t} \leq l_t \cdot \mu_{s,d}^{S} \; \forall t \in T_{w,d} \tag{D.4}$$

$$\lambda_{s,w,b,t} \leq l_t \cdot \mu_{s,w,b,h}^{B} \; \forall t \in T_{w,h}, \tag{D.5}$$

and an equation that makes certain that all load is allocated:

$$\sum_{s\in S, w\in W, b\in B} \lambda_{s,w,b,t} = l_t \; \forall t \in T. \tag{D.6}$$

Doing so provides enough information to calculate the TOU revenue, which is a bilinear function of allocated load $\lambda_{s,w,b}$ multiplied by the chosen TOU rate $\pi_{s,w,b}$:

$$\rho_t^{\text{TOU}} = \sum_{s\in S, w\in W, b\in B} \pi_{s,w,b} \cdot \lambda_{s,w,b,t} \; \forall t \in T. \tag{D.7}$$

Unit commitment-like constraints enforce minimum uptimes for seasons and minimum continuous hours for blocks, both of which are enforced using circular time. Other constraints enforce the sequential nature of seasons and blocks, assign each time period to a season and a block, and ensure each season and block is only used once.

The following constraints apply to all $s \in S$ and all $d \in D$. Season start-up:

$$\sigma_{s,d}^S \geq \mu_{s,d}^S - \mu_{s,d-1}^S \tag{D.8}$$

$$\sigma_{s,d}^S + \mu_{s,d-1}^S \leq 1; \tag{D.9}$$

Season shutdown:

$$\tau_{s,d}^S \geq \mu_{s,d-1}^S - \mu_{s,d}^S \tag{D.10}$$

$$\tau_{s,d}^S \leq \mu_{s,d-1}^S; \tag{D.11}$$

Season linkage:

$$\mu_{s,d}^S = \mu_{s,d-1}^S + \sigma_{s,d}^S - \tau_{s,d}^S; \tag{D.12}$$

Season order:

$$\sigma_{s+1,d}^S = \tau_{s,d}^S; \tag{D.13}$$

Enforce minimum season length of $\underline{n}^S$ days:

$$\sum_{\{dd|(dd>d-\underline{n}^S)\wedge(dd<=d)\}} \sigma_{s,dd}^S + \sum_{\{dd|dd>d+|D|-\underline{n}^S\}} \sigma_{s,dd}^S \leq \mu_{s,d}^S; \tag{D.14}$$

Assign one season per day:

$$\sum_{s\in S} \mu_{s,d}^S = 1; \tag{D.15}$$

Use of each season at most once:

$$\sum_{d\in D} \sigma_{s,d}^S \leq 1. \tag{D.16}$$

These constraints apply to all $s \in S$, all $w \in W$, all $b \in B$, and all $h \in H$. Block start-up:

$$\sigma_{s,w,b,h}^B \geq \mu_{s,w,b,h}^B - \mu_{s,w,b,h-1}^B \tag{D.17}$$

$$\sigma_{s,w,b,h}^B + \mu_{s,w,b,h-1}^B \leq 1; \tag{D.18}$$

Block shutdown:

$$\tau^B_{s,w,b,h} \geq \mu^B_{s,w,b,h-1} - \mu^B_{s,w,b,h} \tag{D.19}$$

$$\tau^B_{s,w,b,h} \leq \mu^B_{s,w,b,h-1}; \tag{D.20}$$

Block linkage:

$$\mu^B_{s,w,b,h} = \mu^B_{s,w,b,h-1} + \sigma^B_{s,w,b,h} - \tau^B_{s,w,b,h}; \tag{D.21}$$

Block order:

$$\sigma^B_{s,w,b+1,h} = \tau^B_{s,w,b,h}; \tag{D.22}$$

Enforce minimum block length of $\underline{n}^B$ hours:

$$\sum_{\{hh|(hh>h-\underline{n}^B)\wedge(hh<=h)\}} \sigma^B_{s,w,b,hh} + \sum_{\{hh|hh>h+|H|-\underline{n}^B\}} \sigma^B_{s,w,b,hh} \leq \mu^B_{s,w,b,h}; \tag{D.23}$$

Assign one block per hour:

$$\sum_b \mu^B_{s,w,b,h} = 1; \tag{D.24}$$

Use of each block at most once:

$$\sum_h \sigma^B_{s,w,b,h} \leq 1. \tag{D.25}$$

Altogether, this formulation is a non-convex nonlinear integer program with a convex quadratic objective, $|T|$ bilinear constraints and $O(|S|\cdot|D|)+O(|S|\cdot|W|\cdot|B|\cdot|H|)$ binary variables.

D.2.3 Practical Implementation

The above formulation can be transformed into a convex MIQP by linearizing the bilinear term in Equation D.7. We do this by assigning:

$$x_{s,w,b,t} = \frac{1}{2}\left(\pi_{s,w,b} + \lambda_{s,w,b,t}\right) \tag{D.26}$$

$$y_{s,w,b,t} = \frac{1}{2}\left(\pi_{s,w,b} - \lambda_{s,w,b,t}\right). \tag{D.27}$$

Then, our quantity of interest:

$$z_{s,w,b,t} = \pi_{s,w,b} \cdot \lambda_{s,w,b,t} \tag{D.28}$$

can also be computed as:

$$z_{s,w,b,t} = x^2_{s,w,b,t} - y^2_{s,w,b,t}. \tag{D.29}$$

Linearization is completed by replacing $x^2_{s,w,b,t}$ and $y^2_{s,w,b,t}$ with piecewise linear approximations. The resulting formulation has many more continuous and binary variables, and it generally scales with $|S|\cdot|W|\cdot|B|\cdot|T|$.

TOU tariffs can also be computed with clustering, either to use directly or to provide a starting point for the mathematical programming formulation. Because of our need to form contiguous

seasons and blocks, we chose to use the agglomerative clustering module[17] available in Python package scikit-learn.[18]

We apply agglomerative clustering first to define seasons and then to define blocks. Seasons are clustered based on average RTP per day. Blocks are clustered based on average RTP per hour within a given season and day type. We supply the algorithm with explicit linking graphs that define which days are adjacent to which other days (for clustering days into season) and which hours are adjacent to which other hours (for clustering hours into blocks). The algorithm returns the requested number of clusters, and all clusters consist of contiguous days or hours, where contiguity is defined circularly by specifying that December 31 and January 1 are adjacent as are 11 p.m.-12 a.m. and 12 a.m.-1 a.m. However, the algorithm does not have an option for specifying minimum cluster sizes. We therefore enforce that constraint as a post-processing step. After clustering days into seasons, and clustering hours into blocks for each combination of season and day type, we have a complete specification of the TOU temporal structure. TOU rates are then computed by assigning the average RTP price within each season, day type and block combination.

[17] https://scikit-learn.org/stable/modules/generated/sklearn.cluster.AgglomerativeClustering.html
[18] https://scikit-learn.org/stable/index.html

Appendix E. Optimal Dispatch Formulations

The general charging flexibility model:

$$\Delta S_k(t) = \Delta S_k(t-1) + \Delta P_k(t)\delta t \tag{E.1}$$

$$\underline{\Delta P_k}(t) \leq \Delta P_k(t) \leq \overline{\Delta P_k}(t) \tag{E.2}$$

$$\underline{\Delta S_k}(t) \leq \Delta S_k(t) \leq \overline{\Delta S_k}(t), \tag{E.3}$$

which in this study appears in individual vehicle (4.12-4.14), aggregate outer approximation (4.16-4.18), and aggregate scaled outer approximation (4.16, 4.27, 4.28) flavors, can be dispatched optimally once an objective function is specified. In this case, $k \in \mathbb{K}$ represents a single flexibility resource k in an arbitrary collection of flexibility resources $\mathbb{K}$, each of which could be at a single vehicle or an aggregate level.

E.1 Price-taking Dispatch

The RTP and TOU dispatch mechanisms rely on dispatching (E.1-E.3) against a price signal $p(t)$. In this study, $p(t)$ is an hourly profile in \$/MWh, specified for each of 8,760 hours in the year. In the RTP case, it consists of the system-level energy prices for the simulated Reference scenario (SEAMS 2038 model with EV load but without EVMC). In the TOU case, after calculating the TOU tariff we expand it again into an "8760" profile that has many repeated values. (The same price applies in all hours assigned to a given season and weekday or weekend time block.) The simplest form of price-taking model maximizes the value of dispatching flexibility:

$$\max_{\Delta P_k(t), \Delta S_k(t)} \sum_{k,t} -p(t)\Delta P_k(t)\delta t \tag{E.4}$$

subject to the constraints (E.1-E.3), which is equivalent to minimizing charging costs.

At high shares of EVMC participation, we find the dispatch produced by (E.1-E.4) increases overall system costs because the amount of load that is shifted is able to create, e.g., new system peaks. To mitigate this effect, we perform price-taking dispatch regularized by an aggregate ramp penalty price ρ (\$/MW):

$$\max_{\Delta P_k(t), \Delta S_k(t), \Delta P(t), \Delta P^+(t), \Delta P^-(t)} \sum_{k,t} -p(t)\Delta P_k(t)\delta t - \rho \sum_t \left(\Delta P^+(t) + \Delta P^-(t)\right) \tag{E.5}$$

where $\Delta P^+(t)$ and $\Delta P^-(t)$ are the positive and negative parts of the aggregate ramp profile, calculated with the constraints:

$$\Delta P(t) = \sum_k \Delta P_k(t) \tag{E.6}$$

$$\Delta P^+(t) - \Delta P^-(t) = \Delta P(t) - \Delta P(t-1) \tag{E.7}$$

$$\Delta P^+(t),\ \Delta P^-(t) \geq 0. \tag{E.8}$$

We find that exactly how we group flexibility resources into sets $\mathbb{K}$ that are dispatched in the same linear program does not significantly impact results, even for the formulation (E.1-E.3, E.5-E.8). In this study, ramp penalties are applied at the county level; that is, we dispatch individual vehicles in batches where each linear program contains all sample vehicles for a single county.

E.2 Disaggreation of Aggregate Dispatch Signal

The disaggregation experiments in Section 4.2 calculate individual dispatch profiles to fulfill an aggregate dispatch request $d(t)$. In this study, we measure error with a 1-norm and solve the linear program:

$$\min_{\Delta P_k(t), \Delta S_k(t), E^+(t), E^-(t)} \sum_t E^+(t) + E^-(t) \tag{E.9}$$

$$\text{s.t. } (E.1 - E.3) \tag{E.10}$$

$$E^+(t) - E^-(t) = \left(\sum_k \Delta P_k(t) \right) - d(t) \tag{E.11}$$

$$E^+(t),\ E^-(t) \geq 0, \tag{E.12}$$

which is equivalent to minimizing the mean absolute error. Future work could explore solving the disaggregation problem in the least-squares sense or directly factoring in the expected effects of buying back dispatch deviations at real-time prices.